

Report E-0260

Increasing Onshore Wind Energy in Ukraine

Alexandre Pereira, Poul Sørensen, Matti Koivisto, Malte Jansen, Aikaterini Mitsakou, Joan Piera, Brian O. Hansen, and Polyneikis Kanellas

Final Report

July, 2025



Increasing Onshore Wind Energy in Ukraine

Final Report

July, 2025

Contractor: Danish Energy Agency

Report E-0260

By Alexandre Pereira, Poul Sørensen, Matti Koivisto, Malte Jansen, Aikaterini Mitsakou, Joan Piera, Brian O. Hansen, and Polyneikis Kanellas

Copyright: Reproduction of this publication in whole or in part must include the customary

bibliographic citation, including author attribution, report title, etc.

Cover photo: wind farm in Denmark by Alexandre Pereira

Published by: DTU Wind, Department of Wind and Energy Systems

ISBN: [978-87-87335-88-1] (electronic version)

Technical University of Denmark

DTU Wind

Department of Wind and Energy Systems

DTU Risø Campus
Frederiksborgvej 399, building 125
4000 Roskilde, Denmark
www.wind.dtu.dk

Executive Summary

The Danish Energy Agency (DEA) requested DTU Wind to undertake a pre-feasibility study within three provinces of Ukraine: Chernihiv, Kirovohrad, and Ternopil. The study included a preliminary analysis of the wind resources, the identification of the wind potential for each province, the energy production simulation for three hypothetical wind farms, and the estimation of the levelized cost of energy (LCOE).

DTU Wind received several inputs during online meetings organised by DEA with several local stakeholders.

The wind resources as well as digital maps of orography and roughness were obtained from the Global Wind Atlas (GWA). The most relevant wind climate parameters used in the study can be found in chapter 2.

A geospatial assessment of the provinces identified most suitable areas for the development of wind energy projects. Several site-specific constraints were considered as exclusion or restriction zones. The databases used for the geospatial analysis, described in chapter 3, are available and may be used in the future for enhancing the current study, in case that new data or different constraints become available.

Three hypothetical wind farms were modelled in chapter 4 using WAsP, the industry-standard software for wind resource assessment and wind farm planning. The layouts were defined using best practices to maximise the energy yield and the preliminary estimations indicate capacity factors of 46% to 48%.

The LCOE for the wind projects described in chapter 5 shows lower costs compared to the Urgent Ukraine Technology Catalogue. The lowest LCOE is observed in Kirovohrad (44.7 €/MWh), followed by Ternopil (46.0 €/MWh) and Chernihiv (46.8 €/MWh). The comparison with German and UK's markets highlights that Ukraine's LCOE is more competitive than Germany's but remains higher than the UK's. As such, for the LCOE calculation, certain external factors, particularly those stemming from the ongoing geopolitical situation, have not been explicitly incorporated into our analysis.

The wind generation time series simulations calculated with DTU's CorRES in chapter 6 shows low correlations between the sites (on average around 0.45) reducing the likelihood of zero aggregate generation. CorRES has also been used to simulate solar photovoltaic (PV) generation. Negative correlation between wind and solar generation is observed at each site, enabling reduction in generation variability when combining wind and solar power.

The preliminary assessment of system integration aspects of variable renewable energy generation indicates promising perspectives for accelerating the use of wind power in Ukraine. Geographically dispersed implementation of wind farms shall be considered when planning the new renewable generation projects. And hybridization with solar PV and/or with solar PV and bat-

teries might improve the feasibility of new projects due to the potential complementarity of wind and solar technologies in Ukraine.

Although this report shows a preliminary analysis, it could be interpreted as guidance for planning the next steps of the development of wind projects in Chernihiv, Kirovohrad, and Ternopil, which might include measurement campaigns, environmental assessments, and a more detailed conceptual design of wind farms and/or hybrid wind-solar power plants.

Contents

1	intro	oduction	1
2	Win	d Meteorology	3
	2.1		3
	2.2	·	6
			6
		2.2.2 Wind Speed Frequency Distribution	
		2.2.3 Monthly Variability of Wind Speed	
	2.3	Summary	
•	0	omatical Ameliania	^
3		spatial Analysis 1	-
	3.1	Site Selection Criteria	
		3.1.1 Wind Energy Potential	
		3.1.2 Environmental Protected Areas	
		3.1.3 Roads	
		3.1.4 Railways	
		3.1.5 Airports	3
		3.1.6 Aspects of Land Use	3
		3.1.7 Other Restrictions	4
	3.2	Selected Areas	6
	3.3	Wind Power Potential	6
4	Ene	rgy Yield Assessment 2	20
	4.1	Inputs	20
		4.1.1 Site Locations	
		4.1.2 Digital Maps	
		4.1.3 Wind Data	
		4.1.4 Wind Turbine	
	4.2	Wind Farm Calculations	
	⊤.∠	4.2.1 Wind Flow Modeling	
		4.2.2 Wake Model	
		4.2.3 Wind Farm Layouts	
		·	
		4.2.4 Energy Yield Results with Wake Losses	
	4.3	4.2.5 Net Energy Yield Results with Additional Losses	
	4.4	Recommendations for a Wind Measurement Campaign	
	4.5	Summary and Discussion	
	7.5	duffinary and Discussion	
5	Lev	elised Cost of Energy 3	
	5.1	Methods and Data	
		5.1.1 Net Annual Energy Production	1
		5.1.2 CapEx	1
		5.1.3 Operation and maintenance expenditure (OpEx)	1
		5.1.4 WACC	2

		5.1.5 Interpretation	3
	5.2	LCOE Results	3
	5.3	Summary and Discussion	5
6	Ren	newable Energy Integration 36	3
	6.1	Wind and Solar Power Simulations: Time Series	3
		6.1.1 The CorRES Tool	3
		6.1.2 Input Data	3
		6.1.3 Wind Generation Time Series	7
		6.1.4 Solar Generation Time Series	7
	6.2	Correlation Analysis	1
		6.2.1 Wind Generation Correlation	1
		6.2.2 Correlation Between Wind and Solar Generation	1
	6.3	Hybridization Analysis	3
		6.3.1 Applied Data for the Analyses	3
		6.3.2 Hybridization with Solar	3
		6.3.3 Hybridization with Solar and Battery	5
	6.4	Load Following	3
	6.5	Summary and Discussion	3
7	Con	nclusion 51	I
Re	fere	nces 54	1
Αŗ	pend	dix 57	7
	A.1	WAsP inputs: elevation and land cover maps	7
	A.2	CorRES inputs: wind farm power curves	3

List of Abbreviations

AEP	Annual Energy Production	GWA	Global Wind Atlas
AGL	Above Ground Level	GWC	Generalised Wind Climate
BZ	Bessel Zooming	IEC	International Electrotechnical Commis-
CAPEX	Capital Expenditures		sion
DEVEX	Development Expenditures	LCOE	Levelised Cost of Energy
DTU	Technical University of Denmark	OPEX	Operational Expenditures
DTU Wind	Department of Wind and Energy Sys-	UTM	Universal Transverse Mercator
	tems	WACC	Weighted Average Cost of Capital
GIS	Geographic Information System	WAsP	Wind Atlas Analysis and Application
GPS	Global Positioning System		Program

1 Introduction

The Ukraine-Denmark energy partnership program – UDEPP – financed by the Danish Neighbourhood Program under the Ministry of Foreign Affairs aims to strengthen the enabling environment for investments in sustainable energy, and to assist Ukraine in achieving its renewable energy, energy efficiency, and energy independence targets. Considering that the Ukrainian energy system could be rebuilt with focus on renewables and energy-efficient solutions, after a special request from Ukraine's Energy Minister for Danish assistance in the field of wind power, and considering that there is a need for more and better data to serve as the foundation for construction of additional wind farms, the Danish Energy Agency (DEA) asked the Department of Wind and Energy Systems of the Technical University of Denmark (DTU Wind) to conduct a study of onshore wind energy potential in Ukraine.

The objective of the study is to generate relevant accurate information to serve as a framework for investors, private companies and other stakeholders engaged in the development of onshore wind in Ukraine. It includes the selection of suitable areas for wind power projects based on geospatial analysis of available information; use of best practices, data and tools for the preliminary assessment of the wind resources; estimation of wind power installed capacity targets; design of hypothetical wind farms to estimate annual energy production and LCOE; simulation of the hypothetical wind farms and solar PV plants to obtain production time series and investigate the correlation among different renewable energy technology and location; and recommendations for necessary surveys and studies to allow for comprehensive and less uncertain feasibility studies.

The provinces included in this study are Chernihiv, Kirovohrad, and Ternopil, indicated in Figure 1. The provinces were selected based on the existence of large areas with reasonably good wind resources according to the *Global Wind Atlas* ([1]), and their geographical location (at different regions of the country) which allows us to investigate the potential advantages of geographically distributed wind generation for Ukraine. The borders of the areas have been retrieved from the World Bank data catalog *World Bank Official Administrative Boundaries* ([2]).

The report provides a comprehensive overview of inputs, methods, and assumptions collaboratively discussed with local stakeholders, supporting the preparation for the next steps in planning the development of large wind energy projects in Ukraine: specific measurement campaigns, environmental assessments, and feasibility studies.



Figure 1: Ukraine and the provinces Chernihiv, Kirovohrad and Ternopil. Country borders obtained from [2].

2 Wind Meteorology

In this study, the methodology described in the Global Wind Atlas¹ (GWA) has been used to analyze the wind meteorology of the selected Ukrainian provinces of Chernihiv, Kirovohrad, and Ternopil.

The main wind parameters and statistics presented in this report may be used for the prefeasibility study of wind power projects and for determination of suitable wind measurement locations.

Details about the Global Wind Atlas are given by Davis et al. [1], outlining the general method, specific development, and application of the Global Wind Atlas.

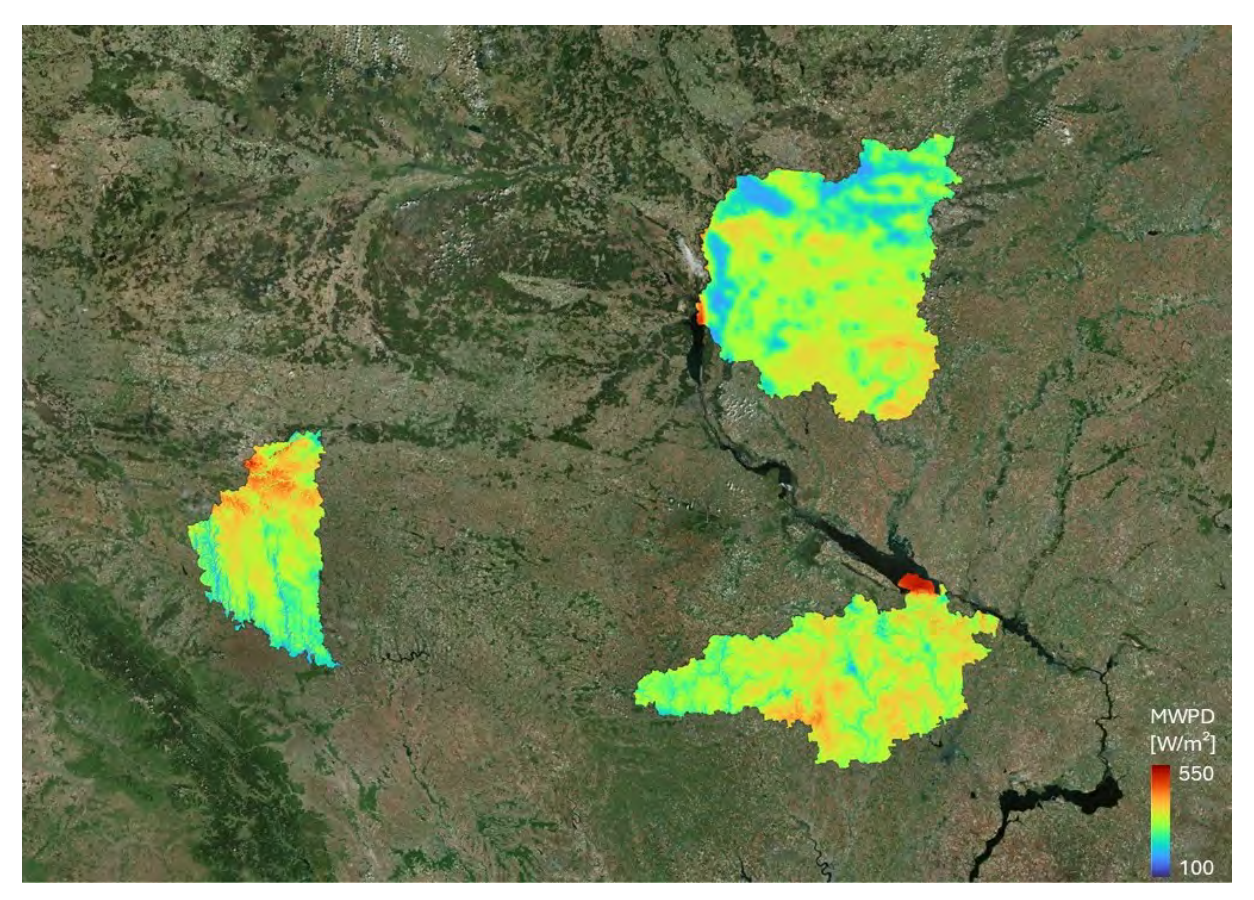
2.1 Wind Meteorology

The estimated wind resources are shown in Figure 2 for all three provinces. The estimated annual mean wind power density at 100 meters varies across the provinces from 100 W/m² to 550 W/m², with a concentration of higher wind resource areas in the southeastern region of Chernihiv, around the centre of Kirovohrad, and in the northern region of Ternopil.

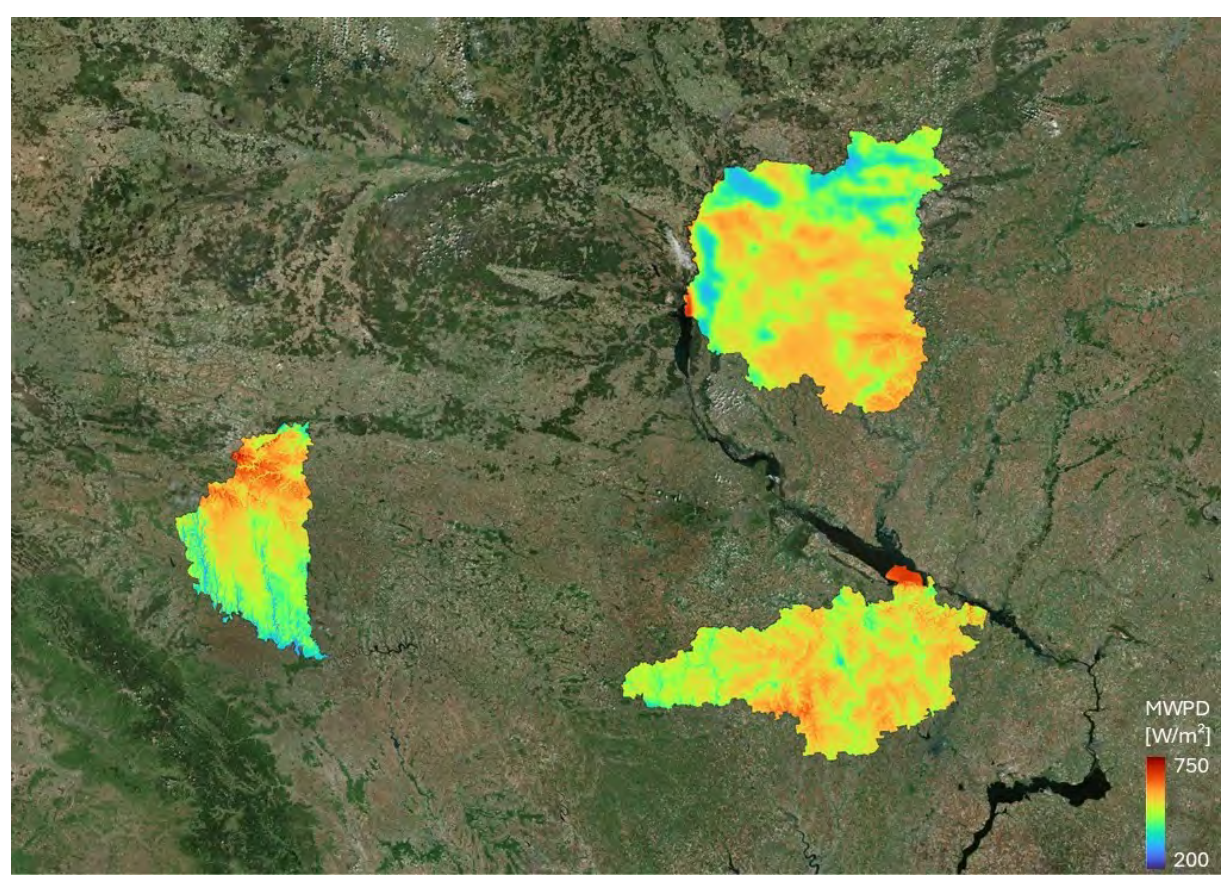
The wind resource normally increases with height, and the increase in mean wind speed at increasing heights has been modelled by the GWA using a roughness length and a modified log law. Figure 2 depicts the estimated mean wind power density at two heights, 100 and 150 meters, showing an expected increase in wind potential for most of the areas and maximum values of around 750 W/m². According to this information, the three provinces are classified as having moderate to low wind resources, and further investigation of the GWA data confirms this assumption. In Figure 3b, for example, all provinces are predominantly classified as IEC Class III, the lowest wind speed class of the IEC 61.400 international standard. The figure shows the IEC class based on the criterium of fatigue loads calculation, which takes into account the average wind speeds (class I, II, III and S) and turbulence intensity (turbulence category A+, A, B and C).

Figure 3 shows a) the Capacity Factor for IEC class III and b) the IEC class - Fatigue Loads layer at 100 m AGL. The Capacity Factor is a measure of the annual energy yield of a wind turbine, and higher capacity factors indicate higher energy yield. More specifically, the capacity factor is the ratio of a) the estimated annual energy production (at varying wind speed and power production) to b) the theoretical maximum annual energy production of the wind turbine (at continuous rated power). These two parameters, along with the mean wind power density, are used in this project to identify the most suitable areas for wind energy development.

¹DTU owns and continues to develop the Global Wind Atlas, a web-based application designed to assist policy-makers, planners, and investors in identifying high-wind areas suitable for wind power generation anywhere in the world. It offers preliminary calculations and allows users to conduct online queries, providing access to up-to-date datasets and modeling methodologies.

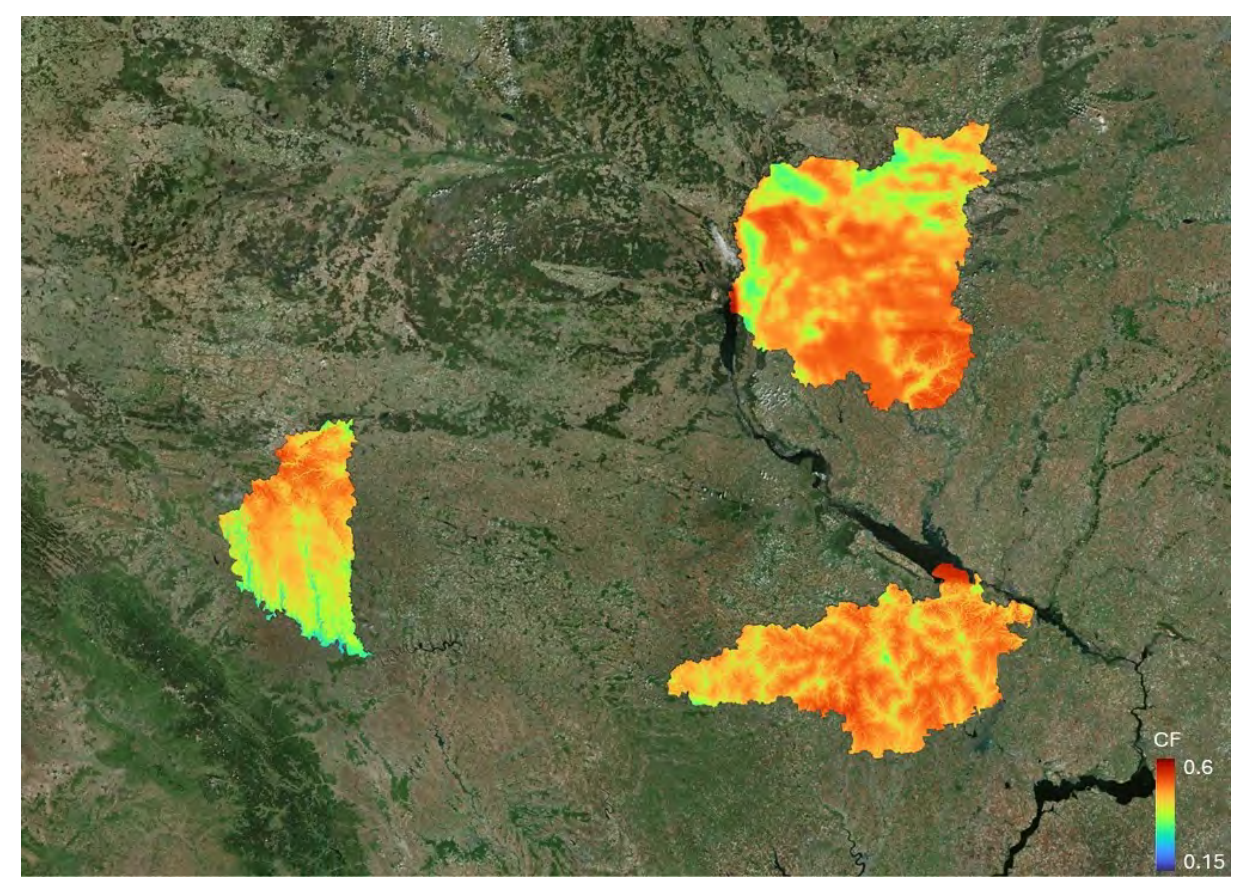


(a) Mean wind power density in W/m² at 100 m AGL. Data from the Global Wind Atlas.

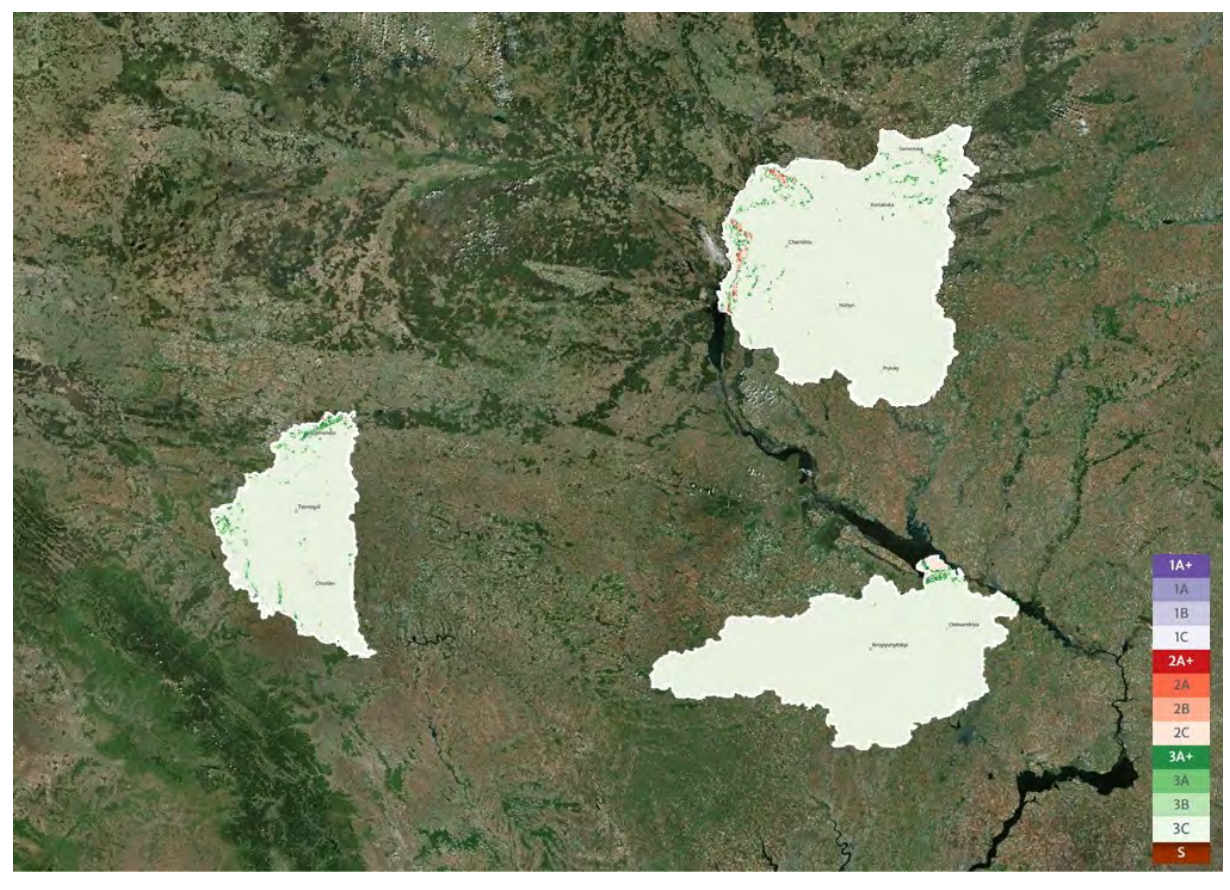


(b) Mean wind power density in W/m^2 at 150 m AGL. Data from the Global Wind Atlas.

Figure 2: Annual Mean Wind Power Density at Chernihiv, Kirovohrad, and Ternopil.



(a) "Capacity Factor - IEC class III" at 100 m AGL. Data from the Global Wind Atlas.



(b) "IEC Class - Fatigue Loads" at 100 m AGL. Data from the Global Wind Atlas.

Figure 3: Capacity Factor and IEC Class at Chernihiv, Kirovohrad, and Ternopil.

A location with relatively good wind resources was selected in each province to investigate and compare their wind characteristics. The reference locations are indicated in Figure 4 and by the following coordinates:

• Reference location in Chernihiv: $50.430\,684^{\circ}$ N, $32.700\,806^{\circ}$ E

• Reference location in Kirovohrad: $48.131\,879^\circ$ N, $31.816\,406^\circ$ E

• Reference location in Ternopil: 49.878118°N, 25.464478°E

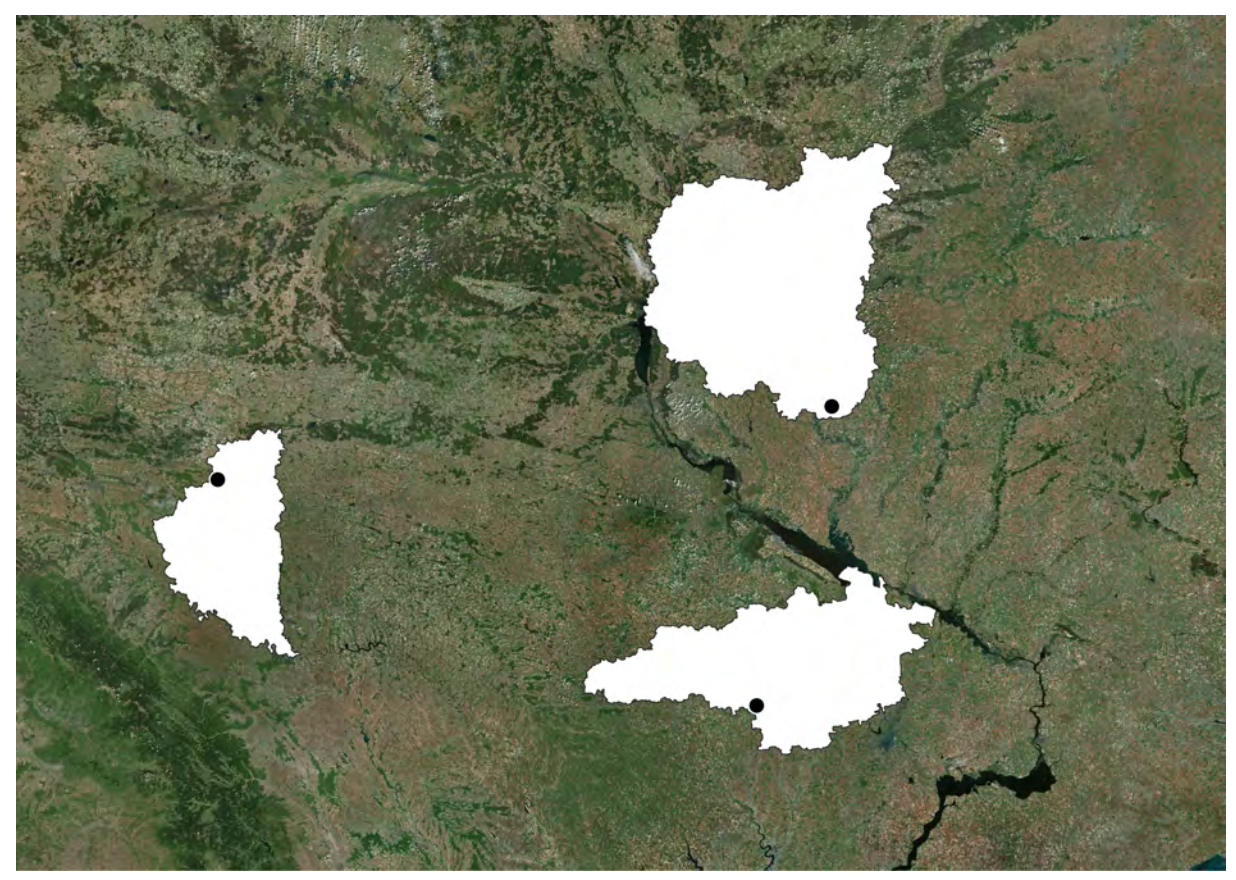


Figure 4: Reference locations shown as black dots.

2.2 Wind Characteristics

All of the wind characteristics described in this section can be obtained from the Global Wind Atlas [3] and the industry-standard software WAsP 12.9 (Wind Atlas Analysis and Application Program) [4] for the reference locations.

The Generalized Wind Climate (GWC) data was obtained from the Global Wind Atlas (GWA), introduced into WAsP, and used to calculate a Predicted Wind Climate (PWC) for the three locations mentioned above.

2.2.1 Wind Direction Frequency Distribution

The wind direction frequency distributions at 100 m AGL are shown in Figure 5. The wind rose for the reference location in Chernihiv appears largely omnidirectional; however, the southern (S) direction emerges as predominant. In Kirovohrad, the prevailing wind spans a broad sector from north-northwest (NNW) to east-northeast (ENE). Meanwhile, Ternopil exhibits two dominant

wind sectors: one from west (W) to west-northwest (WNW), centered around 300°, and another from south-southeast (SSE) to south (S), centered near 150°.

2.2.2 Wind Speed Frequency Distribution

The wind speed frequency distributions at 100 m AGL for the three locations are shown in Figure 5 as Weibull curves. Several wind characteristics indicated in the graphs are also summarised in Table 1, such as the estimated Weibull parameters, A, and k; the estimated mean wind speed; the estimated mean wind power density; and the estimated air density. The air density is calculated by WAsP using the parameters mean temperature, mean pressure and mean humidity obtained from the Global Wind Atlas for each location.

Table 1: Main wind parameters onshore for the three regions of interest at 100 m. Data obtained from GWA.

Parameter	Chernihiv	Kirovohrad	Ternopil
Mean Wind Power Density	401 W/m²	427 W/m²	429 W/m²
Mean Wind Speed	7.62 m/s	7.73 m/s	7.63 m/s
Mean Weibull Shape Factor	2.71	2.58	2.39
Mean Weibull Scale Factor	8.6 m/s	8.7 m/s	8.6 m/s
Mean Air Density	1.214 kg/m ³	1.200 kg/m ³	1.186 kg/m ³

2.2.3 Monthly Variability of Wind Speed

All three areas mentioned previously present similar intra-annual variations of mean wind speed. There is a significant monthly variability of wind potential with a low wind season from May to September and a peak windy period from November to March, as shown in Figure 6.

2.3 Summary

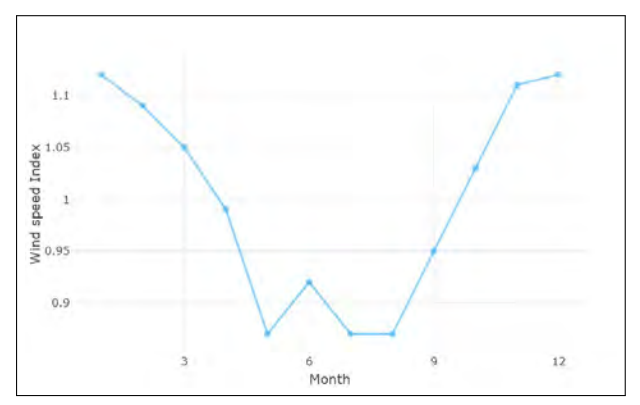
The main wind characteristics of reference locations of Chernihiv, Kirovohrad and Ternopil have been obtained from the GWA and presented here. This data can be used for preliminary estimation of wind generation in the regions of interest, although the uncertainties of the wind characteristics might be as high as around 20%.

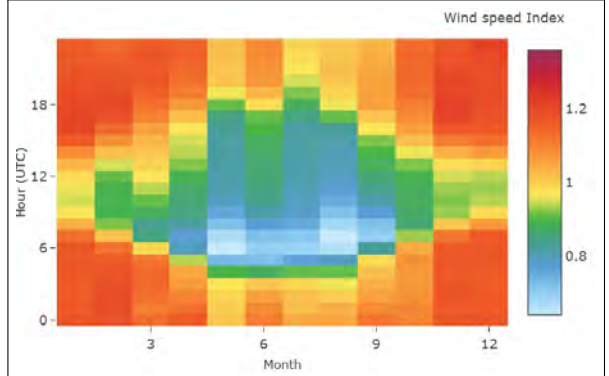
According to the IEC 61400-1 classification and based on the parameters described in this report, wind turbines with IEC class III shall most probably be suitable for the three provinces.



Figure 5: Wind direction frequency distributions (left) and wind speed frequency distributions (right) at 100 m AGL for the reference locations.

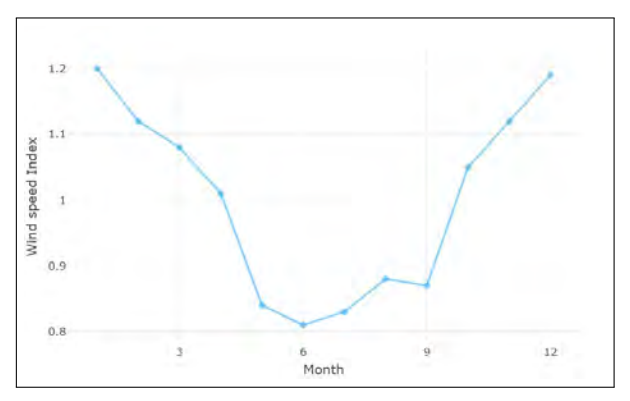
8

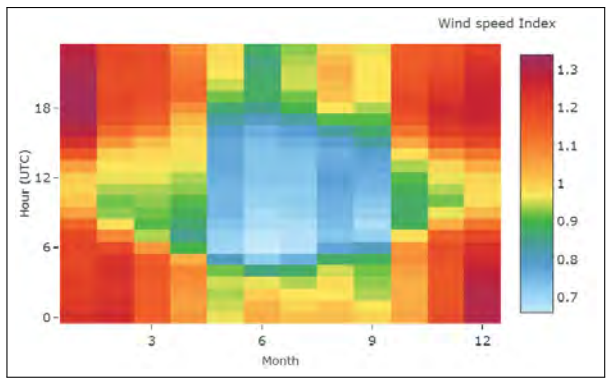




(a) Chernihiv: Monthly variability of mean wind speed index at 100 m AGL.

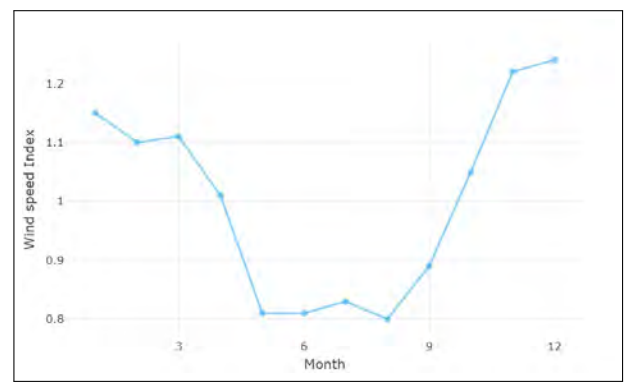
(b) Chernihiv: Variability of the wind speed index over the month and hour of day at 100 m AGL.

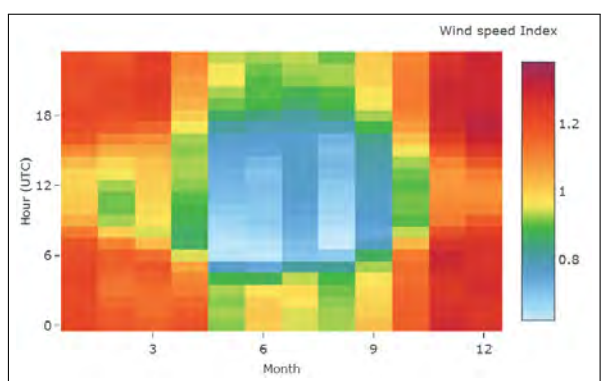




(c) Kirovohrad: Monthly variability of mean wind speed index at 100 m AGL.

(d) Kirovohrad: Variability of the wind speed index over the month and hour of day at 100 m AGL.





(e) Ternopil: Monthly variability of mean wind speed index at 100 m AGL.

(f) Ternopil: Variability of the wind speed index over the month and hour of day at 100 m AGL.

Figure 6: Monthly variability of mean wind index (left) and variability of the wind speed index over the month of year and hour of day (right) at 100 m AGL for the reference locations. Data and graphs from the GWA.

3 Geospatial Analysis

This section outlines the spatial GIS analysis conducted to incorporate various spatial constraints, including environmental impact mitigation, into our early-stage pre-feasibility assessments. However, it is important to emphasize that a full Environmental Impact Assessment (EIA) lies beyond the scope of this study.

QGIS, a free and open-source geographic information system application, was used to create a GIS workspace that incorporates relevant data from publicly available sources and site-specific information from three key regions of Ukraine: Chernihiv, Kirovohrad, and Ternopil. A set of criteria has been used to determine the most suitable areas for developing onshore wind projects.

While the list of constraints in this report is not exhaustive, it includes the most important layers of information related to potential environmental and social impacts. The analysis method described below can be extended in future updates or studies to include additional relevant spatial constraints.

3.1 Site Selection Criteria

Several criteria may be taken into account for site selection, ranging from wind resource and environmental restrictions to available infrastructure and commercial interests, the relevance of them depending on site-specific and project-specific conditions. The criteria described in this section were based on a combination of experience from previous projects and interaction with project stakeholders. The same set of criteria was applied to all provinces.

3.1.1 Wind Energy Potential

The first step of the geospatial analysis is to select the zones with the best wind resources inside the area of interest, i.e. the provinces. Considering the wind characteristics described in section 2.1, the "Capacity Factor for IEC Class III" layer was selected from the GWA as an adequate representation of wind energy potential, see Figure 3a. Then a mask was applied to include only areas with Capacity Factor (CF) greater than or equal to 45%. The Figure 7 illustrates the selected areas for the three provinces.

Similarly to the Capacity Factor analysis, the "IEC Class - Fatigue Loads" layer from the GWA was selected to identify suitable areas for IEC Class III wind turbines based on wind speed and turbulence parameters. The accepted turbulence categories include A+, A, B, and C.

3.1.2 Environmental Protected Areas

The second step in the geospatial analysis is to identify areas where wind farms cannot be built. Several layers help us exclude locations unsuitable for wind turbines. This subsection focuses on the Environmental Protected Areas within the three regions of interest.

These areas were identified using publicly available data from Protected Planet [5]. After discussions with the Ukrainian stakeholders, including the Ukrainian Wind Energy Association (UWEA), it was decided that a 1 km buffer zone would be applied to these protected areas,

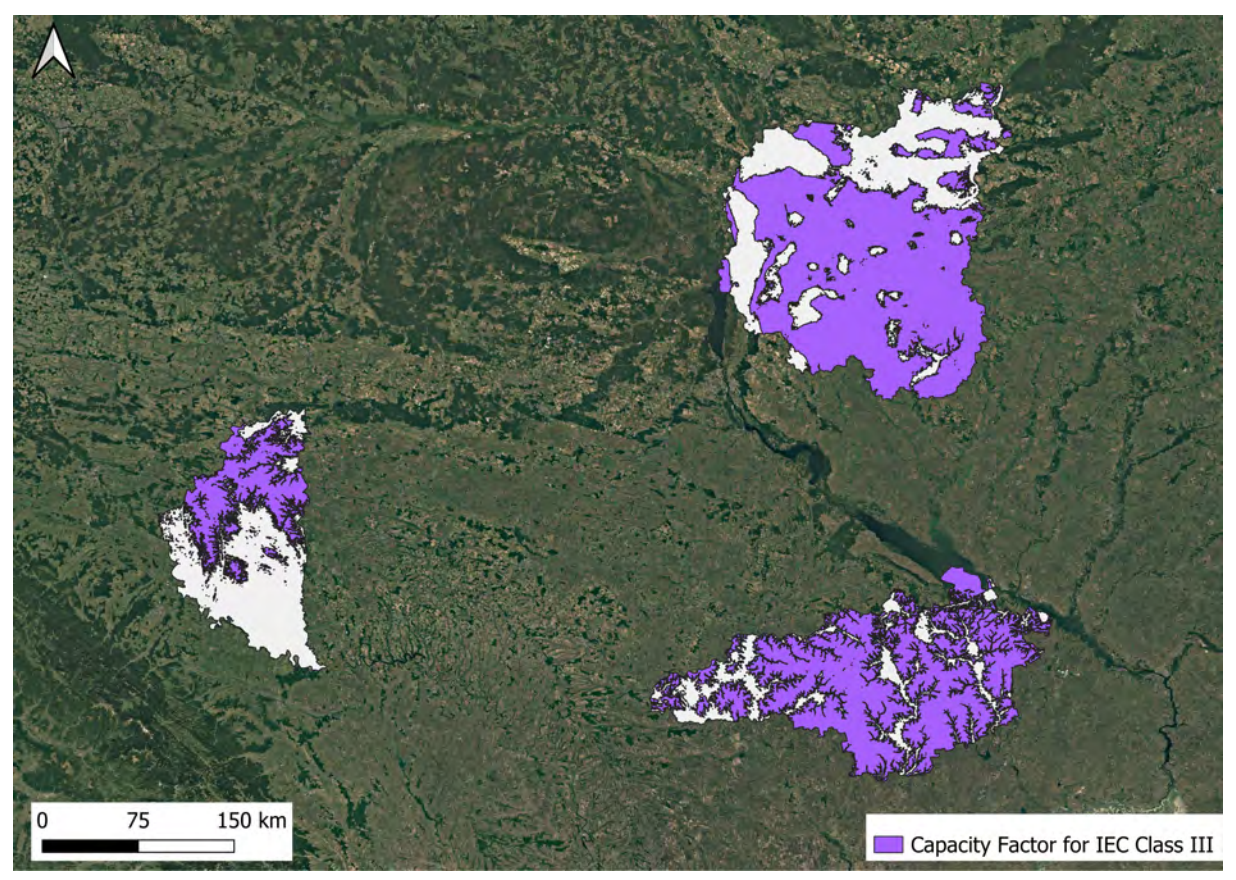


Figure 7: Areas showing capacity factor ≥ 45% for Chernihiv, Kirovohrad, and Ternopil [1].

in accordance with Moskalchuk, N. M., and Adamenko, Ya. O. (2019) [6]. Figure 8 illustrates the protected areas for the three provinces including a buffer zone of 1km.

3.1.3 Roads

Roads are also excluded from the areas considered suitable for installing wind farms. The data was sourced from the GRIP Dataset [7], and a buffer equivalent to the hub height plus rotor radius of the selected wind turbine model was applied, following the recommendations of the Ukrainian Wind Energy Association (UWEA). Figure 9 illustrates the roads within the three provinces of interest, including a buffer zone of 195m, representing the hub height plus rotor radius of the selected wind turbine, which is presented in detail in subsection 4.1.4.

3.1.4 Railways

Similarly to roads, railways were also excluded from the analysis. Data were obtained from a source provided by the Ukrainian Wind Energy Association (UWEA), which is called MegaObzor [8].

To generate the necessary GIS data, the information from this source was combined with Google Earth [9] and a hand-digitized map of the railways was created. A buffer equivalent to the hub height plus rotor radius of the selected wind turbine model was applied, in line with the recommendations of UWEA. Figure 10 illustrates the railways within the three provinces of interest, including a buffer zone of 195m, representing the hub height plus rotor radius of the selected wind turbine, which is presented in detail in subsection 4.1.4.

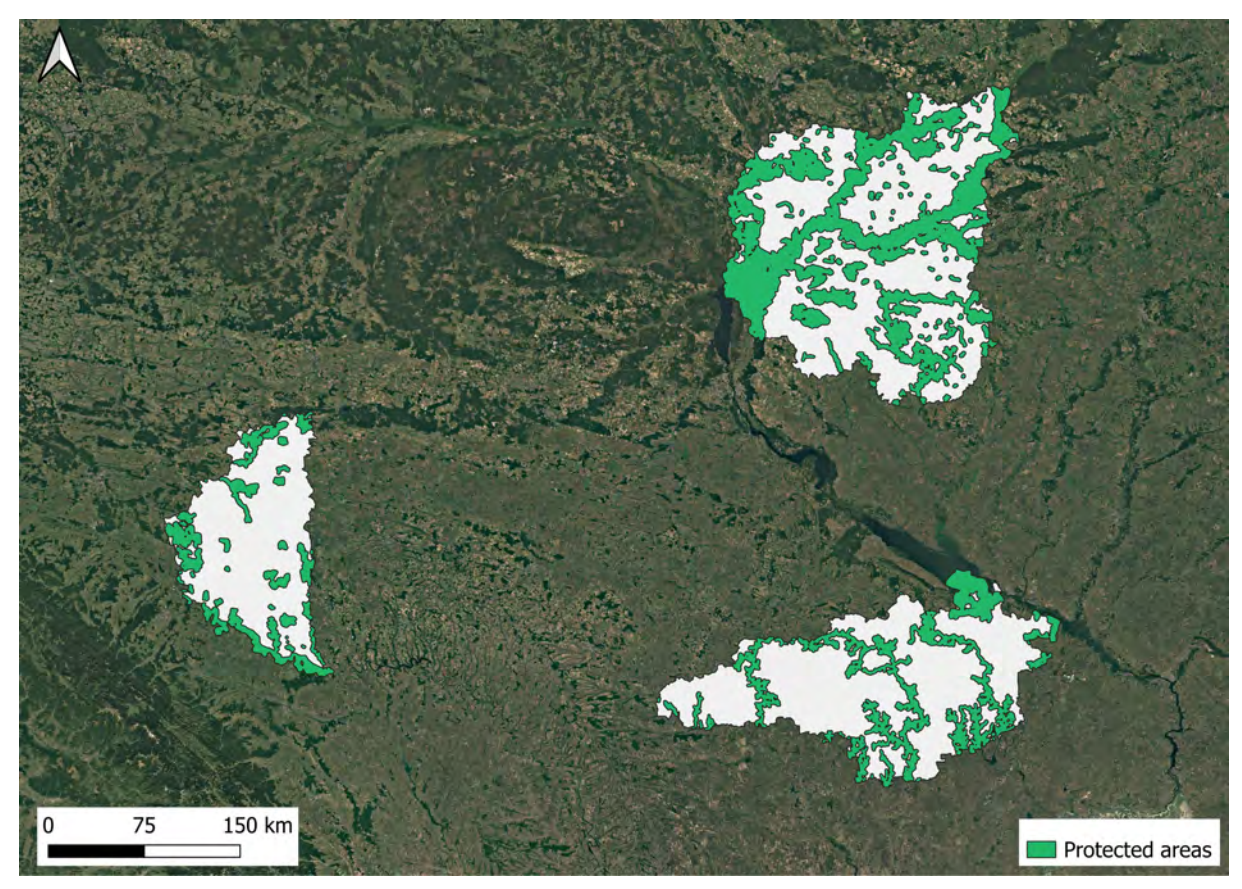


Figure 8: Protected areas for Chernihiv, Kirovohrad and Ternopil. [5]

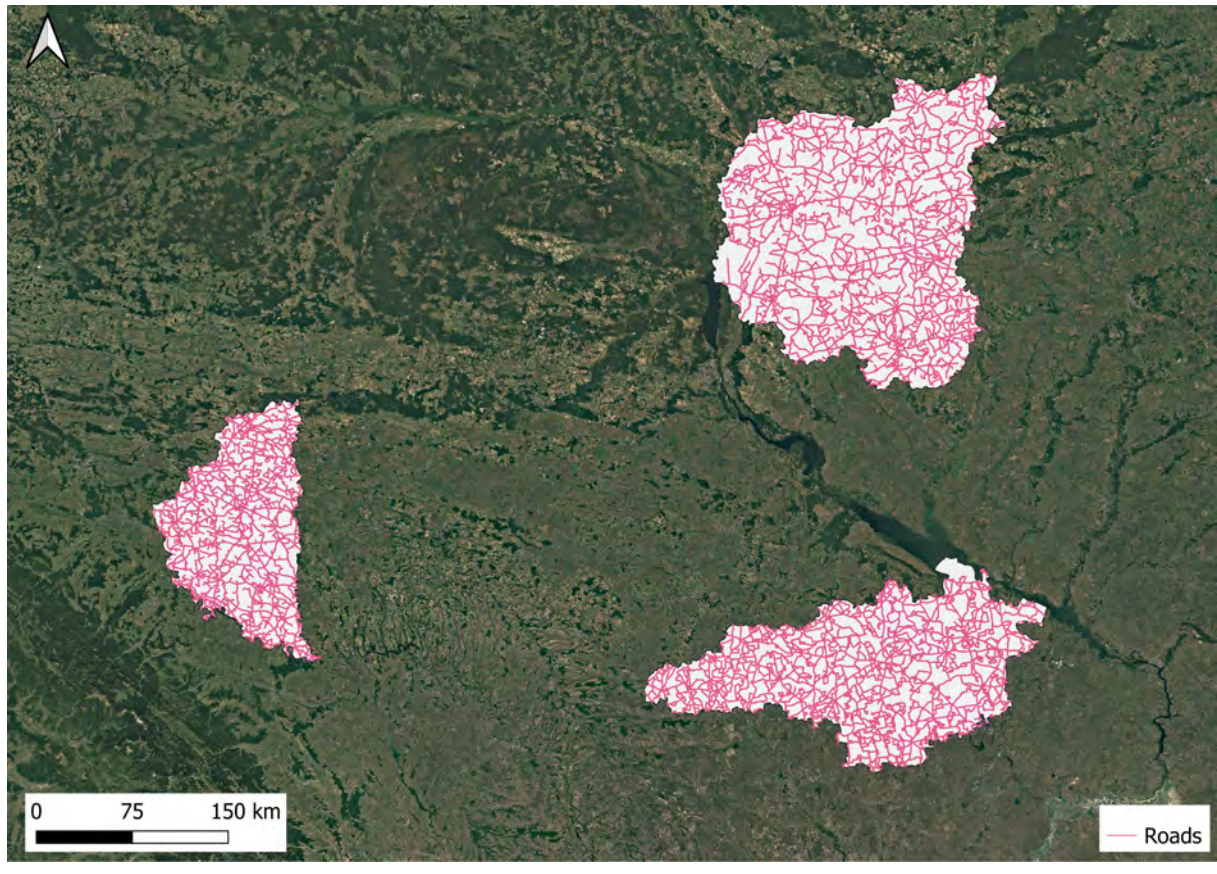


Figure 9: Roads for Chernihiv, Kirovohrad and Ternopil. [7]

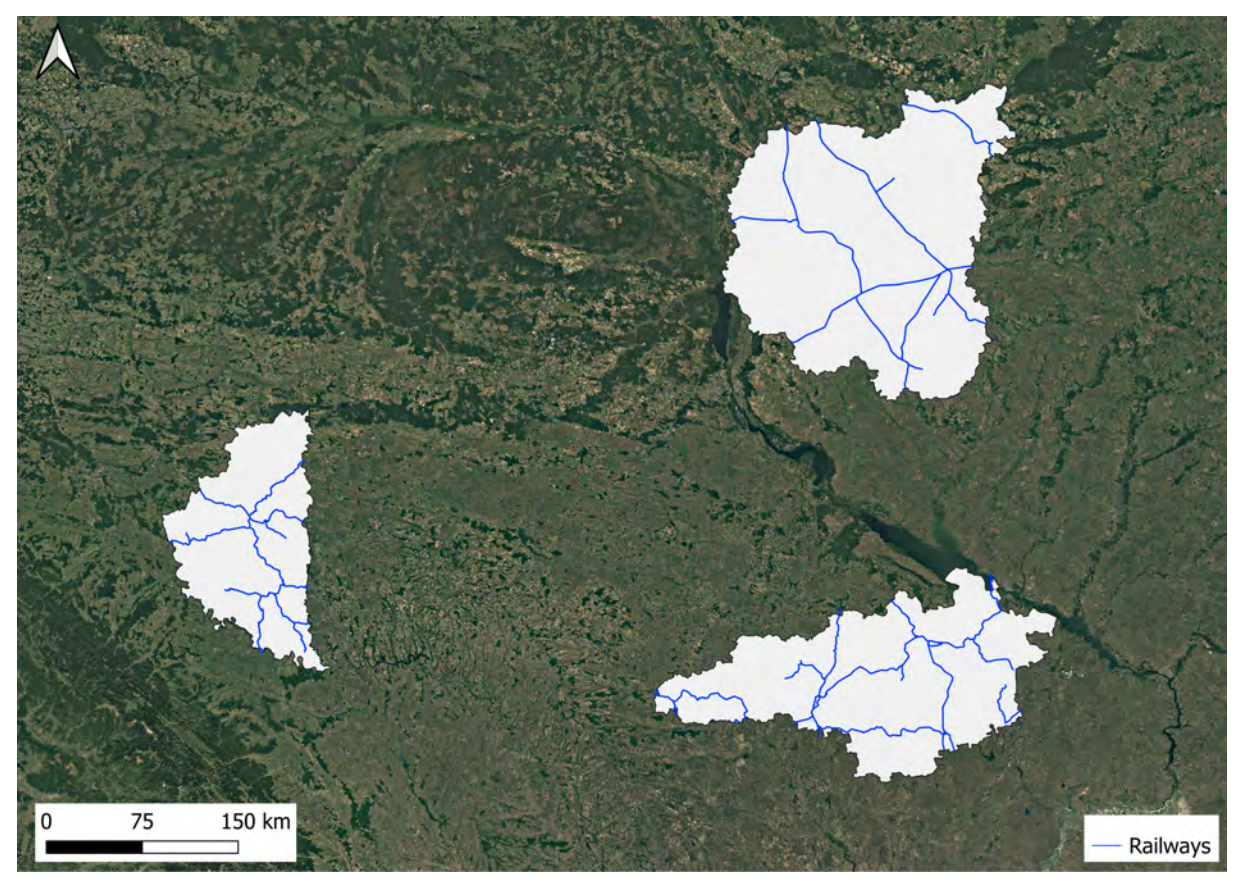


Figure 10: Railways for Chernihiv, Kirovohrad, and Ternopil. [8] [9]

3.1.5 Airports

Airports represent another restriction applied to our study area. Data was sourced from Open-Flights [10]. The Ukrainian Wind Energy Association (UWEA) recommended a buffer of 20 km from both ends of the runway and 20 km on each side, forming an elongated ellipse. However, since most airports have multiple runways, which may intersect or overlap, it was decided to apply a simplified buffer with a 22 km radius centered on each airport.

Figure 11 illustrates the airports for the three provinces, including a buffer zone with a 22km radius centered on each airport.

3.1.6 Aspects of Land Use

In this study, some land cover classes are also considered restrictions. Residential areas classified as Buildings, permanent water bodies (lakes, rivers, reservoirs, etc.), grouped as Water, and herbaceous wetlands, simply called Wetland, are all exclusion zones.

Data were sourced from ESA WorldCover [11]. It is worth mentioning that those GIS raster layers were originally downloaded from ESA WorldCover as rectangular areas of 3 degrees by 3 degrees (216.63 km by 333.58 km) with a spatial resolution of 36000 tiles by 36000 tiles. However, in order to reduce the computational time to handle these files, the spatial resolution was reduced to 3600 tiles by 3600 tiles as the elements of land cover still appeared sufficiently detailed on the map.

From discussions with the project stakeholders and in accordance with Moskalchuk, N. M., and

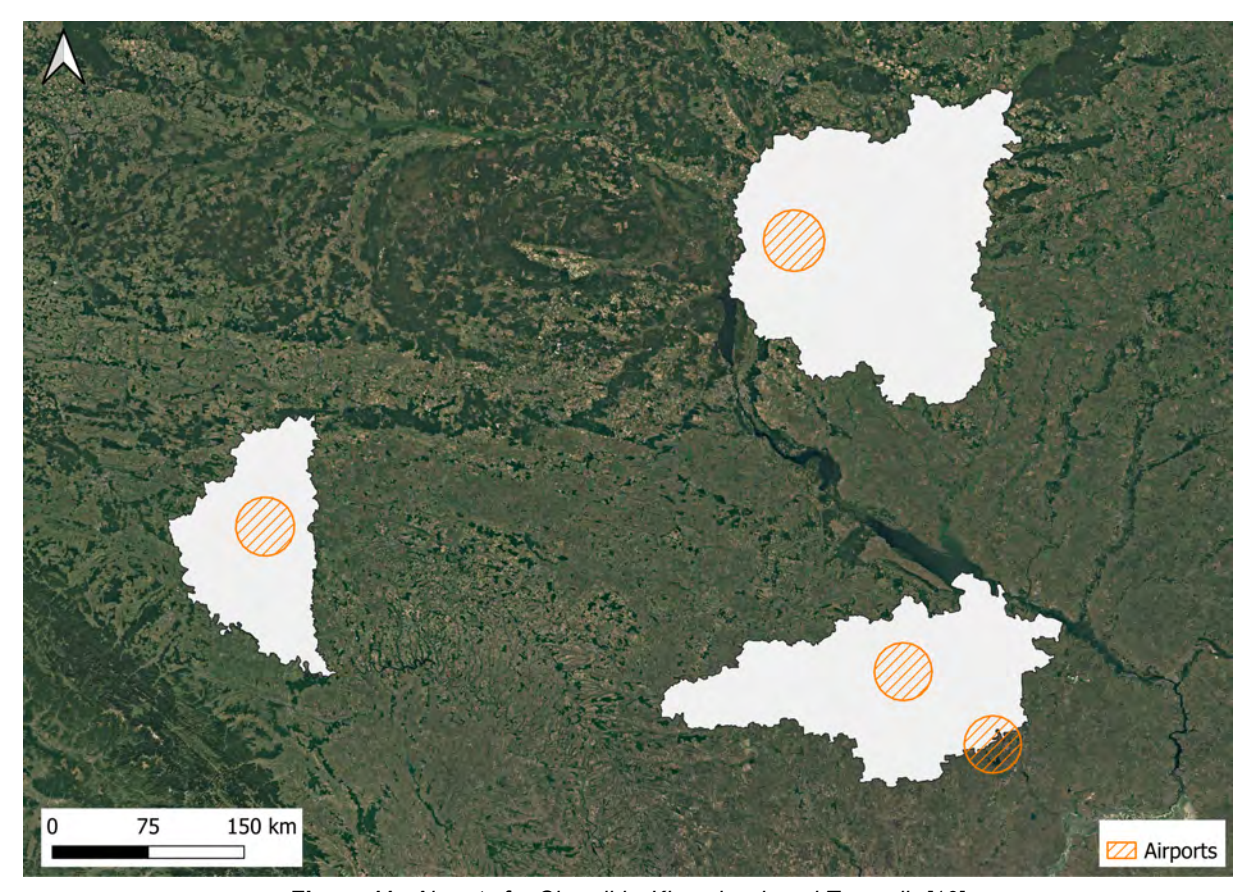


Figure 11: Airports for Chernihiv, Kirovohrad, and Ternopil. [10]

Adamenko, Ya. O. (2019) [6], we decided to select areas with a minimum distance of 1 km from the excluded landcover classes. Therefore, all exclusion zones have a 1 km buffer from their borders. Figure 12 illustrates the areas to be excluded due to the restrictions "Buildings", "Water" and "Wetland" including the 1 km buffer from their borders.

3.1.7 Other Restrictions

The following additional potential constraints were ignored in this study: terrain slope, high-risk areas, energy and electricity infrastructure, bird migration routes, and world heritage sites.

Terrain slope

Steep slopes can pose significant challenges when installing wind turbines and could be considered a restriction in some cases. However, the terrain slope is not included in the present analysis due to the lack of sufficiently accurate data. In addition, the available sources of orography - the GWA maps - indicated insignificant slopes in the areas of interest.

High-risk areas

High-risk areas, such as those experiencing ongoing military conflict and instability, were not considered in this study due to the lack of GIS data.

Energy infrastructure

The energy and electricity infrastructure was not considered in the analysis due to insufficient high-quality GIS data. However, a few sources of information such as ATOM [12], Energo [13] and the Nature Reserve Fund of Ukraine [14] provided inputs for the study. For example, it was

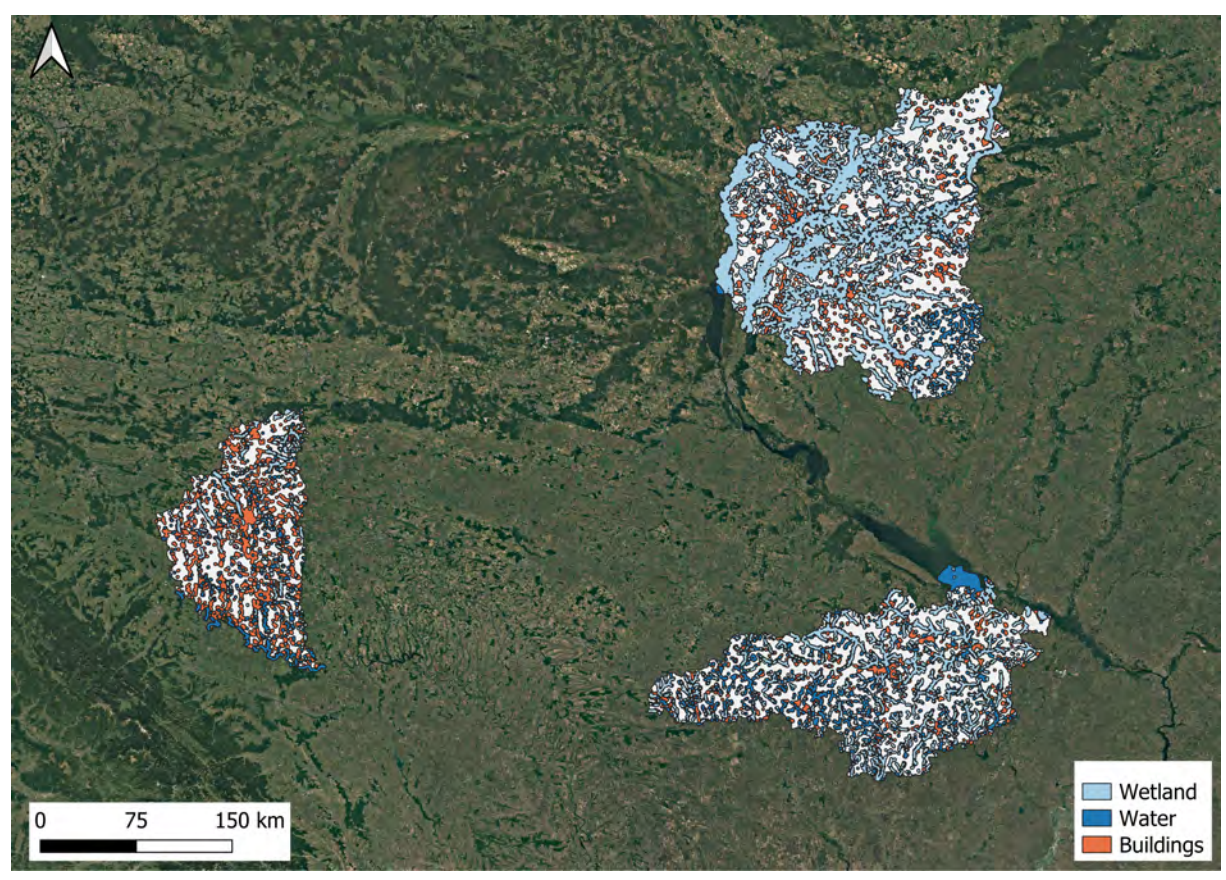


Figure 12: Exclusion areas due to the restrictions "Buildings", "Water" and "Wetland" for Chernihiv, Kirovohrad, and Ternopil. [11]

checked that the area around large conventional power plants have been excluded because most of them are located near rivers, water bodies, or other buildings, three elements that were defined as exclusion zones with a relatively large buffer.

Bird migration routes

The information about bird migration routes provided by the project stakeholders, including Pernati Druzi [15], consists of maps based on bird banding, findings of deceased birds, and GPS tracking within Ukraine. Given the inherent challenges in banding all bird species, it is crucial to assess the presence of migratory corridors at specific project locations. Furthermore, ecologists frequently observe local bird populations, including focal species such as raptors and waterfowl, that may choose not to migrate due to factors such as climate change and an adequate food supply. It is also worth highlighting that migration corridors can shift every five years and have been significantly altered by recent military activities, according to the Ukrainian stakeholders. Consequently, these maps should be considered illustrative and not as definitive or restrictive evidence, as advised by the Ukrainian Wind Energy Association (UWEA). Therefore, this potential restriction is not incorporated in the present study.

World heritage sites

World heritage sites and historical settlement areas were not included in the study due to the unavailability of GIS data.

3.2 Selected Areas

A summary of the criteria described above is included in Table 2. The same set of criteria is applied to all provinces and the result is presented in Figure 13. Kirovohrad is the province with the largest selected area, a total of 7.213 km². In Chernihiv an area of 6.762 km² has been selected while a much smaller area, 1.983 km² resulted for Ternopil. These numbers represent only rough estimates of the total area suitable for the development of wind power plants. A more accurate analysis shall be done with a complete list of restrictions, with all datasets in the highest available resolution and taking into account region-specific exclusion criteria considerations.

Table 2: Summary of the area selection criteria.

OBS: CF = Capacity factor for IEC Class III. IEC Class = IEC Class - Fatigue loads.

Information	Exclusion criterium	Source
CF	CF < 45%	Global Wind Atlas [1]
IEC Class	IEC Class I, II, S	Global Wind Atlas [1]
Protected areas	all + 1km buffer	Protected Planet [5]
Roads	all + 195m buffer	GRIP Datastet [7]
Railways	all + 195m buffer	MegaObzor [8]
Airports	all + 22km radius buffer	OpenFlights [16]
Buildings	all + 1km buffer	ESA WorldCover [11]
Water	all + 1km buffer	ESA WorldCover [11]
Wetland	all + 1km buffer	ESA WorldCover [11]

Figure 14, Figure 15 and Figure 16 show the selected areas, including two additional information useful for the next steps of the study: the wind resource, represented by the Mean Wind Power Density (WPD) at 100 m, and the electrical grid, illustrated by power lines greater than or equal to 11 kV obtained from Open Infrastructure Map [17].

3.3 Wind Power Potential

Preliminary estimates of the wind power potential for each province are presented based on the following procedure and assumptions:

- 1. Wind farms are to be installed in the windy areas of the province. Windy areas are a subgroup of the selected areas (see section 3.2) in which the mean wind power density is greater than or equal to a certain value.
- 2. The total wind power installed capacity is the result of multiplying the windy areas by a pre-defined capacity density, e.g. 2.25 MW/km².
- 3. The wake effect is estimated from the previous parameters (area, capacity density) using the simulation results of large wind farm clusters [18].
- 4. The capacity factor is estimated based on Global Wind Atlas data (capacity factor for a specific IEC Class), averaged for each mean wind power density and reduced from the wake effects calculated in the previous step.

Chernihiv

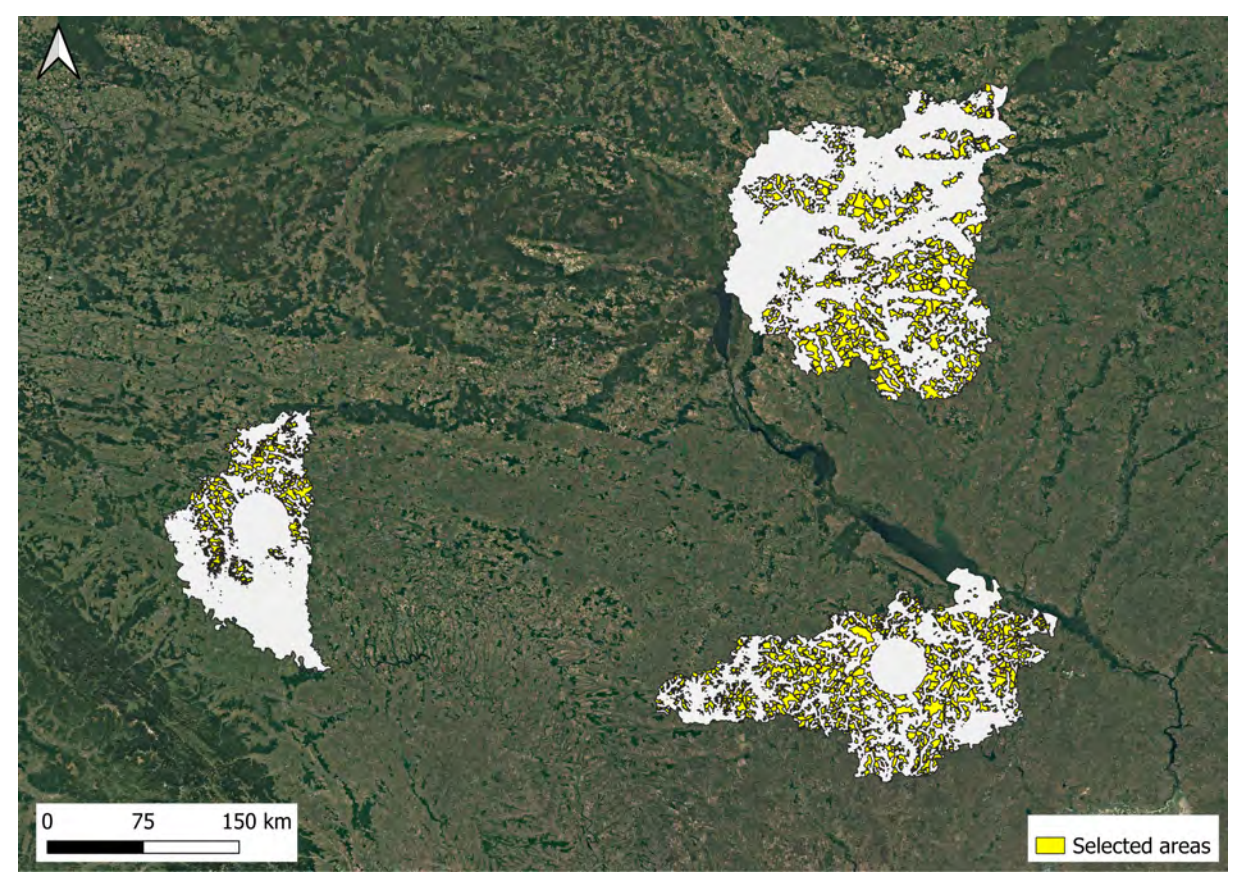


Figure 13: Final result: selected areas for Chernihiv, Kirovohrad, and Ternopil.

Assuming a mean wind power density threshold of 360 W/m^2 , a total area of 1.850 km^2 is selected. The estimated total installed capacity would be 4.180 MW considering a capacity density of 2.25 MW/km^2 . This configuration might create wake effects of approximately 10% resulting in potential capacity factors of 48% to 50%.

Kirovohrad

If the mean wind power density threshold is defined as $375~\text{W/m}^2$, a total area of $2.180~\text{km}^2$ is selected. The estimated total installed capacity would be 4.900~MW considering a capacity density of $2.25~\text{MW/km}^2$. This configuration might create wake effects of approximately 10% resulting in potential capacity factors of 46.7% to 48%.

Ternopil

In Ternopil, an area equivalent to 620 km² has mean wind power densities greater than or equal to 400 W/m². The estimated installed capacity in this area would be 1.395 MW considering the same capacity density (2.25 MW/km²). This configuration might create wake effects of approximately 10% resulting in potential capacity factors of 46% to 47.7%.

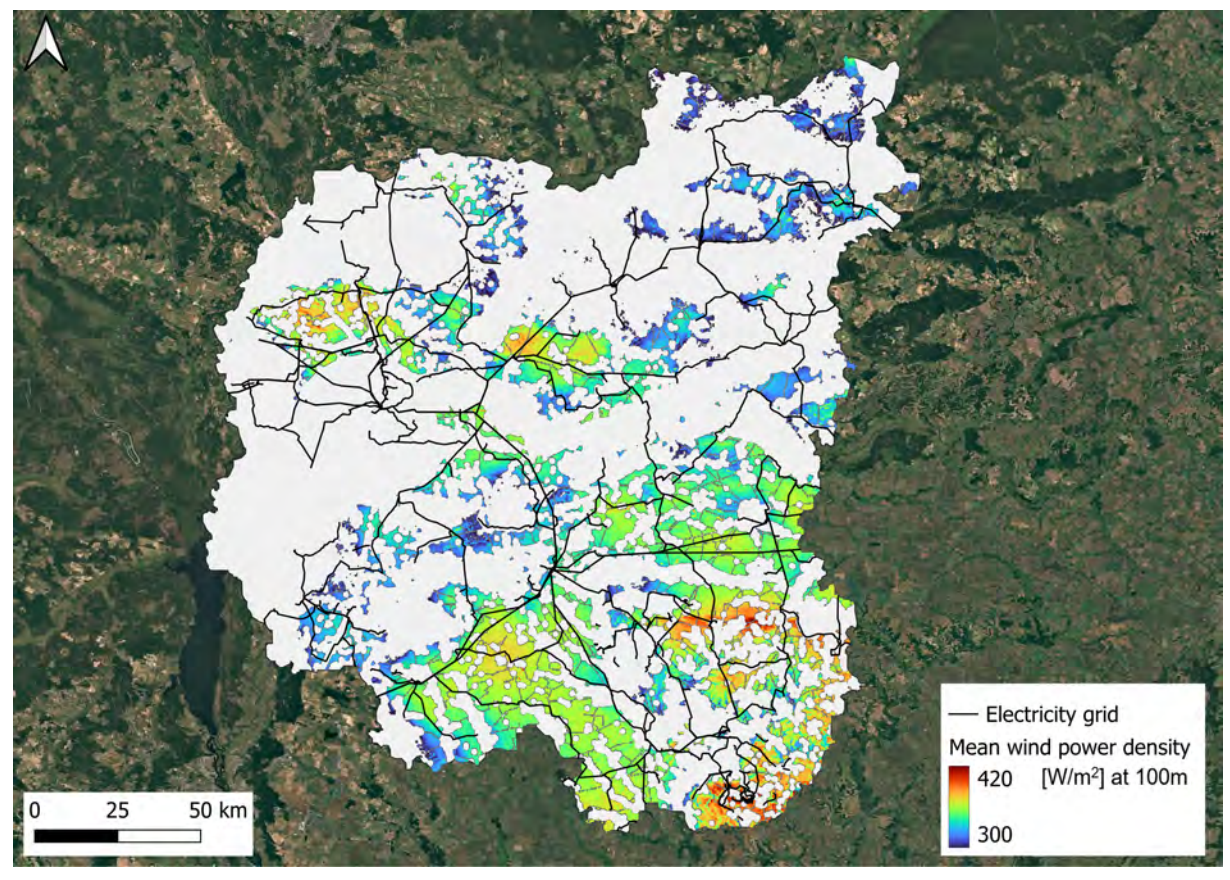


Figure 14: Selected areas for Chernihiv showing wind power density and electricity grid

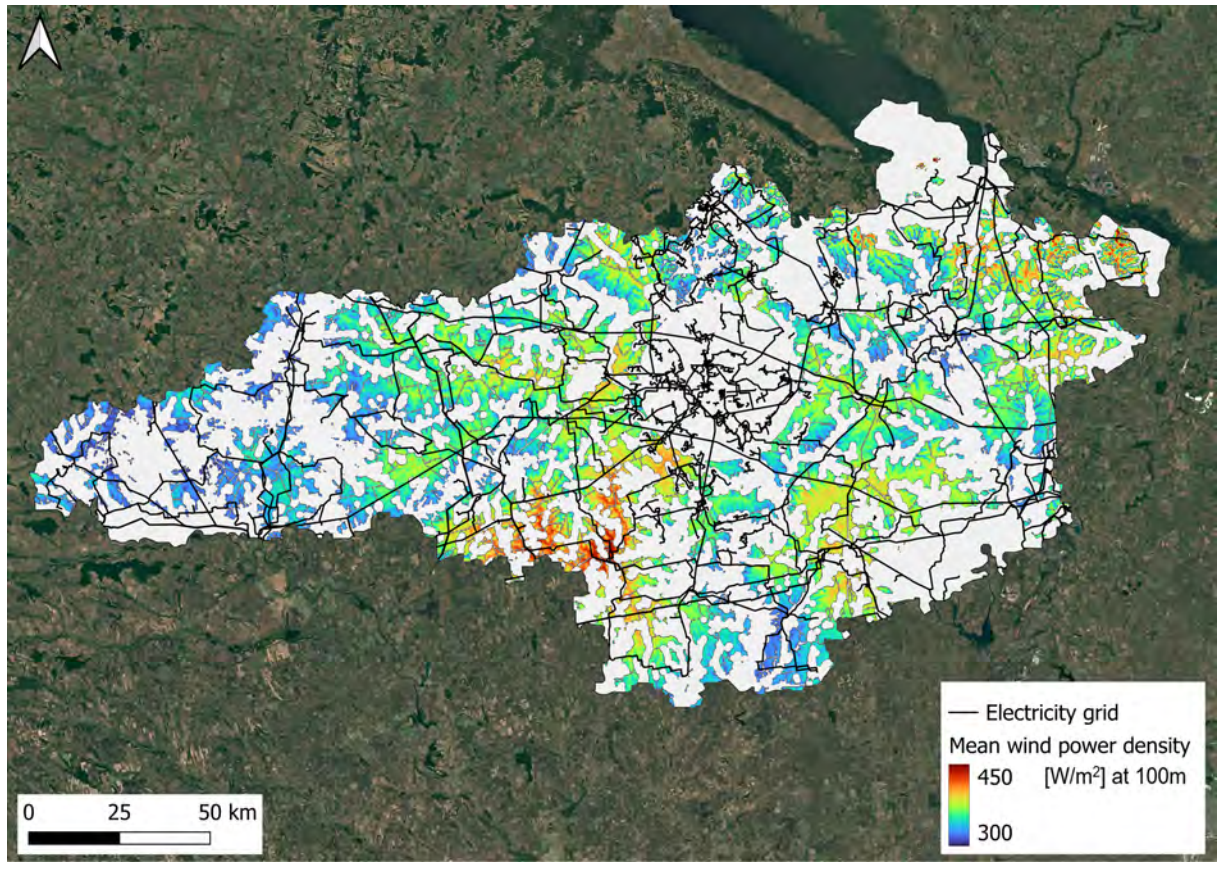


Figure 15: Selected areas for Kirovohrad showing wind power density and electricity grid

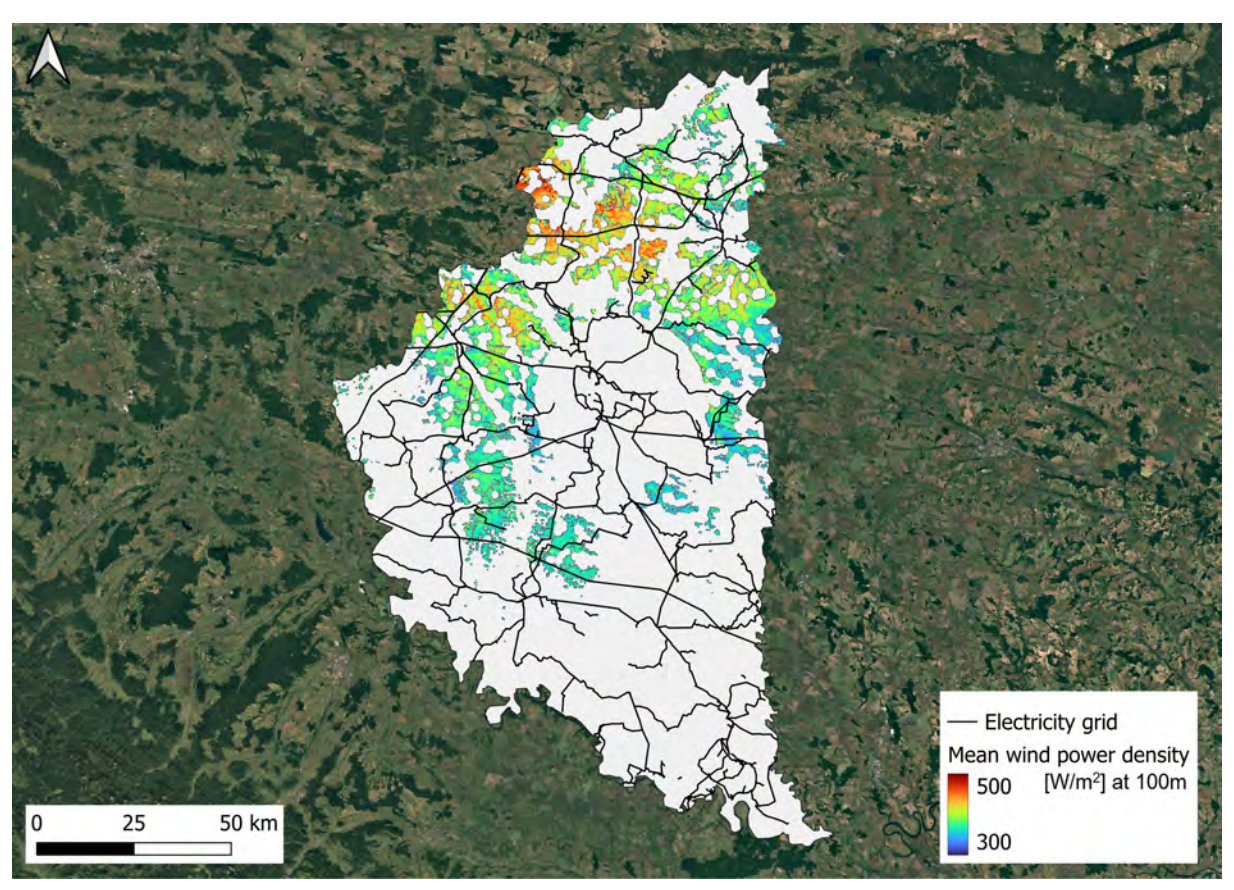


Figure 16: Selected areas for Ternopil showing wind power density and electricity grid

4 Energy Yield Assessment

This chapter describes the basic design of three 250 MW hypothetical wind farms in Ukraine. The primary objective is to estimate the energy yield, employing the best practices, tools and data for a preliminary analysis. The site locations are defined within the designated available areas shown in chapter 3 using primarily the wind resource information.

The Global Wind Atlas is the main data source for digital maps and wind climate data. The models of the software WAsP 12.9 (Wind Atlas Analysis and Application Program) [4], are used to estimate the long-term mean annual energy production. The data, models, and parameters used in the calculations are described below.

4.1 Inputs

4.1.1 Site Locations

Three sites have been selected, one in each of the three provinces, for the development of hypothetical wind farms. The common characteristics of the sites are good wind resources, proximity to the grid (110 kV substations at a distance of 20-30km), and areas consisting primarily of farmland with very few buildings or trees. Figure 17 shows the site locations (red rectangles) for each province. The first wind farm site is located in the southern part of Chernihiv. The second wind farm site is located in the center-south of Kirovohrad. The third wind farm site is located in the northern part of Ternopil with the most favourable wind resources.

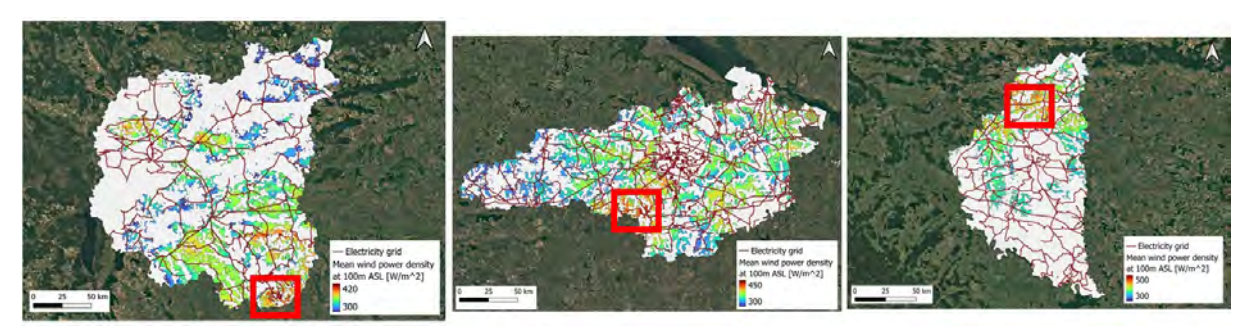


Figure 17: Site locations for the hypothetical wind farms.

4.1.2 Digital Maps

The digital maps (including surface roughness and terrain elevation) for the site locations are downloaded from the GWA Map Warehouse using QGIS. For the elevation, a 10 m interval is chosen for the height contour lines. According to WAsP best practices, the elevation map should extend at least several (2-3) times the horizontal scale of significant terrain features from any mast or wind turbine position, typically 5-10 kilometres. The roughness map should extend at least $\max(150 \times h, 10 \text{km})$, where h is the turbine hub height, which translates to 17 kilometres considering the hub height of 113 m.

The digital maps adopt the UTM coordinate system based on the WGS-84 datum (zone 35 and 36 for Ukraine) and are shown in Appendix A.1.

4.1.3 Wind Data

The Global Wind Atlas (GWA) version 3.4 provides Generalised Wind Climate (GWC) data for any location in the world within 200 km from coastlines. The concept of a generalised wind climate, a key element of the Wind Atlas methodology developed at DTU Wind and fully explained in the European Wind Atlas [19], has been used in numerical wind atlas methodologies, where mesoscale modelling output is generalised before being applied in WAsP microscale modelling.

As explained in chapter 2, the present study relies on the GWA for wind data due to the absence of high-quality energy-specific wind measurements in the areas of interest. In wind power development, the GWA data is predominantly applied during the exploration phase and the preliminary stages of wind resource assessment before on-site meteorological measurement stations are deployed. It is important to note that relying solely on GWA data does not meet the requirements of investors and stakeholders for bankable wind resource assessment and site assessment, including e.g. specific siting of wind turbines and wind farms.

The current GWA version 3.4 uses large-scale wind climate data provided by atmospheric reanalysis data, available from ERA5 dataset for the period 2008-2017 [3]. The generalised wind climate file, used as input in the present study, contains the sector-wise frequency of occurrence of the wind (the wind rose) and the wind speed frequency distributions in the same sectors (as Weibull A- and k-parameters, seen in chapter 2). This information is a generalised site-independent description of the wind climate in a certain area.

DTU has adopted the procedure of downloading one GWC data file for each of the turbine positions to ensure that the spatial variation of the wind conditions in the area due to mesoscale effects would be included in the analysis. The air density was also calculated for each wind turbine position using the meteorological information obtained from the GWC data.

4.1.4 Wind Turbine

The wind turbine selection focused on shortlisting current commercial models which present a combination of the following requirements: 1) IEC Class III design and certification; 2) availability of a tested power curve; 3) nominal capacity greater than 4 MW; 4) hub height above 100 m; 5) proven track record.

A commercial wind turbine rated at 4.5 MW, with a hub height of 113 m and a 163 m rotor diameter has been selected for this study. Its main characteristics are presented in Table 3 and Figure 18. The wind turbine power curve is the blue curve in the figure and the thrust coefficient (C_t) curve is depicted as a gray curve using a secondary Y-axis (right).

Each hypothetical wind farm is composed of 55 wind turbines with a total installed capacity of 247.5 MW (55 x 4.5MW), approximately 250 MW.

4.2 Wind Farm Calculations

4.2.1 Wind Flow Modeling

The WAsP software utilises the IBZ flow model, derived from the BZ model of Troen [20], to calculate the wind velocity perturbations induced by orographic features such as single hills or

Table 3: Basic specifications for the 4.5 MW wind turbine used in the study.

Parameter	Value
Rated power	4.5 MW
Hub height	113.0 m
Rotor diameter	163.0 m
Cut-in wind speed	3.0 m/s
Rated wind speed	11.5 m/s
Cut-out wind speed	24.0 m/s
IEC Class	III and S
Power control	pitch

more complex terrain. The IBZ model was developed with the specific purpose of detailed wind energy siting in mind and has the following general features:

- It employs a high-resolution, zooming, polar grid (with the centre point located at a selected point of interest). The polar grid has 72 rays separated by 5° and 100 radial stations on each ray with each radial interval 6% larger than the previous interval). This is coupled with a map analysis routine to calculate the potential flow perturbation profile at the central point of the model.
- It integrates the roughness conditions of the terrain surface into the spectral or scale decomposition. The inner-layer structure is calculated using a balance condition between surface stress, advection, and the pressure gradient.
- It uses an atmospheric boundary layer thickness of approximately 1 km to force the largescale (say, more than a few kilometres) flow around high-elevation areas.

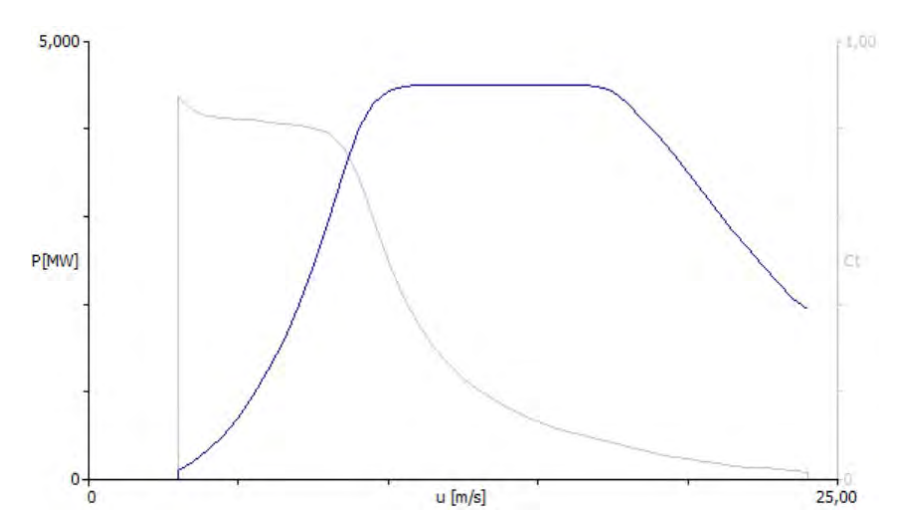


Figure 18: Power and thrust coefficient curves for modelling the wind turbine in WAsP.

The recommended operational envelope of the WAsP model corresponds to terrain slopes up to about 0.3. Given the location of the sites and the clear absence of challenging land features in the vicinity of the wind farms, the use of WAsP is considered suitable.

4.2.2 Wake Model

WAsP includes the PARK2 wake model to consider internal wake losses from one wind turbine to another within a wind farm. The PARK2 wake model has been calibrated and validated against production data from several wind farms at different conditions [21]. In this study, the PARK2 model was configured with the wake decay constant of 0.09.

4.2.3 Wind Farm Layouts

For each site location, red rectangles in Figure 17, the procedure for area selection described in chapter 3 was repeated with landcover data in high resolution. The objective is to guarantee that all restrictions (Buildings, Water and Wetland) are excluded while the recalculation is applied only to the site locations to optimise computational resources. Read more about the landcover resolution reduction in subsection 3.1.6.

The siting of 55 wind turbines for each wind farm - the wind farm layout - was carried out using an optimization procedure that aimed at maximising the energy yield. The wind farm layouts, are presented in Figure 19, Figure 20 and Figure 21 for Chernihiv, Kirovohrad and Ternopil respectively. The different layouts are the result of the optimization considering the following variables/conditions: the boundaries of the selected areas (shown in the figures), the various wind direction frequencies (or wind roses) in each location (wind data obtained from GWA), the site-specific topographic features (digital maps of elevation and roughness), and the technical characteristics of the wind turbine.

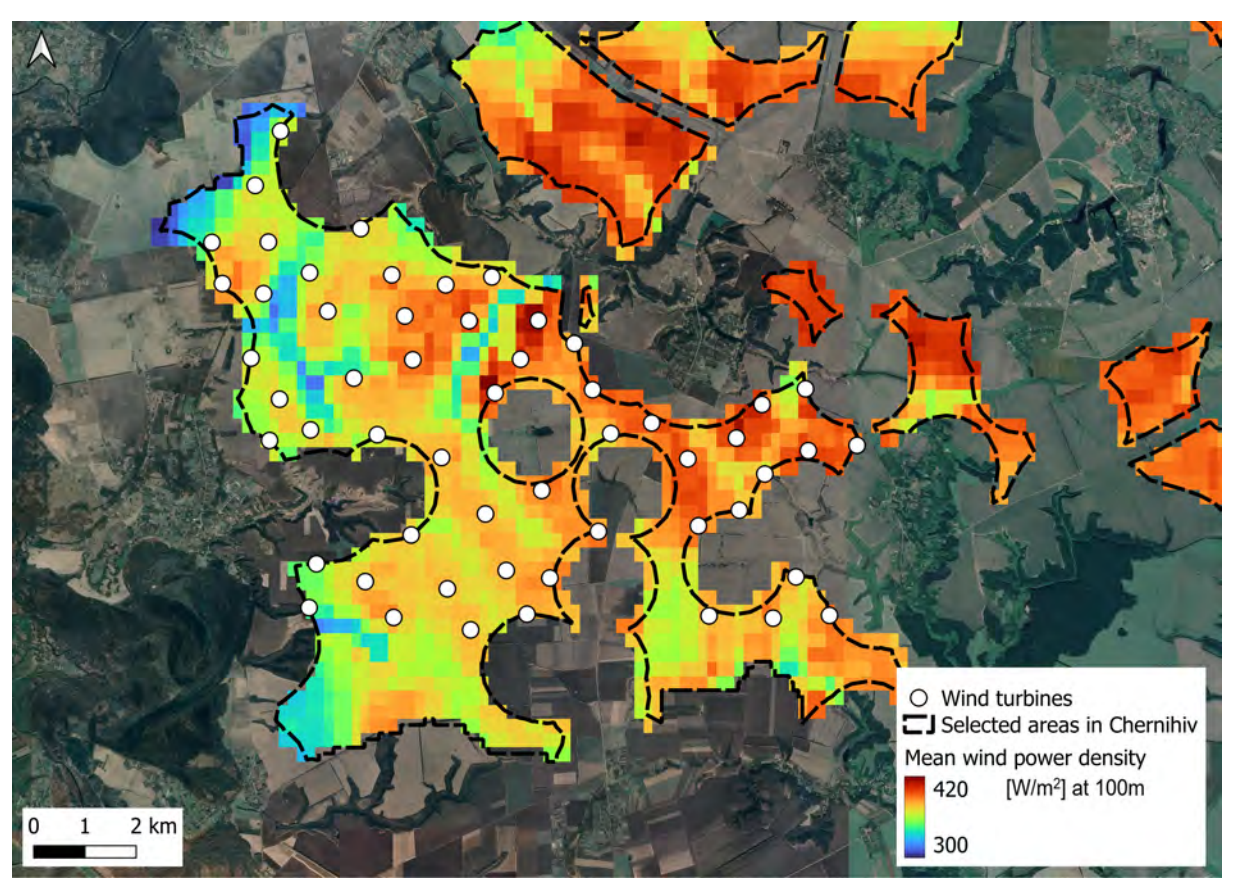


Figure 19: Map showing the Chernihiv site location and layout of the hypothetical wind farm.

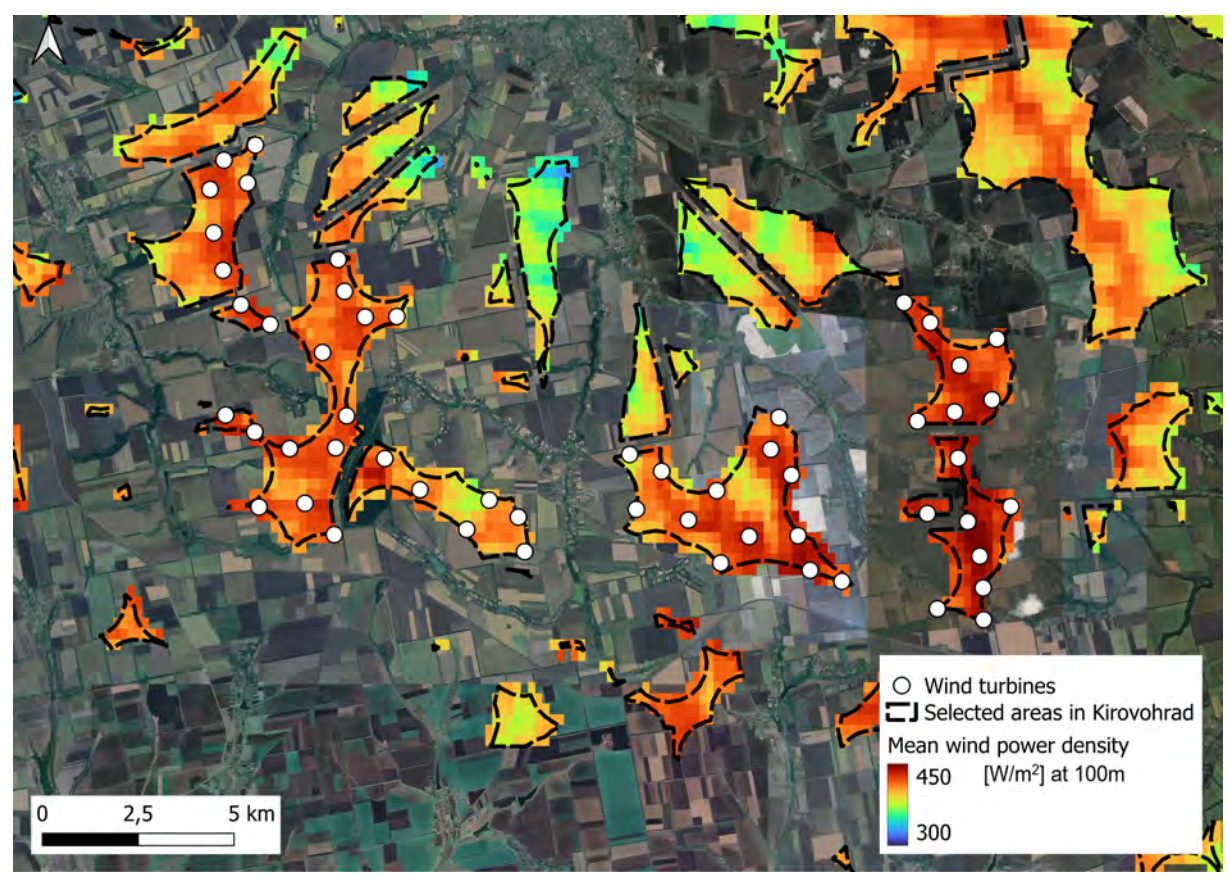


Figure 20: Map showing the Kirovohrad site location and layout of the hypothetical wind farm.

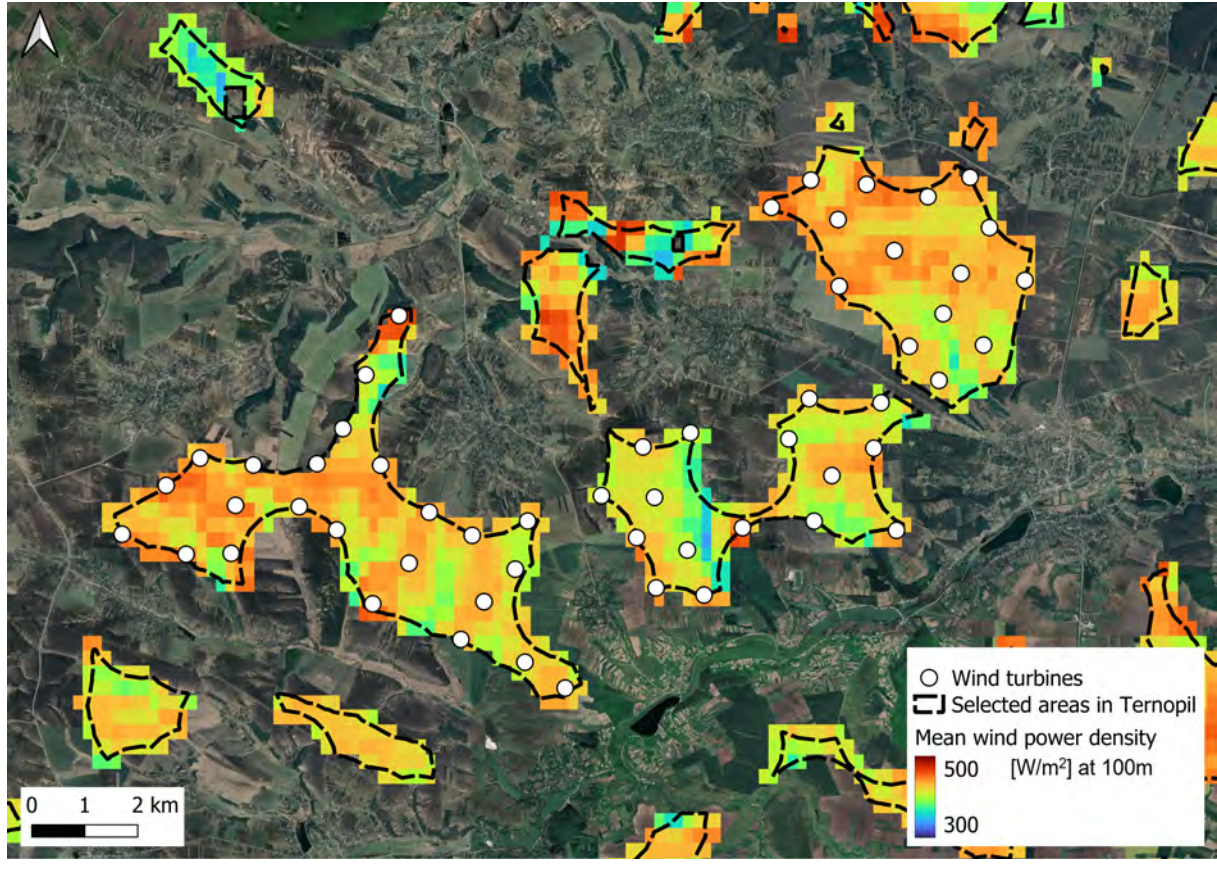


Figure 21: Map showing the Ternopil site location and layout of the hypothetical wind farm.

4.2.4 Energy Yield Results with Wake Losses

The annual energy production results are presented in Table 4. The mean wind speed (wake-reduced) is the mean wind speed at hub height - an average value of all wind turbine positions taking wake effects into account. The wake loss is sum of all wake losses in the wind farm. The Potential AEP shown in the table is the gross annual energy production reduced by the wake losses only. The energy yield differences are due to the distinct wind energy resources of the sites combined with the wake losses for each layout.

Parameter	Chernihiv	Kirovohrad	Ternopil
Mean wind speed (wake-reduced)	7.25 m/s	7.52 m/s	7.51 m/s
Wake loss	6.87%	3.97%	5.36%
Potential AEP	1087 GWh	1138 GWh	1106 GWh

Table 4: Initial results for wind farm sites.

4.2.5 Net Energy Yield Results with Additional Losses

The calculation of the potential AEP, shown in the previous section, only includes the wake loss. In reality, wind farms might be impacted by several factors or losses such as blockage loss, turbine availability loss, balance of plant availability loss, grid availability loss, electrical efficiency loss, sub-optimal wind farm performance loss, high-wind hysteresis loss, high-temperature derating loss, blade degradation loss, non-technical curtailments, etc.

The losses used in this study are calculated or estimated according to methodologies described in *CREYAP 2021* by Badger et al. [22]. A total loss of the order of 8% is assumed for all hypothetical wind farms. Then, the net annual energy production, also described as P50, is derived from the potential AEP multiplied by a factor of 0.92, representing the estimated total additional losses of a typical onshore wind farm.

The final results of net AEP (P50) and the capacity factors, which account for all losses, are presented in Table 5. The capacity factor for a wind farm is defined as the ratio of its net AEP over a period of time to its potential output had it operated at its full nameplate capacity throughout the same time frame.

The annual mean capacity factor (CF) can be expressed as:

$$\mathrm{CF} = \frac{\mathrm{Net}\,\mathrm{AEP}}{\mathrm{Wind}\,\mathrm{farm}\,\mathrm{capacity}\,\mathrm{rating}\times8766} \tag{1}$$

where the denominator represents the maximum possible AEP calculated based on the wind farm capacity and the total number of hours in a year (365.25 days multiplied by 24 hours per day).

4.3 WASP Workflow

As a summary of this chapter, the workflow of a wind farm energy production calculation using WAsP is outlined below.

1. Site Identification: Based on restrictions described in chapter 3, an area suitable for

Table 5: Final results for wind farm sites.

Parameter	Chernihiv	Kirovohrad	Ternopil
Total losses	14.9%	12.0%	13.4%
Net AEP	1000 GWh	1047 GWh	1018 GWh
CF	46.1%	48.3%	46.9%

wind power projects is determined. Three potential sites with superior wind resources, relatively close to the grid and adequate orographic features have been identified

- 2. **Digital Mapping:** Using tools such as QGIS, the area was modelled with a high-resolution digital map, capturing details of the terrain: Orography (elevation) and land cover (roughness).
- 3. Wind Turbine: The power and thrust coefficient curves for a 4.5 MW Vestas wind turbine, model V163 Class III, were adopted for the simulations. A hub height of 113 m was considered, and the Svenningsen method was applied to correct the power curve based on the calculated mean air densities at the wind turbine positions.
- 4. **Wake Effects:** The applied wake model was PARK2 with decay coeficient 0.090, 5 subsectors and 1 m/s resolution for the wind speed. The terrain context for the simulation was onshore.
- 5. Wind Farm Layout: Each wind farm consists of 55 turbines with a total installed capacity of 247.5 MW. The wind farms were positioned in locations with favourable wind resources. The wind farm layouts were optimised according to the wind conditions and topographic features to maximise energy yields.
- 6. **Wind Resource Data:** Generalised wind climates from the Global Wind Atlas were applied for each wind turbine position, including wind resource, atmospheric stability inputs and meteorological parameters for air density calculation.
- 7. **Simulations:** WAsP computed the wind resources and meteorological parameters at the hub height, calculated the wake effects, the potential Annual Energy Production (AEP) and the Capacity Factor (CF) of the wind farm.
- 8. **Technical Losses:** After calculating the potential AEP, the results are refined by including all technical losses and contingencies expected in a wind farm. The estimated losses used in this study are based on methodologies described in *CREYAP 2021* by Badger et al. [22]. The final result is the wind farm's annual net energy production.

4.4 Recommendations for a Wind Measurement Campaign

The wind data used for the energy yield calculations in the previous sections have not been obtained from measurement stations, they were obtained from the Global Wind Atlas which is associated with relatively high uncertainties.

In order to build more confidence in the estimated AEP of the hypothetical wind farms, and

perhaps generate inputs for a detailed feasibility study, DTU recommends carrying out on-site wind measurement campaigns to validate the wind climate data used in the WAsP Workflow.

A site-specific measurement campaign following the international standard IEC 61400-50-1 and the MEASNET procedure "Evaluation of Site-specific Wind Conditions" shall be implemented to evaluate the wind resource and the wind turbine design parameters. For each province, two locations are suggested: one in the "center" of the hypothetical wind farm - a location that would be relevant for the final design of the wind farm - and another one to cover another part of the province - useful for a potential validation of the global wind atlas - when combined with the measurements of the first location.

The suggested met masts locations are presented in Figure 22, Figure 23 and Figure 24 for Chernihiv, Kirovohrad and Ternopil respectively. The approximate coordinates of the measurement points 1 (in the wind farm area) and 2 (covering another part of the province) are included in Table 6.



Figure 22: Map showing the location, triangle, for the wind measurements inside the area of the hypothetical wind farm in Chernihiv.

Table 6: Recommended met mast locations. Point 1 (wind farm). Point 2 (Province). UTM Zones 35U and 36U.

Province	Point 1	Point 2
Chernihiv	473.373 m E, 5.582.466 m N	421.684 m E, 5.663.327 m N
Kirovohrad	406.814 m E, 5.333.484 m N	478.858 m E, 5.384.858 m N
Ternopil	400.512 m E, 5.528.737 m N	362.504 m E, 5.493.178 m N

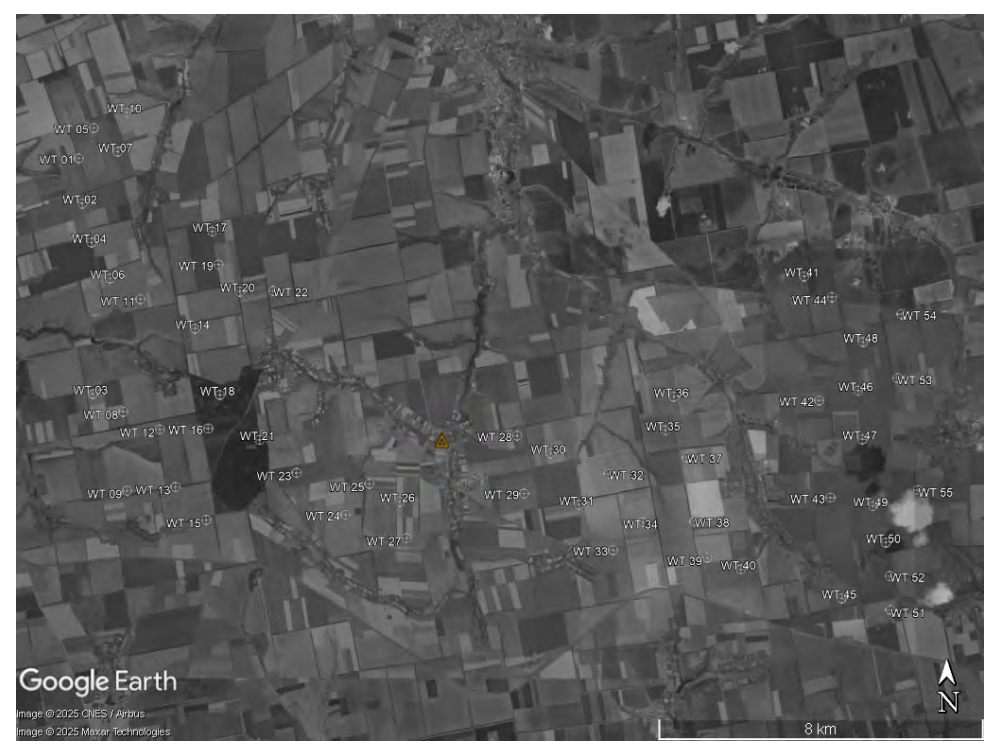


Figure 23: Map showing the location, triangle, for the wind measurements inside the area of the hypothetical wind farm in Kirovohrad.

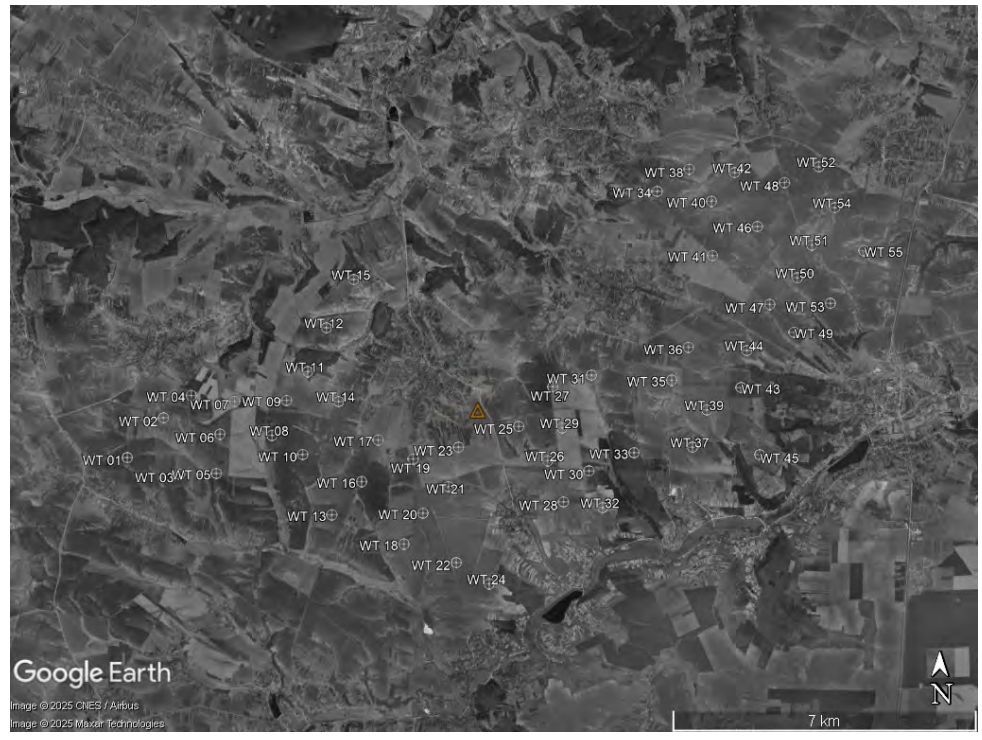


Figure 24: Map showing the location, triangle, for the wind measurements inside the area of the hypothetical wind farm in Ternopil.

4.5 Summary and Discussion

Three hypothetical wind farms, one for each region: Chernihiv , Kirovohrad and Ternopil, were modelled using WAsP, the industry-standard software for wind resource assessment and wind farm planning. All three sites share similar terrain characteristics, consisting mainly of farmland with very few buildings or trees.

Wind data from the Global Wind Atlas were used due to the lack of high-quality wind data. An on-site measurement campaign is recommended in order to reduce the uncertainties of the estimated wind conditions and energy yields. It is important to consider that bankable wind resource assessment and site assessment can only be carried out after an on-site measurement campaign is completed, compliant to the international standard IEC 61400-50-1 and the MEASNET procedure "Evaluation of Site-specific Wind Conditions".

The wind farm layouts were defined using best practices for maximising energy yields. And the estimated annual energy production was obtained based on benchmark losses assumptions.

The preliminary estimations indicate capacity factors of 46.1%, 48.3% and 46.9% for Chernihiv, Kirovohrad and Ternopil, respectively.

The procedure described in this chapter may be used for updating the energy yield calculation whenever relevant site and project-specific data becomes available such as local meteorological data from site-specific wind energy measurement campaigns. New calculations would also be required when a change of wind turbine model and height, or a different layout is adopted.

5 Levelised Cost of Energy

This section outlines our estimates of the levelised cost of energy (LCOE) for the three hypothetical onshore wind farms in Ukraine, in the regions of Chernihiv, Kirovohrad and Ternopil. The LCOE is the cost of electricity generation and is therefore the minimum price at which energy produced must be sold for the duration of the project's operating phase to break even. The LCOE does not include any system costs, such as balancing, deep network reinforcement and increased dispatch costs for thermal generation units.

5.1 Methods and Data

The following equation is used for the calculation of the Levelised Cost of Energy. Whilst the model uses the more accurate cash-flow method, we assume that all upfront cost occurs in year 1, and electricity generation commences in year 2. This is a reasonable assumption, given the nature of onshore wind, with little site accessibility issues assumed over the installation period. The assumption for all costs to occur allows us to express the LCOE using the simplified equation Equation 2 [23].

$$LCOE = \frac{\sum_{t=0}^{n} \frac{CapEx_{t} + OpEx_{t} + DecEx_{t}}{(1+r)^{t}}}{\sum_{t=0}^{n} \frac{AEP_{t}}{(1+r)^{t}}}$$
(2)

where, $CapEx_t$: Investment costs for year t (euros); $OpEx_t$: operation and maintenance costs for year t (euros/year); AEP_t : electricity generation in year t; r: discount rate (%), i.e. WACC - weighted average cost of capital; n: Operational lifetime of the asset (years).

We estimate LCOE ranges for the three hypothetical onshore wind projects in Ukraine using country-specific financing cost. Where available, we use Ukraine specific numbers for CapEx and OpEx. Following the conclusion of data gathering, we use a discounted cash flow model to calculate the LCOE from the electricity generation and cost estimates. The model allows for a number of additional finance-related inputs, such as cost of debt and cost of equity.

We calculate the LCOE for onshore wind in Germany and the UK for reference using the same methodology and sources using country-specific average numbers from IRENA[24]. In addition to the three proposed wind farms, we calculate the LCOE for an average wind farm in Ukraine using data from the Urgent Technology Catalogue [25].

Additionally, we decompose the LCOE into its component shares: WACC, CapEx, and OpEx. This is done by comparing each LCOE estimate to a scenario where the (real) WACC is 0%. The financing cost share is determined by the percentage change from the LCOE to the LCOE with a 0% WACC. The shares for CapEx, OpEx, and taxes are then calculated for the 0% WACC scenario and adjusted by subtracting the financing cost share.

5.1.1 Net Annual Energy Production

The net Annual Energy Production (AEP) estimated for the three 250 MW wind farms are 1,000 GWh/year, 1,047 GWh/year and 1,018 GWh/year in Chernihiv, Kirovohrad, and Ternopil, respectively (see chapter 4), which equates to capacity factors of 46.1%, 48.3% and 46.9%, respectively.

5.1.2 CapEx

The total installed capital expenditure CapEx is available in the literature. All sources to date state 2023 data, although publication date is in 2024, Table 7. More recent numbers were not available at the time of writing. We assume 1,600 €/kW for onshore wind Ukraine as a baseline, utilising country specific data from IRENA [24]. The IRENA numbers are for wind turbines in the 4-5 MW class, which align with the wind turbine model chosen in this study, whereas NREL data refers to lower capacity wind turbines, average rated power of around 3.3 MW.

We assume four years of development, with wind farms going online 2029/2030. Explicit figures on development expenditures (DevEx) are not available, thus we assume a DevEx equal to 3% of total CapEx [26], which is added to the overall installed CapEx. Decommissioning costs (DecEx) as set to zero, as the scrap value at the end of wind turbine life is likely to exceed any decommissioning costs.

Location	Mean Cost [€/MWh]	Notes	Source
Noth America	1,811	with construction financing, insurance, warranty	NREL [27]
Noth America	1,539	without construction financing, insurance, warranty	NREL [27]
Noth America	1,484		IRENA [24]
Europe	1,583	Min: 1,092 Max: 2,213 SD: 458	IRENA [24]
Ukraine	1,600		IRENA [24]

Table 7: Overview on total installed cost, CapEx, for onshore wind for 2023 data.

We further investigate how these CapEx value would change by location. For this we have identified three cost items which are location specific and may change with the distance to the next grid connection point, and the access to suitable roads for the transport of the turbines. Table 2 shows the cost share of these components. However, we acknowledge that these costs are highly variable, with grid connection cost accounting between 1% and 5% of total CapEx in Ukraine, where installation and logistics vary between 5-7% and 10-13%, respectively. The inputs on installation and logistics were kindly provided by the Ukrainian Wind Energy Association and thus represent most accurate local knowledge. We account for these cost variations adjusting CapEx by ±100 €/kW in scenarios around our baseline value of 1,600 €/kW. The range was kindly provided by the Ukrainian Wind Energy Association.

5.1.3 Operation and maintenance expenditure (OpEx)

Operation and maintenance expenditure (OpEx) is also quoted in aforementioned sources. NREL states 40 €/kW/year for North America [27], whereas IRENA differentiates OpEx by coun-

Table 8: Location variable components of an onshore wind farm.

Component	Cost	Source
Grid Connection	5% of total installed capital cost	NREL [27]
Installation	6% of total installed capital cost	NREL [27]
Transport	13% of total installed capital cost	NREL [27]
Grid Connection	9% of wind turbine cost	IRENA [24]

try and country groups [24], with an average of 35 €/kW/year. The most appropriate category, 'other non-OECD' is at 30 €/kW/year, which is the value employed in this study for the baseline. We also assess an OpEx of 45 €/kW/year to account for potentially higher OpEx costs, which is the midpoint of the range provided by the Ukrainian Wind Energy Association.

5.1.4 WACC

For the estimation of the WACC we follow Damodaran [28],[29] and IRENA's methodology [30], described by the equations in this section. Actual data is from Damodaran's website[31], which contains most up-to-date figures. Following this, we can establish base line for the WACC.

The overall WACC is obtained from:

$$\mathit{WACC} = \delta*(1-\tau)*K_D + (1-\delta)*K_E \tag{3}$$

where, δ is the gearing ratio or leverage; τ is the corporate tax rate; K_D is the cost of debt; and K_E is the cost of equity.

The cost of debt is in Equation 4. Note that LM and TP are calculated together and not explicitly shown.

$$K_D = GRF + CDS + LM + TP (4)$$

where, GRF is the global risk-free rate; CDS is the country default spread; LM is the lender margin; and TP is the technology premium.

And the cost of equity is given by:

$$K_E = GRF + CRP + ERP + TP \tag{5}$$

where, CRP is the country risk premium; and ERP is the equity risk premium.

The inputs for WACC calculation are summarised in Table 9 for the baseline cost assumptions. In addition, a lender margin of 3% is evaluated in different cost scenarios as well as a debt-to-equity ratio of 70:30.

The weighted average cost of capital (WACC) is key as it represents the average rate of return required by both debt and equity investors, adjusted for the tax rate. It combines the cost of

Table 9: Inputs to WACC calculation.

Variable	Value	Source
GRF (ECB Rate Fixed Rate)	2.9%	ECB (2035) [32]
Debt to Equity Ratio (d)	60:40	IRENA [30]
Country Default Spread (CDS)	11.88%	Damodaran [31]
Lender Margin (LM)	2%	IRENA [30]
Technology Premium (TP)	Included in lender margin	IRENA [30]
Equity Risk Premium (ERP)	4.33%	Damodaran [31]
Country Risk Premium (CRP)	16.02%	Damodaran [31]
Corporate Tax Rate (T)	18%	Damodaran [31]
Inflation	12%	National Bank of Ukraine [33]

debt (interest on borrowed funds) and the cost of equity (expected return on equity investments). The resulting nominal WACC for onshore wind projects is estimated to be 18.9%. This is higher than a quoted WACC of 12.2% [30] for the years 2019-2021, but also to be expected, reflecting on the investment uncertainty. To convert this to a real WACC, we assume a 12% inflation rate [33] for 2024. This adjustment results in a real WACC of 6.1% (post tax).

5.1.5 Interpretation

The actual cost of onshore wind development for any specific project cannot be determined until the development process begins. Developers need to invest significant resources in conducting site studies to estimate more accurately the energy yield of the wind farms and determining the actual costs of materials, transportation, installation, etc., for that particular site, based on proprietary data, models, and discussions with potential contractors.

Moreover, our primary data sources, NREL, IRENA and Damodaran only partially cover Ukraine in sufficient details for onshore wind. Therefore, our results should not be considered precise estimates of the LCOE. They can be used for comparison between different projects in Ukraine, as well as to a baseline project, to gain a broad understanding of where Ukraine's onshore wind resources stand in relation to more mature markets.

5.2 LCOE Results

The analysis of wind energy costs in Ukraine reveals some differences between the Urgent Ukraine Technology Catalogue and the three wind farms examined in this study. While the wind farms in this study demonstrate lower LCOE values compared to the Urgent Ukraine Technology Catalogue, the difference is not substantial, which indicates a good alignment between both independent studies.

A key distinction between the Ukraine Technology Catalogue and the case study wind farms lies in capital expenditure (CapEx) and annual energy production (AEP). The Ukraine Technology Catalogue assumes a lower CapEx (-21%) than the three wind farms; however, this is accompanied by a considerably lower AEP (-31%), ultimately affecting the LCOE calculations.

A sensitivity analysis highlights the extent to which various financial and operational parameters impact the LCOE:

- Raising or lowering CapEx by ±100 €/kW (total CapEx 1500-1700 €/kW) alters the LCOE by approximately 5.2%.
- An increase in lender margin to 3% (up from 2% in the baseline) results in a 3.9% rise in LCOE.
- OpEx of 45 €/kW/a, up from 30 €/kW/a, leads to an 8% increase in LCOE.
- A financing structure with an increased debt-to-equity ratio of 70:30 would result in a 5.8% reduction in LCOE compared to the baseline one, i.e., a 60:40 debt-equity configuration.

These results highlight the importance of financing conditions and cost structures in determining the overall economic viability of wind power in Ukraine. The relatively strong alignment between our case study wind farms and the Urgent Ukraine Technology Catalogue suggests that while there are differences in cost assumptions, the overall findings are robust.

Table 10: LCOE results in real terms for the baseline assumptions. Values in brackets are the respective minimum and maximum values for the full set of scenarios.

Project / Reference	Real LCOE in 2024 [€/MWh]	Financing cost share	CapEx share	OpEx share	Taxes share
Chernihiv	46.8 (44.1/50.6)	37.1% (36.0/39.1)	36.3% (33.7/38.6)	19.7% (17.2/23.7)	5.8% (5.4/6.2)
Kirovohrad	44.7 (42.1/48.3)	38.6% (36.1/40.6)	35.4% (33.7/36.7)	19.2% (16.8/23.7)	5.7% (5.4/5.9)
Ternopil	46.0 (43.3/49.7)	40.2% (36.1/44.0)	34.5% (33.7/35.8)	18.8% (16.0/23.7)	5.4% (5.0/5.8)
Urgent Technology Catalogue	49.3 (41.5/55.3)	46.2% (46.0/46.3)	35.9% (35.9/36.0)	11.0% (11.0/11.0)	5.8% (5.8/6.0)
Germany (Average)	56.2	17.1%	42.1%	34.6%	4.9%
United Kingdom (Average)	36.1	17.8%	46.9%	26.9%	4.3%

The LCOE (in real terms) for wind projects in Ukraine varies across the three case studies – Ternopil, Chernihiv, and Kirovohrad – but all three projects demonstrate lower costs compared to the Urgent Ukraine Technology Catalogue. The lowest LCOE is observed in Kirovohrad (44.7 €/MWh), followed by Ternopil (46.0 €/MWh) and Chernihiv (46.8 €/MWh).

Using CapEx and OpEx numbers – but same financing costs - from the Urgent Technology Catalogue yields 49.3 €/MWh, which is higher than all three case studies, indicating that these three projects may perform better in overall cost terms due to the excellent wind resource. Compared to international benchmarks, Ukraine's wind projects have significantly lower costs than Germany (56.2 €/MWh) but remain higher than the UK (36.1 €/MWh).

The financing cost share in Ukrainian projects ranges from 37.% (Chernihiv) to 40.2% (Ternopil), which is lower than the Urgent Technology Catalogue estimate (46.2%). CapEx shares are

relatively consistent across the three projects (34.5%–36.3%), which is within the range of the Urgent Technology Catalogue estimate (35.9%). However, they remain higher than in Germany (42.1%) and the UK (46.9%), which is logical considering the lower financing costs in both countries. The OpEx share for the Ukrainian projects (18.8%–19.7%) is significantly higher than the Urgent Technology Catalogue value (11.0%), suggesting that real-world projects face higher operational costs than assumed in the technology catalogue. Tax shares are consistent across all Ukrainian projects, ranging between 5.4% and 5.8%, in line with the Urgent Technology Catalogue results (5.8%).

5.3 Summary and Discussion

The LCOE for wind projects in Ukraine demonstrate lower costs compared to the Urgent Ukraine Technology Catalogue. The lowest LCOE is observed in Kirovohrad (44.7 €/MWh), followed by Ternopil (46.0 €/MWh) and Chernihiv (46.8 €/MWh).

The comparison with German and UK's markets highlights that Ukraine's LCOE is more competitive than Germany's but remains higher than the UK's. It is noteworthy that CapEx and OpEx are lower in Ukraine than in Germany and UK, but the cost reduction will most heavily depend on the significantly higher capacity factors in Ukraine, which rivals offshore locations in Germany and UK. These cost reducing aspects are somewhat offset by significantly higher financing costs, which account for almost 40% of overall project costs, which is double the share in Germany and UK. While Ukraine benefits from lower capital investment requirements, its higher financing burden remains a key challenge, emphasising the need for improved access to low-cost capital and more favourable debt terms to reduce overall LCOE.

6 Renewable Energy Integration

The aim of this chapter is to discuss grid integration aspects of renewable energy generation - focus on wind and solar power - in Ukraine. It also recommends additional studies to analyse the impact of increasing shares of renewable energy generation on the power system in Ukraine.

6.1 Wind and Solar Power Simulations: Time Series

This section presents wind generation time series simulations for the wind farms modelled in Chernihiv, Kirovohrad, and Ternopil, each with 250 MW of installed capacity. The simulations supplement the annual energy yield calculated from WAsP in chapter 4 by adding a time series perspective to the results. The time series can be used in assessing system integration aspects of variable renewable energy generation.

In addition, solar photovoltaic (PV) hypothetical power plants are also simulated to support a preliminary analysis of potential complementarity of wind and solar technologies in the region.

The time series simulations are carried out using the CorRES software [34]. The CorRES runs are synchronised to the detailed WAsP modelling by using the wind farm power curves from WAsP and aligning the average wind speed of each site to the WAsP results. The time series results thus benefit from WAsP's high-resolution wind resource assessment capabilities.

6.1.1 The CorRES Tool

The analyses in this chapter are based on simulated wind and solar generation time series at the locations of the hypothetical wind power plants in Chernihiv, Kivorohrad, and Ternopil. The simulations are carried out using the CorRES tool [34]. CorRES is used in many academic and industry collaboration projects [35], including the work for European Network of Transmission System Operators for Electricity (ENTSO-E) for their Pan-European Climate Database (PECD). The PECD data are used, e.g., in the TYNDP [36] and ERAA [37]studies. Thus, the wind and solar generation time series generated in this project can be used in potential further studies considering broader European power and energy system integration.

The CorRES tool links weather data and power curves to produce the generation time series [38]. The core weather time series are from ERA5 [39]. However, as shown in [38], it is important to use more detailed local wind resource data for accurate capacity factor estimates. In this project, the high-resolution wind resource data are obtained from the WAsP results (chapter 4).

6.1.2 Input Data

The wind and solar generation are simulated on hourly resolution, based on the ERA5 [39] reanalysis data, with the WAsP high-resolution wind data used to scale the ERA5 data for more accurate representation of plant-level wind speeds (the scaling is carried out following the procedure in [38]). The data obtained from ERA5 are wind speed and wind direction for wind generation and irradiance and temperature for solar generation (temperature is used in panel efficiency calculations). The time series simulations are carried out from 1980 to 2022.

The wind power plant specifications are the same as described in chapter 4. CorRES uses power curves at the wind power plant level [38] to model wind farms, which are obtained from the WAsP calculation section A.2 including wake losses and terrain effects for all directions.

Note that only wake losses are considered because all other systematic losses do not affect the results of this study. An overview of the wind power plant inputs are provided in Table 11 and the solar power plant inputs are provided in Table 12, where Overpower shows how much the panel-side (DC-side) installed capacity is oversized compared to the grid-connection (AC-side). The solar generation time series are simulated both considering fixed tilt (south-facing) and 1-axis tracking.

 Table 11: Wind power plant CorRES inputs

Name	Latitude [°]	Longitude [°]	Hub height [m]	Wind	farm
				power cu	ırve
Chernihiv	50.3941	32.6161	113	From WA	∖sP
Kirovohrad	48.1547	31.7605	113	From WA	∖sP
Ternopil	49.9085	25.6330	113	From WA	∖sP

Table 12: Solar power plant CorRES inputs

Name	Latitude [°]	Longitude [°]	Surface az-	Surface tilt [°]	Overpower
			imuth [°]		
Chernihiv	50.3941	32.6161	180 (south)	40.6411	1.25
Kirovohrad	48.1547	31.7605	180 (south)	38.9302	1.25
Ternopil	49.9085	25.6330	180 (south)	40.2701	1.25

6.1.3 Wind Generation Time Series

Overview of the wind generation time series for a hypothetical wind farm in Chernihiv is provided in Figure 25, for Kirovohrad in Figure 26, and for Ternopil in Figure 27. The capacity factors are very high for all locations (above 0.5) but note that only wake losses are included in the CorRES runs. The high capacity factors are driven by the selection of an adequate site, the design of an optimized wind farm layout and the selection of a wind turbine power curve with low specific power (more details in chapter 4). The small differences between capacity factors estimated in CorRES compared to WASP are due to differences in the two softwares.

The year-to-year variation is moderate, with all years showing capacity factor of 0.45 or higher for all locations (Figure 25, Figure 26, and Figure 27).

6.1.4 Solar Generation Time Series

Overview of the solar PV generation time series for a hypothetical solar power plant farm in Chernihiv is provided in Figure 28, for Kirovohrad in Figure 29, and for Ternopil in Figure 30. The graphs show two distinct outputs, one for fixed south-facing installations and another one for power plants with tracking mechanisms (1-axis tracking). The capacity factors with tracking are higher, but arguably the most important benefit of tracking is the increased generation in the morning and evening (as the panels are moved to be better aligned towards the sun).

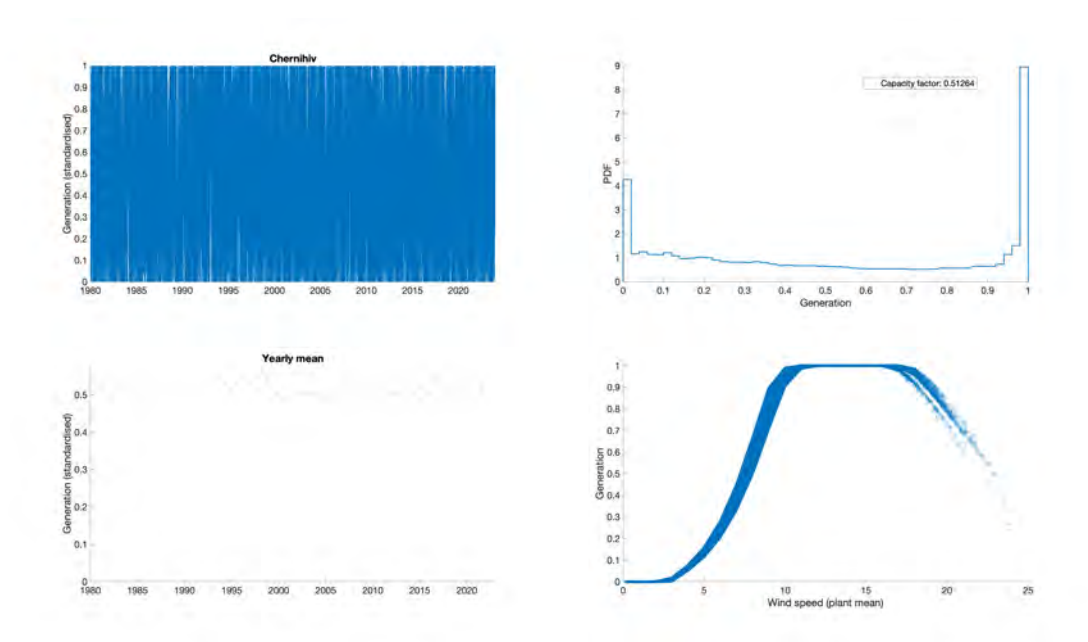


Figure 25: Overview of the CorRES wind generation simulations for Chernihiv (in per unit values: 1.0 = generation at full installed capacity). The capacity factor (top-right subplot) is average of all the simulated years. PDF = probability density function.

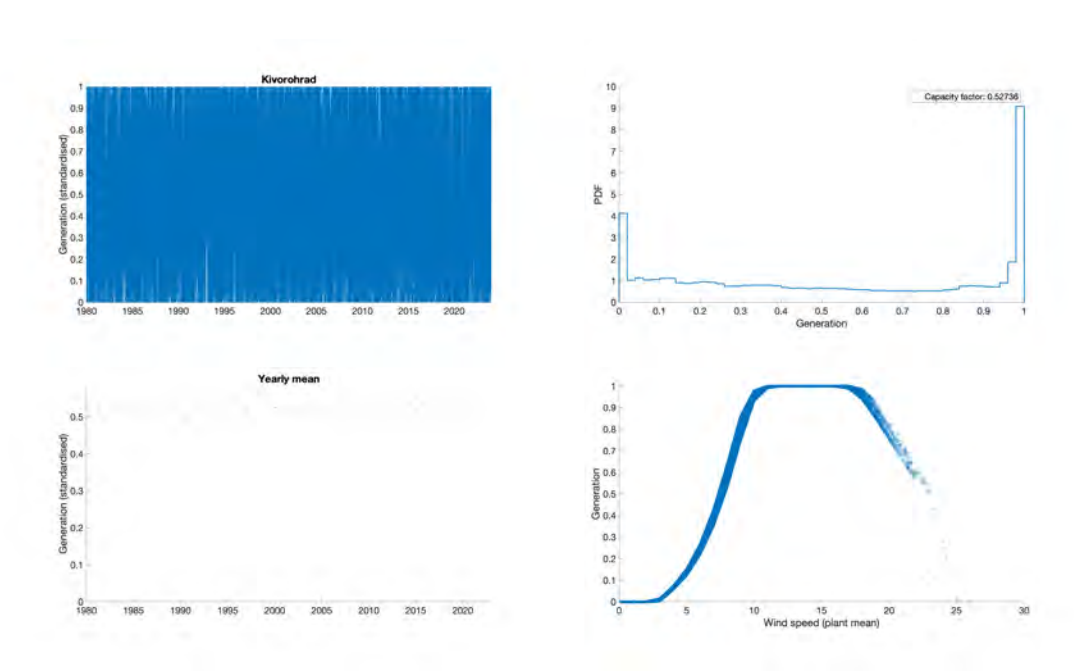


Figure 26: Overview of the CorRES wind generation simulations for Kirovohrad (in per unit values: 1.0 = generation at full installed capacity). The capacity factor (top-right subplot) is average of all the simulated years. PDF = probability density function.

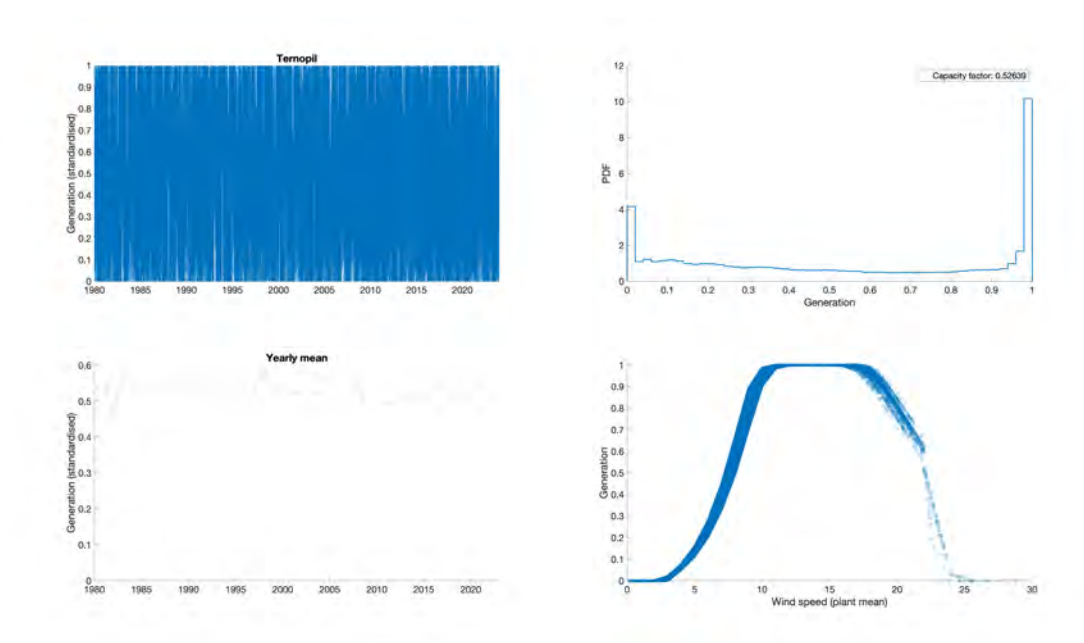


Figure 27: Overview of the CorRES wind generation simulations for Ternopil (in per unit values: 1.0 = generation at full installed capacity). The capacity factor (top-right subplot) is average of all the simulated years. PDF = probability density function.

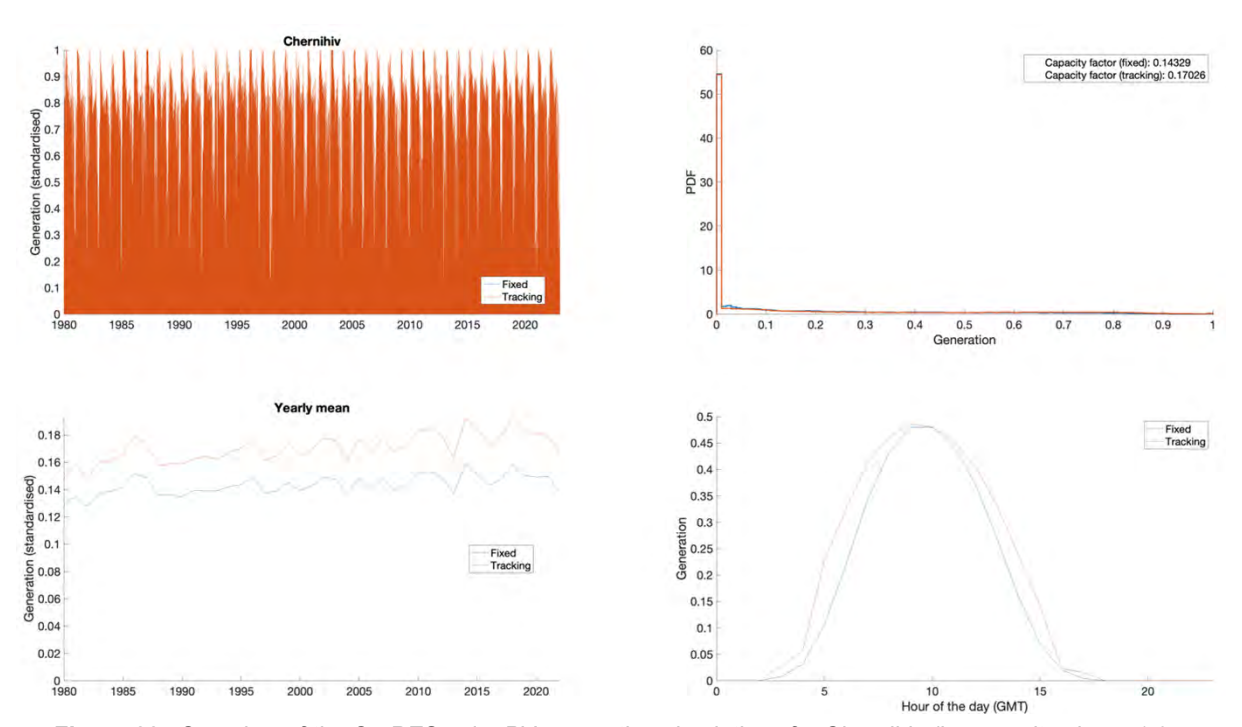


Figure 28: Overview of the CorRES solar PV generation simulations for Chernihiv (in per unit values: 1.0 = generation at full installed capacity). The capacity factor (top-right subplot) is average of all the simulated years. PDF = probability density function.

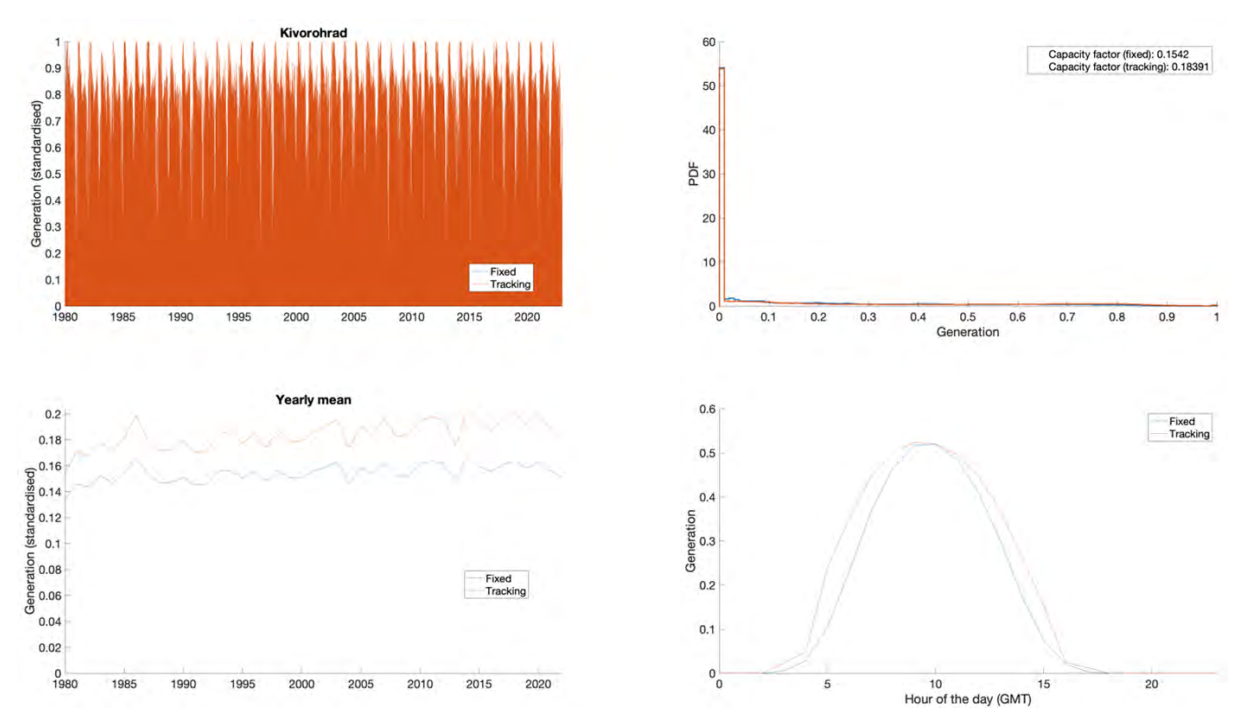


Figure 29: Overview of the CorRES solar PV generation simulations for Kirovohrad (in per unit values: 1.0 = generation at full installed capacity). The capacity factor (top-right subplot) is average of all the simulated years. PDF = probability density function.

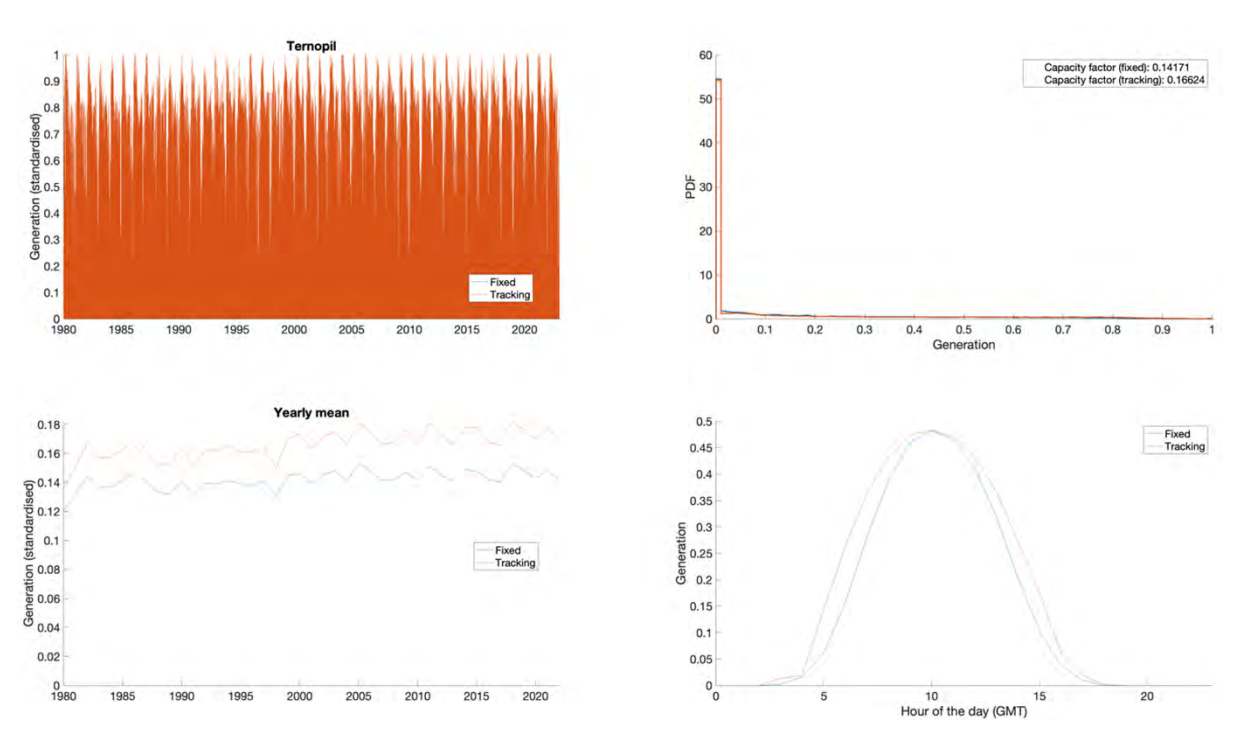
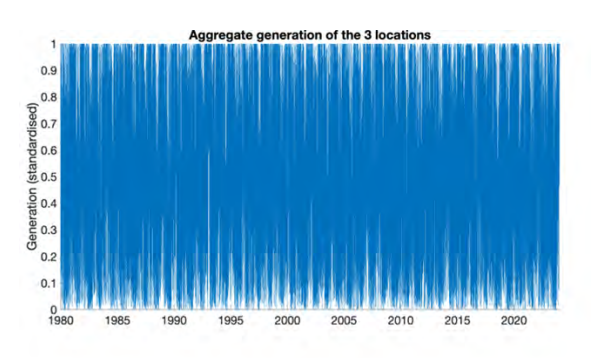


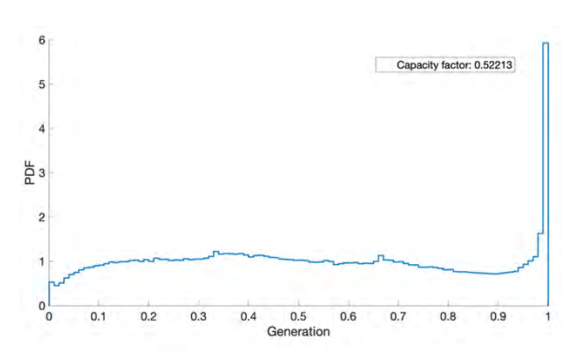
Figure 30: Overview of the CorRES solar PV generation simulations for Ternopil (in per unit values: 1.0 = generation at full installed capacity). The capacity factor (top-right subplot) is average of all the simulated years. PDF = probability density function.

6.2 Correlation Analysis

6.2.1 Wind Generation Correlation

In addition to looking at the individual wind farms, it is of interest to consider the correlations between the time series generation of the wind power plants. Low correlations can be beneficial for system integration as they can reduce the variability of the aggregate wind generation (sum of all wind farms) [40]. The correlations between the wind farms are shown in Table 13. With the correlations on average around 0.45, significant geographical smoothening is expected for the aggregate output. The aggregate generation (sum of the three wind farms) is visualised in Figure 31. The generation distribution (the PDF in the top-right subplot) shows significantly reduced likelihood of zero generation compared to the individual locations.





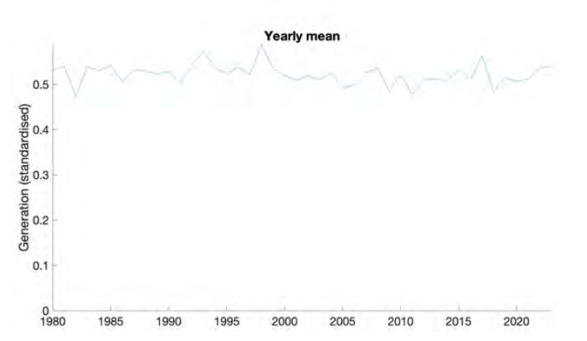


Figure 31: Overview of the CorRES wind generation simulations for the aggregate (sum) of the three analysed locations (in per unit values: 1.0 = generation at full installed capacity). The capacity factor (top-right subplot) is average of all the simulated years. PDF = probability density function.

Table 13: Correlations between the three simulated wind power plants.

	Chernihiv	Kirovohrad	Ternopil
Chernihiv		0.67	0.37
Kirovohrad	0.67		0.31
Ternopil	0.37	0.31	

6.2.2 Correlation Between Wind and Solar Generation

Figure 32 shows wind and solar generation monthly averages (period 1980-2022) for the Ternopil site. There is significant synergy between wind and solar generation: when the solar generation is high in late Spring and Summer, wind generation shows low generation, and vice versa. Table 14 shows that such negative correlation is evident also in hourly resolution data, suggesting that there exist an opportunity for exploring the benefits of the negative correlation between wind and solar in Ukraine.

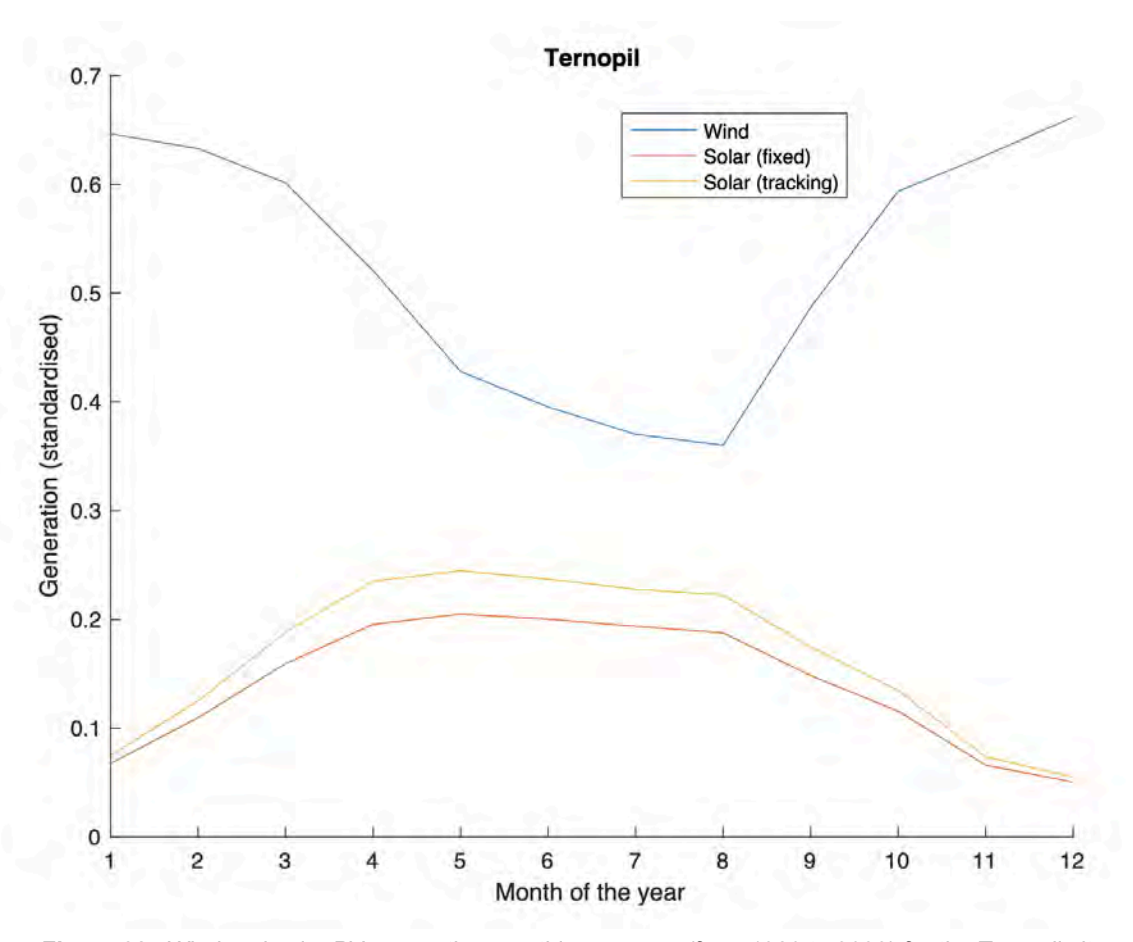


Figure 32: Wind and solar PV generation monthly averages (from 1980 to 2022) for the Ternopil site

Table 14: Correlations between wind and solar PV generation at the three sites (calculated from hourly data).

	Wind vs. Solar (fixed)	Wind vs. Solar (tracking)
Chernihiv	-0.18	-0.20
Kirovohrad	-0.17	-0.18
Ternopil	-0.19	-0.20

6.3 Hybridization Analysis

The analysis in this section demonstrates how hybridization of wind farms with solar PV and battery storage affects the performance of renewable generation, both from a national perspective and from the perspective of wind farm owners. The analysis presented here is purely technical, meaning that the economic consequences of the technical results have not been quantified. The performance metrics are the annual energy production, the curtailment of renewable generation and utilization of grid.

The basic assumption for this analysis is that the wind farm capacity and the grid connection capacity remain the same also after the wind farm is hybridized with solar PV and battery, in this case 250 MW. Therefore, hybridizations cause the so-called overplanting, which means that the sum of installed capacity is greater than the grid connection capacity. Therefore, the hybrid system is expected to improve grid utilization, but it will also cause some curtailment of renewable energy generation to avoid grid overload.

6.3.1 Applied Data for the Analyses

The analyses in this chapter are based on simulated historical wind and solar generation time series at the locations of the three hypothetical wind farms in Chernihiv, Kirovohrad, and Ternopil, supplemented with historical time series of the electricity demand in Ukraine. The historical wind and solar generation time series are described in section 6.1 while the electricity demand data is obtained from the ENTSO-E database.

The available electricity demand data is limited to a little more than four years of data over a period of six years from 2017 to 2022. Therefore, wind and solar data is only used for the same concomitant period, Figure 33. The resolution of renewable generation time series and of electricity demand time series is 1 hour. It is observed that the seasonal variations in electricity demand and solar generation is very visible from the figure, and also the seasonal variation with less wind generation during summer can be observed from the time series.

6.3.2 Hybridization with Solar

The impact of wind farm hybridization with solar PV is presented in Figure 34 considering several aspects: the increase in the annual energy production, the curtailment of the combined renewable power generation (based on the limited grid capacity assumption), the increase in duration of available renewable power generation, and the increase of grid utilization (or capacity factor) of the hybrid system. This analysis is based on hourly calculations for all wind and solar PV generation for the period 2017-2022 showed in the previous subsection.

The impact on the annual energy production is shown in Figure 34a. The hybridization of the 250MW wind farms with solar power plants increases the annual energy production between 9% and 10% for 100MW solar power plant and between 21% and 22% for a hybrid system with both wind and solar plants rated at 250MW.

The expected curtailment of a hybrid wind-solar system is illustrated in Figure 34b. The result does not establish if it is the wind generation or the solar generation which is curtailed, but the curtailment is obviously caused by the additional solar PV installation. The trends are the same for all three locations, but it is noted that the curtailment is highest for the location Kirovohrad

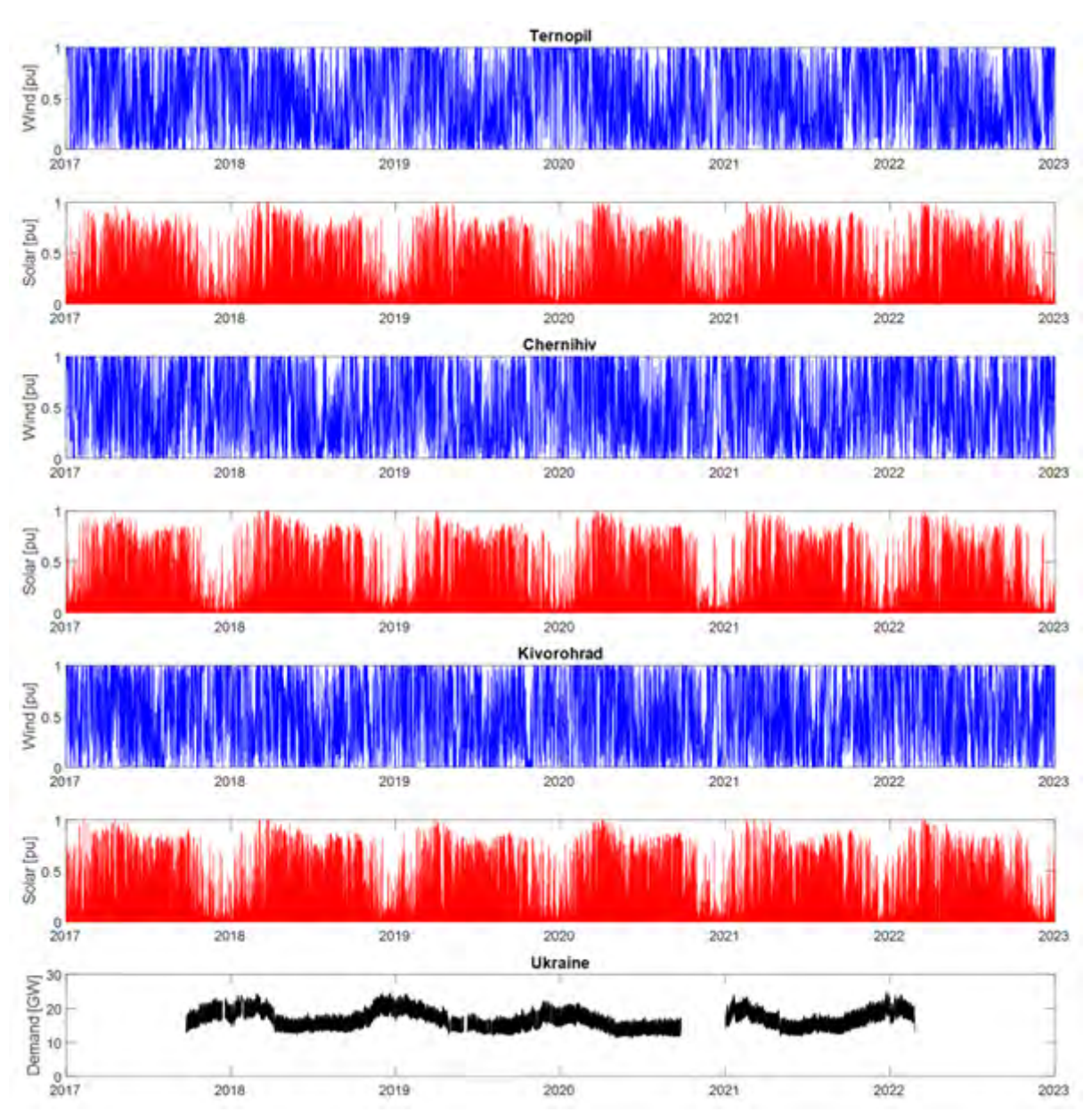


Figure 33: Applied data for the analysis of grid integration aspects.

which also has the highest annual wind energy production. The curtailment is moderate (approximately 2%) considering a solar power plant of 100MW and more significant (approximately 6%) with a 250MW solar power plant.

Figure 34c and Figure 34d show the duration curves of available wind generation for the three wind farms and the available wind-solar generation for the hybrid systems considering a 100MW solar PV plant, and considering a 250MW solar PV plant, respectively. The available wind power generation is shown for Benchmarking purpose. For each duration curve, the curtailed renewable generation is the area above 250MW power level (grid capacity threshold) and the annual energy production is the area below this threshold.

Figure 34e and Figure 34f show the duration curves for grid utilization which are obtained from Figure 34c and Figure 34d disregarding the power above the grid capacity threshold. The Grid utilization factor, Table 15, is calculated as the ratio between the annual energy production and the maximum energy which can be transmitted considering the grid capacity. The maximum energy is calculated from the area below 100% and the annual energy production is calculated from the area below the duration curve. The grid utilization factors of the wind farms are very good (>50%) but the hybridization with solar PV shows significant improvement of the grid utilization factor, around 57% for a hybrid system with 100MW solar PV capacity and more than 62% with 250MW solar PV capacity.

0 6: 4:	O la	17:	T
Configuration	Chernihiv	Kirovohrad	Ternopil
Wind only	51%	52%	52%
Hybrid with 100MW solar	56%	58%	57%
Hybrid with 250MW solar	62%	64%	63%

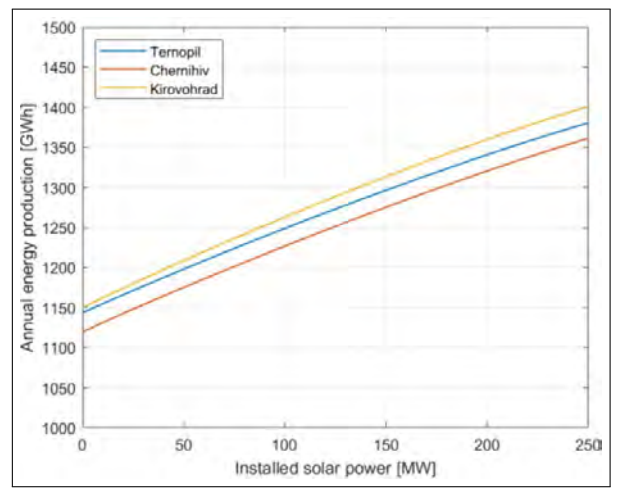
Table 15: Grid Utilization Factor for three locations with 250 MW wind farms

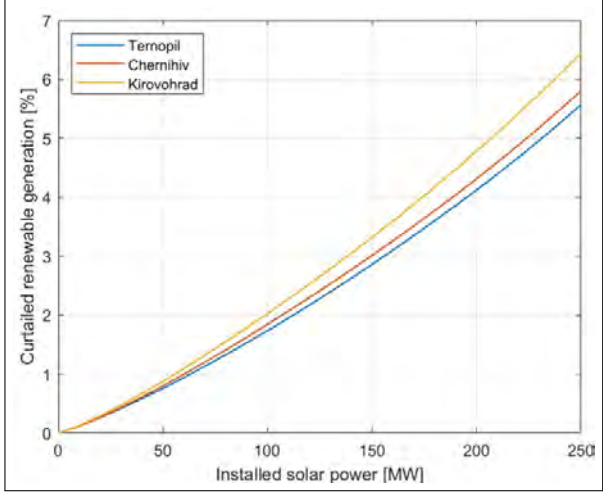
6.3.3 Hybridization with Solar and Battery

A hybrid wind-solar-battery configuration is studied to analyse the impact on the energy production. The addition of a battery bank to the hybrid wind-solar system might reduce curtailment resulting in an increased annual energy production. In order to quantify the possible reduction in curtailment and increase in annual energy production, a simple charge/discharge algorithm has been applied. This algorithm assumes that the only purpose of the battery is to reduce the curtailment. Therefore, the battery is discharged towards minimum state of charge (SOC) (0%) at times where there is additional grid capacity beyond the current wind and solar generation, and the battery is charged towards maximum SOC (100%) at times where the available wind plus solar generation exceeds the grid capacity.

It is assumed that the C-rate of the battery system is C/4, i.e. that a time full charging from 0% SOC to 100% SOC with maximum charging power will take 4 hours. The analysis is done from 0 battery capacity up to battery capacities which are up to 2 hours multiplied by the PV capacity, i.e. C/4 batteries which can charge 50% of the maximum PV output. This choice is made to limit the scope of the analysis what is considered to be financially relevant although the curtailment could be further reduced with larger battery systems.

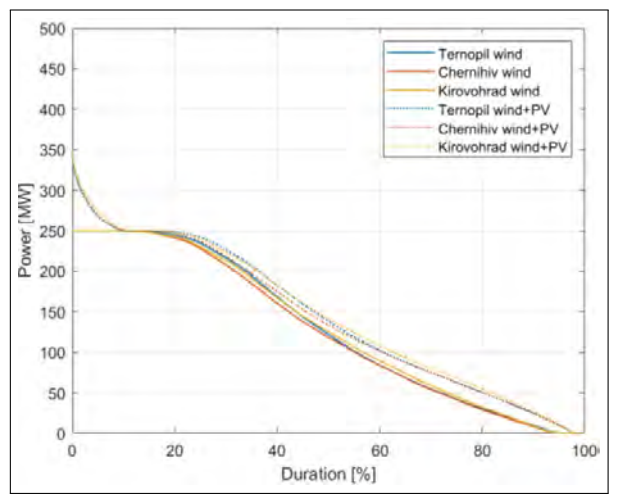
Figure 35 shows the impact of the battery size on the annual energy production for a hybrid

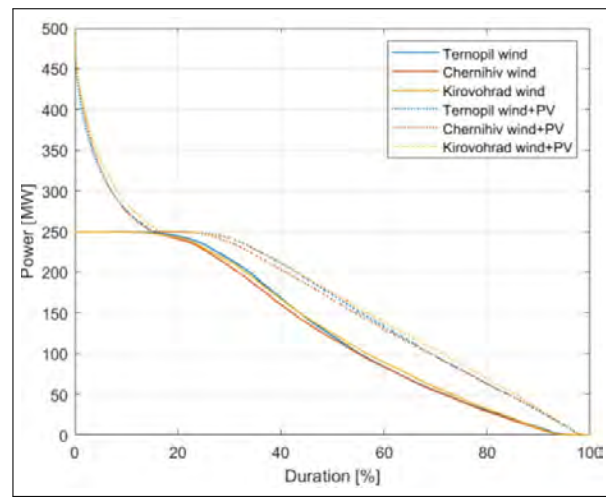




(a) Estimated annual energy production of a hybrid system vs. solar PV capacity.

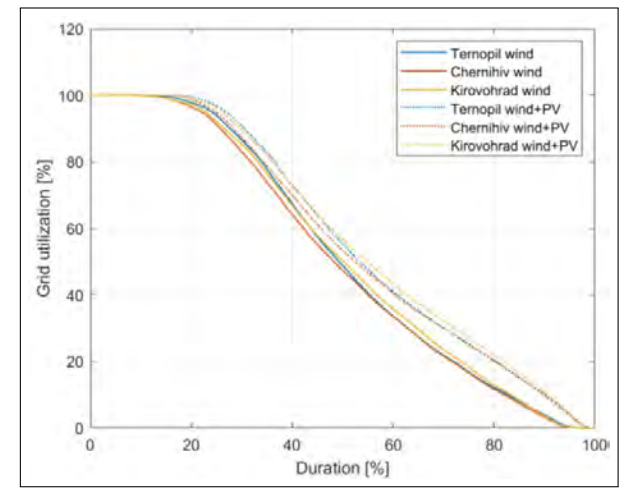
(b) Estimated curtailment of a hybrid system vs. solar PV capacity.

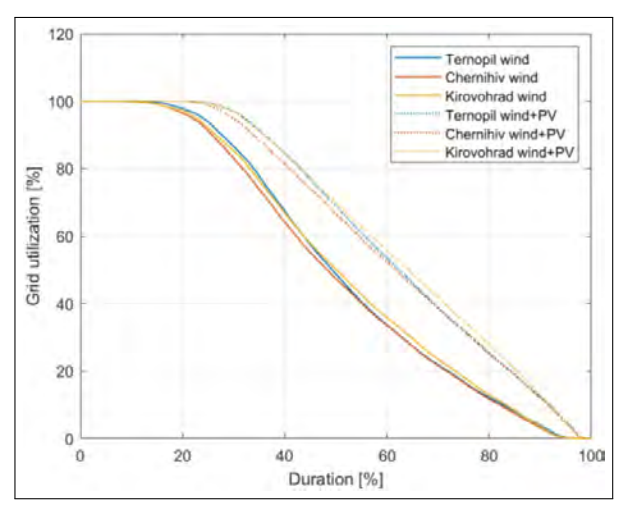




(c) Duration curves for 250MW wind farms with and without 100MW solar PV hybridization.

(d) Duration curves for 250MW wind farms with and without 250MW solar PV hybridization.





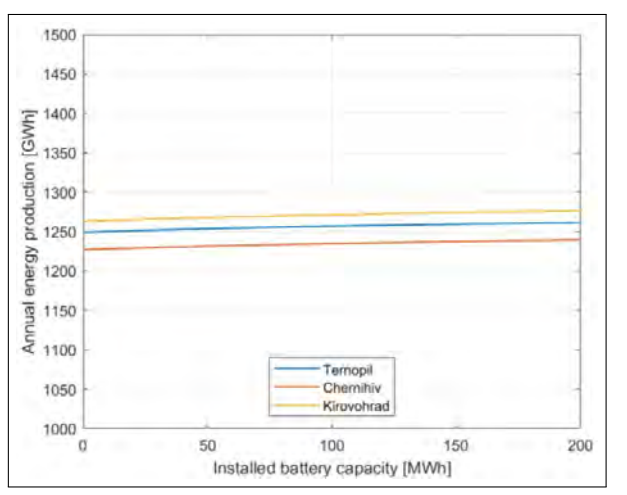
(e) Grid utilization curves for 250MW wind farms with and without 100MW solar PV hybridization.

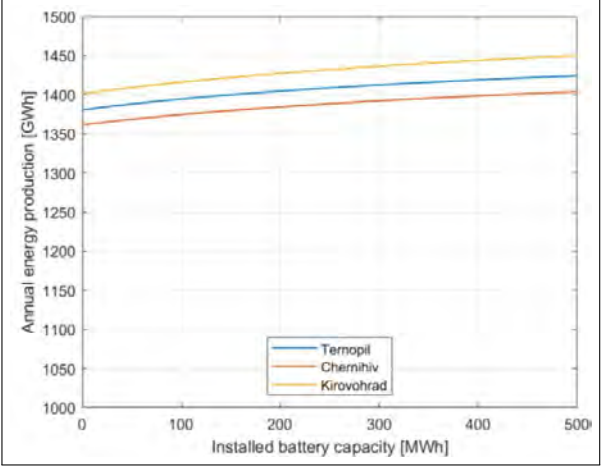
(f) Grid utilization curves for 250MW wind farms with and without 250MW solar PV hybridization.

Figure 34: Annual energy production, curtailment, duration curves and grid utilization curves for 250MW wind farms with and without solar PV hybridization.

system with 100MW and 250MW solar PV, respectively. In the first case, for a hybrid system with 250MW wind and 100MW solar, the addition of a 200MWh battery system would increase the annual energy production by approximately 1%, Figure 35a. For the second case, the hybrid system with 250MW wind and 250MW solar, the addition of a 500MWh battery system would increase the annual energy production by approximately 3.1% to 3.5%, Figure 35b.

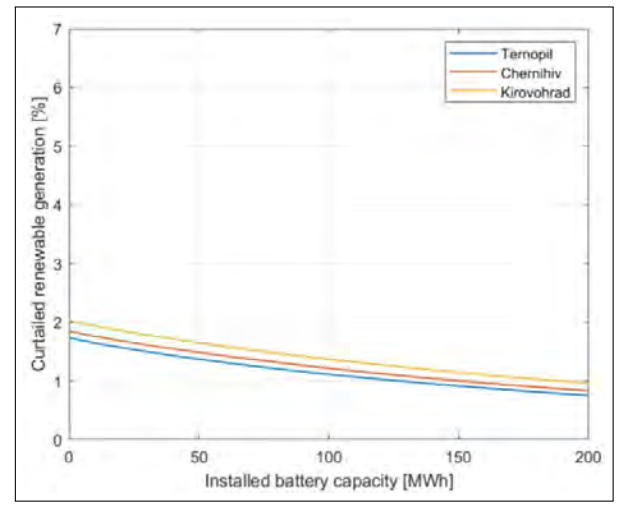
Figure 35c and Figure 35d show the curtailment of renewable generation of hybrid systems with 100MW and 250MW solar PV, respectively. It can be seen that the curtailment for a hybrid system with 100MW solar and a 200MWh battery would reduce the curtailment to approximately half the curtailment of the same hybrid system without storage. Similarly, the curtailment for a hybrid system with 250MW solar and a 500MWh battery would reduce the curtailment to approximately half the curtailment of the same hybrid system without storage.

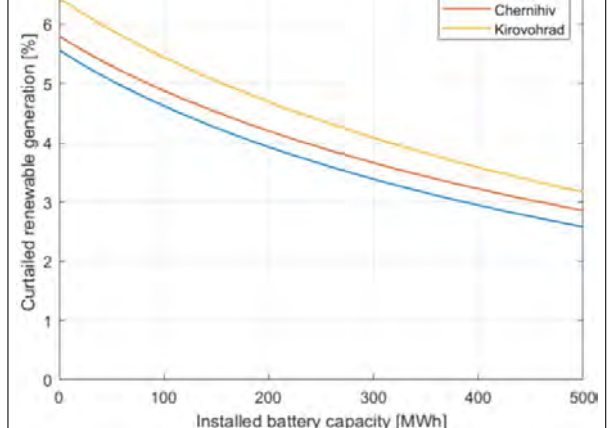




(a) Estimated annual energy production vs. battery size. Hybrid system with 100MW solar.

(b) Estimated annual energy production vs. battery size. Hybrid system with 250MW solar.





(c) Curtailment vs. battery size. Hybrid system with 100MW solar.

(d) Curtailment vs. battery size. Hybrid system with 250MW solar.

Figure 35: Impact of adding storage to hybrid wind-solar systems.

Ternopil

6.4 Load Following

The load following characteristics of the wind farms is analysed in ths section. For this purpose, the deviation time series, $\delta(t)$, between the generation profile of renewable power plants, $P_{\rm RE}(t)$, and the load profile, $P_{\rm demand}(t)$, is defined as

$$\delta(t) = \frac{P_{\rm RE}(t)}{\langle P_{\rm RE}(t) \rangle} - \frac{P_{\rm demand}(t)}{\langle P_{\rm demand}(t) \rangle} \tag{6}$$

With this definition, the mean value of $\delta(t)$ is zero because the mean value of each term on the right side is one. It is also important to notice that this definition is not only considering the fluctuations in renewable energy generation but also considers the "base load contribution" by normalizing with the mean value.

Now the demand deviation index is defined as the mean absolute of $\delta(t)$, i.e.

$$I_{\delta} = \langle | \delta(t) | \rangle * 100\% \tag{7}$$

The demand deviation index is used to compare the deviation between generation profile and demand profile for different solar PV sizing in the hybridization with wind farms. It is noticed that the demand deviation index is 0% if there is a perfect match between the generation profile and demand profile.

Figure 36 shows the demand deviation index calculated for hybridization with different solar power capacities. The demand deviation index is represented by the Y-axis ranging from 0% to 70%, and the solar PV installed capacity, ranging from 0 (wind only case) to 250MW, is in the X-axis. The solid red curve is the result for the hybridization of the 250MW wind farm in Chernihiv with a Solar PV with fixed solar panels, the yellow curve is the result for the Kirovohrad site and the blue curve for the Ternopil site. The dotted color curves are similar results but considering solar PV plants with 1-axis tracking systems instead of fixed structures.

The demand deviation index is reduced from 61%-65% with wind only to 45%-49% with 250MW solar PV hybridization and to 44%-47% for Solar PV with tracking. The black curves in the figure, solid for fixed solar PV and dotted for solar PV with tracking, represent the sum of all three locations. It simulates the combined renewable energy generation from three geographically dispersed locations. Only combining the energy generation of the three wind farms - case where x-axis "installed solar power" is zero - causes a drop in the demand deviation index from 61%-65% to around 47%. Finally, the total impact of the smoothening effect caused by the differences in wind speed variations between the locations and the hybridization of each wind farm with 250MW solar PV reduces the demand deviation index to 35%-36%.

6.5 Summary and Discussion

Wind generation time series simulations for the 250MW hypothetical wind farms modelled in Chernihiv, Kirovohrad, and Ternopil are presented to assess system integration aspects of variable renewable energy generation. In addition, solar photovoltaic (PV) hypothetical power

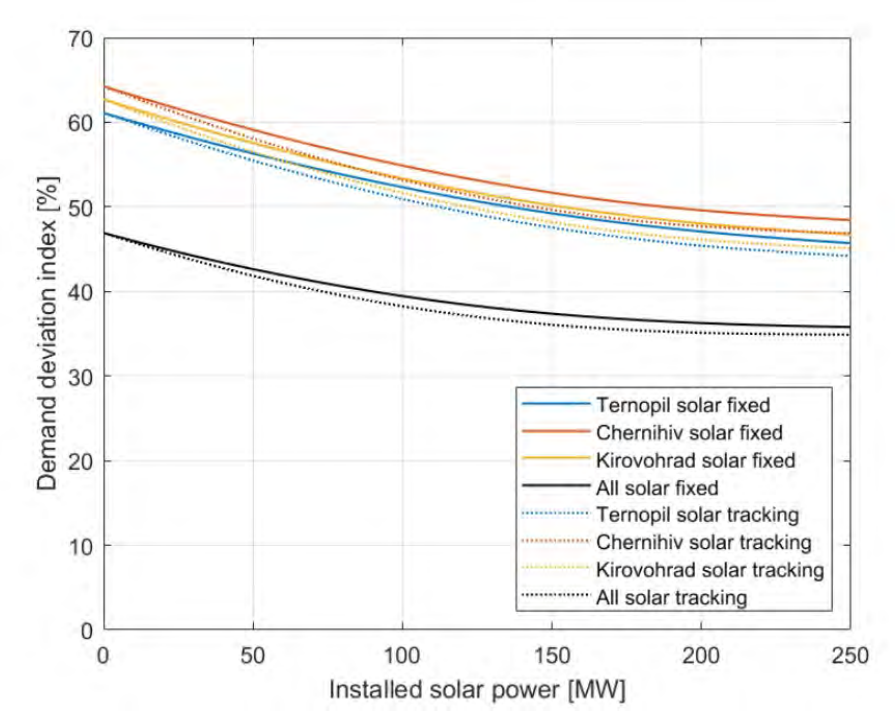


Figure 36: Load following indexes as a function of installed solar power for each site and for the sum of 3 sites.

plants are also simulated to support a preliminary analysis of potential complementarity of wind and solar technologies. The analysis of possible hybridization with PV assumes overplanting, meaning that the hybridized wind farms will need a hybrid power plant controller to ensure that the grid is never overloaded with more than 250MW generation. The following conclusions can be made based on the analyses presented in this chapter:

- The analysed wind power plants provide high capacity factors (above 0.5) at all three sites, with moderate year-to-year variation (all annual capacity factors above 0.45). Note that only wake losses are considered.
- The correlations between the sites (on average around 0.45) enable significant geographical smoothening in wind generation, reducing the likelihood of zero aggregate generation.
- Negative correlation between wind and solar generation is observed at each site, enabling reduction in generation variability when combining wind and solar power.
- calculations assuming 100% availability of wind turbines and solar PV systems show that
 hybridization wind farms with solar PV results in approximately 2%-6% curtailment. It is
 worth noting that if wind turbine and solar inverters outages were included in the calculations then the curtailment would be reduced.
- The grid capacity is better utilised if the wind farms are hybridized with PV. The grid utilization factor of a hybridized wind farm is higher (62%-64%) than only wind farm (51%-52%).
- The inclusion of a storage system could reduce the curtailment of the hybrid wind-solar power plant in approximately 50%.

- A demand deviation index is defined so that 0% corresponds to complete match between
 the electricity demand profile and the renewable generation profile. The demand deviation
 index shows a significant reduction for hybridized wind-solar plants compared to wind
 farms only (from 61%-65% for wind farms, to 45%-49% for wind farms hybridized with
 250MW solar without tracking, and to 44%-47% for wind farms hybridized with 250MW
 solar with tracking).
- The combination of the generation from all three locations (portfolio effect) resulted in the largest reduction of the mismatch between the renewable power generation and the demand, with the demand deviation index of around 35%-36%.

7 Conclusion

This report presents a preliminary feasibility study for three hypothetical wind farms in Ukraine. The work involved the identification of wind power potential and main wind characteristics of the region, the creation of a GIS workspace to aggregate all relevant information, the application of procedures for selecting the most suitable areas, simulation of wind farms with a microscale flow model, estimation of a minimum price at which energy produced must be sold for the wind projects, and an assessment of system integration aspects of variable renewable energy generation using generation annual generation time series in hourly resolution.

DTU Wind has been helping the wind industry to develop tools and methods for wind farm development based on state-of-the-art technology. This work involves the application of two software developed and owned by DTU Wind: WAsP and CorRES, and a free access web tool and datasource developed and owned by DTU Wind: the Global Wind Atlas (GWA).

This work only applies to three provinces of Ukraine: Chernihiv, Kirovohrad, and Ternopil. The results cannot be extrapolated to other regions without conducting similar analyses.

The wind characteristics over the provinces have been obtained from the GWA, including mean wind speed, mean wind power density, and mean wind power rose. The areas with good wind resources have been identified as candidates for wind energy projects.

Geospatial assessment was used to select suitable areas with the most feasible characteristics for wind farm projects, such as having a combination of good wind potential, proximity to the grid and adequate orographic features, while respecting some site-specific constraints to minimize the potential negative impact of future wind farms on the environment, culture, security, and social and commercial activities.

Three hypothetical wind farms were modelled using the industry-standard wind resource assessment software WAsP with inputs (wind data, meteorological parameters, orography, and surface roughness) obtained directly from the GWA. The wind farms, with approximately 250 MW nominal capacity each, were investigated regarding their estimated performance – annual energy production and capacity factor – and the levelized cost of energy. A capacity factor of 48.3% was determined for the Kirovohrad site, 46.9% for the Ternopil site and 46.1% for the Chernihiv site.

The databases and the procedure used for the geospatial analysis and wind farm simulations are made available by DTU Wind. They may be used in the future to enhance the current study, consider new or different constraints, include other areas, select a different wind turbine model, have access to site and project-specific data, etc.

DTU Wind recommends to carry out a site-specific measurement campaign following the international standard IEC 61400-50-1 and the MEASNET procedure "Evaluation of Site Specific Wind Conditions". Two locations were chosen for measurement stations in each province, one inside the hypothetical wind farm, a location that would be relevant for the final design of the

wind farm, and another one to cover an extended region of the province, which could be useful for a potential validation of the global wind atlas when combined with the measurements of the first location.

The DTU Wind analysis indicates that the LCOE for the wind projects in Ukraine have lower costs compared to the Urgent Ukraine Technology Catalogue. The LCOE for the Kirovohrad site is 44.7 €/MWh, 46.0 €/MWh for Ternopil and 46.8 €/MWh for Chernihiv. The comparison with German and UK's markets highlights that Ukraine's LCOE is more competitive than Germany's but remains higher than the UK's. It is noteworthy that CapEx and OpEx are lower in Ukraine than in Germany and UK, but the cost reduction will most heavily depend on the significantly higher capacity factors in Ukraine, which rivals offshore locations in Germany and UK. These cost reducing aspects are somewhat offset by significantly higher financing costs, which account for almost 40% of overall project costs, which is double the share in Germany and UK. While Ukraine benefits from lower capital investment requirements, its higher financing burden remains a key challenge, emphasising the need for improved access to low-cost capital and more favourable debt terms to reduce overall LCOE.

The wind generation time series simulations using DTU's CorRES was used to assess system integration aspects of variable renewable energy generation. There is a moderate year-to-year variation of energy generation and the correlations of hourly time series between the sites are relatively low (on average around 0.45) indicating a potential significant geographical smoothening in wind generation, reducing the likelihood of zero aggregate generation.

The analysis of wind generation time series and solar photovoltaic (PV) generation time series - both calculated by CorRES for the same site location allows us to preliminary study the potential complementarity of wind and solar technologies. Negative correlation between wind and solar generation is observed in all three sites. Calculations assuming 100% availability of wind turbines and solar PV systems and grid capacity equal to the wind farm rated power show that hybridization wind farms with solar PV might result in approximately 2% to 6% curtailment depending on the size of the solar PV plant. The inclusion of a storage system could reduce the curtailment of the PV-hybridized wind farms in approximately 50%.

The grid capacity is better utilised if the wind farms are hybridized with PV. The grid utilization factor of hybridized wind farms is higher (62% -64%) than only wind farms (51% -52%).

A demand deviation index is defined so that 0% corresponds to complete match between the electricity demand profile and the renewable generation profile. The demand deviation index shows a significant reduction for a combination (sum) of the wind generation of the three wind farms. The demand deviation index drops from 61%-65% (individual wind farms) to around 47% for the combined wind generation. If a 250MW solar PV system is added to each wind farm (hybridization with solar PV only) the combined renewable energy generation results in a demand deviation index of around 35%-36%.

The results of this early-stage study should only be interpreted as guidance due to variability in wind energy deployment methods, along with the evolution of technology and changes in costs. The values discussed here can be considered as rough yet qualified estimates of different

installed capacity scenarios, given the applied constraints.

The main recommendations are a) to carry out feasibility studies considering the hybridization of wind farms with PV and batteries due to the complementarity of the two sources; and b) to plan the development of renewable energy projects in different provinces to take advantage of the smoothening effect caused by differences in wind speed variations in different regions of the country.

References

- [1] Neil N. Davis et al. "The Global Wind Atlas: A high-resolution dataset of climatologies and associated web-based application". In: *Bulletin of the American Meteorological Society* 104.8 (2023), E1507–E1525. url: https://doi.org/10.1175/BAMS-D-21-0075.1 (cit. on pp. 1, 3, 11, 16).
- [2] The World Bank. *World Bank Official Administrative Boundaries*. Online. May 2025. url: https://datacatalog.worldbank.org/search/dataset/0038272/World-Bank-Official-Boundaries (cit. on pp. 1, 2).
- [3] DTU. *Global Wind Atlas Methodology*. Online. July 2025. url: https://globalwindatlas.info/en/about/method (cit. on pp. 6, 21).
- [4] WASP. Online. url: https://www.wasp.dk (cit. on pp. 6, 20).
- [5] UNEP-WCMC and IUCN (2024). Protected Planet: The World Database on Protected Areas (WDPA) and World Database on Other Effective Area-based Conservation Measures (WD-OECM). Cambridge, UK: UNEP-WCMC and IUCN. Online. Nov. 2024. url: http://protectedplanet.net/ (cit. on pp. 10, 12, 16).
- [6] N. M. Moskalchuk and Ya. O. Adamenko. "The wind farm site selection on GIS-based approach". In: Scientific Bulletin of UNFU 29.6 (2019), pp. 71–75. url: https://doi.org/10.15421/40290614 (cit. on pp. 11, 14).
- [7] GLOBIO. *Global Roads Inventory Project (GRIP) Dataset*. Online dataset. Accessed: 2024-11-27. 2024. url: https://www.globio.info/download-grip-dataset (cit. on pp. 11, 12, 16).
- [8] MegaObzor. *Maps of Railways in Ukraine*. Online resource. Accessed: 2024-11-27. 2024. url: https://megaobzor.net/kartyi-zheleznyih-dorog-ukrainyi/ (cit. on pp. 11, 13, 16).
- [9] Google. Google Earth. https://www.google.com/earth. Accessed: 2024-11-27. n.d. (Cit. on pp. 11, 13).
- [10] OpenFlights. *OpenFlights: Airport, Airline, and Route Data*. Online. Available at: https://openflights.org. N/A: OpenFlights, Mar. 2024 (cit. on pp. 13, 14).
- [11] European Space Agency (ESA). *ESA WorldCover: Worldwide land cover mapping*. Online. Available at: https://esa-worldcover.org/en. Nov. 2024 (cit. on pp. 13, 15, 16).
- [12] ATOM. Location of Nuclear Reactors in Ukraine. Online. © Atom.org.ua Nuclear Energy in Ukraine and the World 2007-2025. Available at: https://atom.org.ua/map. Atom.org.ua Nuclear Energy in Ukraine and the World, 2024 (cit. on p. 14).
- [13] Energo.ua. *About Energo.ua*. Online. The project is dedicated to increasing transparency for the Ukrainian renewable energy market. Available at: https://www.energo.ua/ua/assets#google_vignette. Energo.ua, 2024 (cit. on p. 14).
- [14] Nature Reserve Fund of Ukraine. *Nature Reserve Fund of Ukraine*. Online. Available at: https://wownature.in.ua/en/. Ministry of Environmental Protection of Ukraine, 2024 (cit. on p. 14).

- [15] Oleksandr Bobko et al. *Seasonal Bird Migration Map of Ukraine*. Online. Available at: https://pernatidruzi.org.ua/karta_sezonnykh_mihratsiy_ptakhiv.html. Pernati Druzi, Mar. 2024 (cit. on p. 15).
- [16] OpenFlights. *Airports*. Accessed in 15-11-2023. Online. 2017. url: Accessed%20from%20% 5Curl%7Bhttps://openflights.org/%7D (cit. on p. 16).
- [17] OpenInfrastructureMap. *Electricity grid*. https://www.openinframap.org/. Accessed: 2024-11 (cit. on p. 16).
- [18] P.J. Volker et al. "Prospects for generating electricity by large onshore and offshore wind farms". In: *Environmental Research Letters* 12 (2017), p. 034022 (cit. on p. 16).
- [19] Ib Troen and Erik Lundtang Petersen. *European Wind Atlas*. Risø National Laboratory Denmark, 1989 (cit. on p. 21).
- [20] Ib Troen. A high resolution spectral model for flow in complex terrain. 1990, pp. 417–420 (cit. on p. 21).
- [21] Ole Steen Rathmann et al. *The Park2 Wake Model Documentation and Validation*. Tech. rep. DTU Wind Energy, 2018 (cit. on p. 23).
- [22] Jake Badger et al. CREYAP 2021. Tech. rep. DTU Wind Energy, 2021 (cit. on pp. 25, 26).
- [23] W. Short, D. J. Packey, and T. Holt. *A Manual for the Economic Evaluation of Energy Efficiency and Renewable Energy Technologies*. Technical Report NREL/TP-462-5173. NREL, 1995. doi: 10.2172/35391. url: http://www.osti.gov/servlets/purl/35391-NqycFd/webviewable/ (cit. on p. 30).
- [24] IRENA. *Renewable Power Generation Costs in 2023*. 2024. url: https://www.irena.org/ Publications/2024/Sep/Renewable-Power-Generation-Costs-in-2023 (cit. on pp. 30–32).
- [25] Danish Energy Agency et al. *Ukraine Urgent Technology Catalogue*. 2024. url: https://www.ea-energianalyse.dk/wp-content/uploads/2024/04/Ukraine_urgent_technology_catalogue.pdf (cit. on p. 30).
- [26] G. Smart et al. *IEA Wind Task 26: Offshore Wind Farm Baseline Documentation*. Technical Report NREL/TP–6A20-66262. NREL, 2016. doi: 10.2172/1259255. url: http://www.osti.gov/servlets/purl/1259255/ (cit. on p. 31).
- [27] T. Stehly, P. Duffy, and D. M. Hernando. *Cost of Wind Energy Review: 2024 Edition*. 2024 (cit. on pp. 31, 32).
- [28] A. Damodaran. *Country Default Spreads and Risk Premiums*. 2024. url: https://pages.stern.nyu.edu/~adamodar/New_Home_Page/datafile/ctryprem.html (cit. on p. 32).
- [29] A. Damodaran. *Country Risk: Determinants, Measures, and Implications The 2024 Edition*. 2024. url: https://doi.org/10.2139/ssrn.4896539 (cit. on p. 32).
- [30] IRENA. *The Cost of Financing for Renewable Power*. 2023. url: https://www.irena.org/-/media/Files/IRENA/Agency/Publication/2023/May/IRENA_The_cost_of_financing_renewable_power_2023.pdf (cit. on pp. 32, 33).
- [31] A. Damodaran. *Damodaran On-line Home Page*. url: https://pages.stern.nyu.edu/~adamodar/New_Home_Page/home.htm (cit. on pp. 32, 33).
- [32] European Central Bank. *Official interest rates*. 2025. url: https://www.ecb.europa.eu/stats/policy_and_exchange_rates/key_ecb_interest_rates/html/index.en.html (cit. on p. 33).

- [33] National Bank of Ukraine. *Inflation Report January* 2025 Summary. 2025. url: https://bank.gov.ua/admin_uploads/article/IR_2025-Q1_eng.pdf?v=9 (cit. on p. 33).
- [34] CorRes webpage. url: https://corres.windenergy.dtu.dk (cit. on p. 36).
- [35] CorRes projects. url: https://corres.windenergy.dtu.dk/projects (cit. on p. 36).
- [36] TYNDP webpage. url: https://tyndp.entsoe.eu (cit. on p. 36).
- [37] ERAA webpage. url: https://WWW.entsoe.eu/outlooks/eraa/ (cit. on p. 36).
- [38] J. P. Murcia and et al. "Validation of European-scale simulated wind speed and wind generation time series". In: *Applied Energy* (2022). doi: 10.1016. url: https://doi.org/10.1016/j.apenergy.2021.117794) (cit. on pp. 36, 37).
- [39] Reanalysis Project at ECMWF webpage. url: https://www.ecmwf.int/en/forecasts/dataset/ecmwf-reanalysis-v5 (cit. on p. 36).
- [40] M. J. Koivisto and et al. "Minimizing Variance in Variable Renewable Energy Generation in Northern Europe". In: *IEEE International Conference on Probabilistic Methods Applied to Power Systems*. 2018. url: https://doi.org/10.1109/PMAPS.2018.8440369 (cit. on p. 41).

Appendix

A.1 WAsP inputs: elevation and land cover maps

The elevation and roughness maps can be seen in Figure A.1, Figure A.2, Figure A.3, Figure A.4, Figure A.5, and Figure A.6. The coordinate system is based on the WGS-84 datum, UTM zone 35 and UTM zone 36.



Figure A.1: Elevation for Chernihiv site

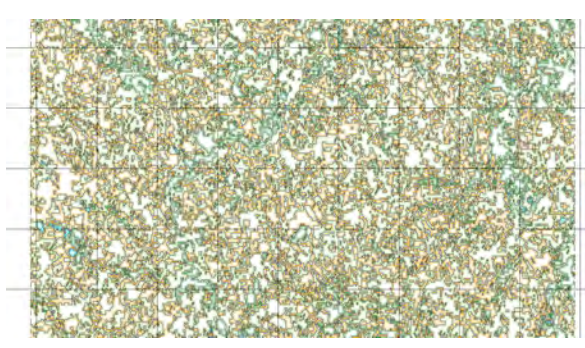


Figure A.2: Roughness for Chernihiv site

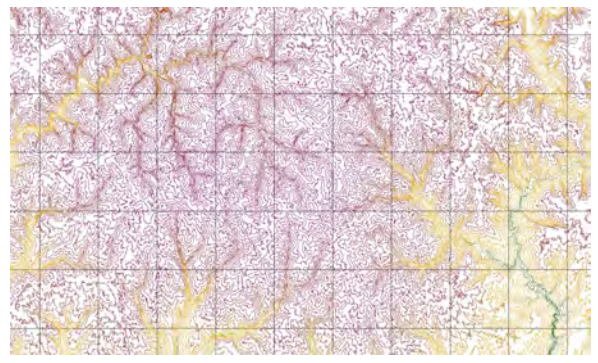


Figure A.3: Elevation for Kirovohrad site

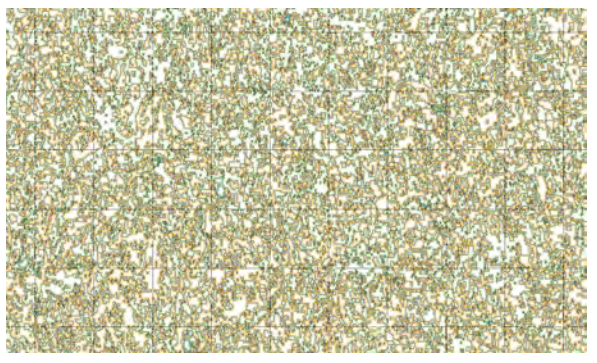


Figure A.4: Roughness for Kirovohrad site

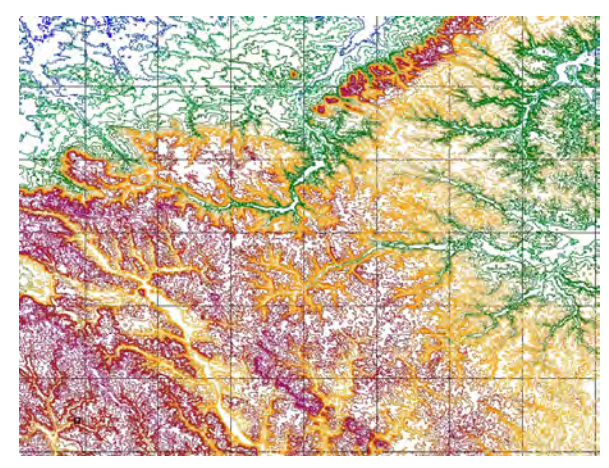


Figure A.5: Elevation for Ternopil site

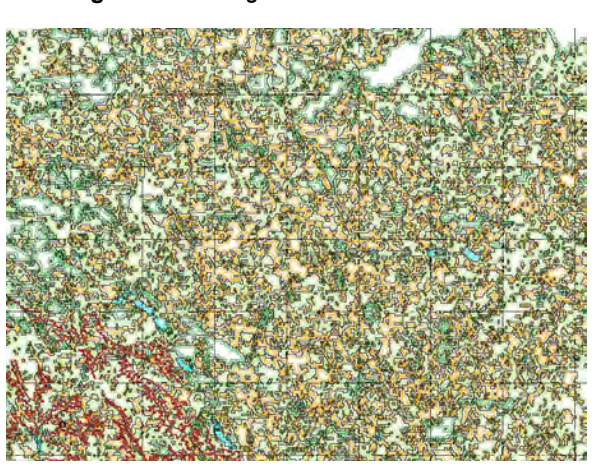


Figure A.6: Roughness for Ternopil site

A.2 CorRES inputs: wind farm power curves

The plant-level power curve for each wind farm is calculated using the WAsP software with the following basic inputs: orography and roughness digital maps, wind turbine power curve and hub height, wind farm layout, and the wind climate information derived from GWA for a reference position in the center of the wind farm.

The power curve for the Chernihiv wind farm is presented in Figure A.7. The power curve for the Kirovohrad wind farm is presented in Figure A.8. The power curve for the Ternopil wind farm is presented in Figure A.9. The values are total wind farm power in MW, for 60 direction bins and 26 wind speed bins.

	2	3	4	5	6	7	8	9	10	11	12	13	14	15	16	17	18	19	20	21	22	23	24	25	26	27
1 (0°)	0.0	1.9	15.9	33.9	60.3	97.0		201.5	237.7	246.4	247.5		247.5		247.5		237.0	218.2	195.3	171.4	148.0	122.4	48.2	18.8	2.1	0.0
2 (6°)	0.0	2.1	16.1	34.2	60.9	97.9		202.4	236.9	246.3	247.4	247.5	247.5	247.5	247.5	246.4	236.9	218.1	195.3	171.3	148.0	122.4	48.2	18.8	2.1	0.0
3 (12°)	0.0	2.1	16.1	34.3	61.0	98.1	_	202.2	237.0			247.5	247.5	247.5	247.5	246.4	236.9	218.1	195.3	171.3	148.0	122.4	48.2	18.8	2.1	0.0
4 (18°)	0.0	3.3	17.5	37.0	65.6	105.3		213.6	242.3	247.2		247.5	247.5	247.5	247.5	244.1	228.6	206.3	181.6	157.3	133.6	83.2	16.6	4.0	0.0	0.0
5 (24°)	0.0	3.1	17.1	36.2	64.3	103.3	_	211.7	242.1	247.2		247.5	247.5	247.5	247.5	244.3	228.7	206.5	181.7	157.4	133.7	87.1	16.6	4.0	0.0	0.0
6 (30°)	0.0	3.0	16.8	35.7	63.4	101.9	152.4	209.7	241.7	247.2	247.5	247.5	247.5	247.5	247.5	244.4	228.8	206.6	181.8	157.4	133.7	89.0	16.6	4.0	0.0	0.0
7 (36°)	0.0	3.3	17.3	36.5	64.9	104.2	155.5	212.2	242.0	247.2	247.5	247.5	247.5	247.5	247.5	244.2	228.7	206.4	181.6	157.3	133.7	87.0	16.5	4.0	0.0	0.0
8 (42°)	0.0	3.3	17.5	37.0	65.6	105.3	157.1	213.8	242.6	247.2	247.5	247.5	247.5	247.5	247.5	244.2	228.6	206.3	181.6	157.3	133.6	87.0	16.5	4.0	0.0	0.0
9 (48°)	0.0	4.2	18.6	39.0	69.1	110.8	165.1	221.8	244.7	247.4	247.5	247.5	247.5	247.5	247.3	241.5	222.3	198.6	173.1	148.7	125.3	55.1	2.0	0.0	0.0	0.0
10 (54°)	0.0	3.7	18.3	38.4	68.0	109.2	163.0	220.9	244.5	247.4	247.5	247.5	247.5	247.5	247.3	241.6	222.4	198.6	173.1	148.7	125.4	55.1	2.0	0.0	0.0	0.0
11 (60°)	0.0	3.8	17.8	37.6	66.7	107.0	159.9	217.7	244.1	247.4	247.5	247.5	247.5	247.5	247.3	241.7	222.6	198.8	173.3	148.8	125.4	55.1	2.0	0.0	0.0	0.0
12 (66°)	0.0	3.8	17.4	36.7	65.3	104.9	156.9	214.9	243.5	247.4	247.5	247.5	247.5	247.5	247.3	241.8	222.8	199.0	173.4	148.9	125.5	57.1	2.0	0.0	0.0	0.0
13 (72°)	0.0	3.9	17.3	36.5	64.9	104.3	156.0	213.4	243.2	247.3	247.5	247.5	247.5	247.5	247.3	241.7	222.8	199.0	173.5	149.0	125.6	57.1	2.0	0.0	0.0	0.0
14 (78°)	0.0	8.0	14.2	30.8	55.0	88.6	133.0	187.9	233.3	246.2	247.5	247.5	247.5	247.5	247.5	247.3	241.7	223.7	201.4	177.2	153.8	131.2	95.1	5.9	0.0	0.0
15 (84°)	0.0	0.9	14.3	31.0	55.4	89.3	134.0	189.4	234.0	246.3	247.5	247.5	247.5	247.5	247.5	247.3	241.6	223.6	201.3	177.1	153.8	131.2	93.2	7.9	0.0	0.0
16 (90°)	0.0	0.9	14.1	30.6	54.7	88.2	132.3	187.2	233.0	246.2	247.5	247.5	247.5	247.5	247.5	247.3	241.7	223.7	201.4	177.2	153.9	131.2	93.2	7.9	0.0	0.0
17 (96°)	0.0	0.7	13.8	30.0	53.7	86.7	_	184.2	231.0	246.0		247.5	247.5		247.5	247.3		223.9	201.6	177.4	154.0	131.3	95.2	5.9	0.0	0.0
18 (102°)	0.0	0.8	13.8	30.3	54.1	87.3	_	185.5	231.7	246.0	247.5	247.5	247.5	247.5	247.5	247.3	241.8	223.8	201.5	177.3	153.9	131.2	95.2	5.9	0.0	0.0
19 (108°)	0.0	0.6	13.6	29.8	53.3	86.0		183.1	230.3	245.8	247.5	247.5	247.5	247.5	247.5	247.4	242.5	225.1	203.0	179.0	155.6	132.9	102.1	11.8	0.0	0.0
20 (114°)	0.0	0.6	13.8	30.1	53.9	86.9	_	184.5	231.7		247.5	247.5	247.5		247.5	247.4		225.0	202.9	178.9	155.5	132.9	102.1	11.8	0.0	0.0
21 (120°)	0.0	0.7	14.2	30.8	55.1	88.7		187.6	232.4	246.1	247.5	247.5	247.5	247.5	247.5	247.4	242.3	224.9	202.8	178.8	155.4	132.8	100.2	11.8	0.0	0.0
22 (126°)	0.0	0.8	14.2	30.8	55.0	88.6	_	187.3	232.3	246.1	247.5	247.5	247.5 247.5	247.5	247.5	247.4	242.3 242.5	224.9	202.8	178.8 179.0	155.5 155.6	132.8	100.2	11.8	0.0	0.0
23 (132°) 24 (138°)	0.0	0.8	13.7	29.8	53.3 51.2	82.6		183.0 176.1	224.4	245.8 244.4	247.5	247.5 247.5	247.5	247.5 247.5	247.5 247.5	247.4	243.4	228.9	203.0	184.5	161.1	138.6	100.2	11.8 39.2	0.0	0.0
25 (144°)	0.0	0.7	13.3	29.2	52.3	84.3		179.5	227.9	245.2	247.4	247.5	247.5	247.5	247.5	247.4	243.3	228.8	207.6	184.3	161.0	138.5	105.4	39.2	0.0	0.0
26 (150°)	0.0	0.3	13.4	29.5	52.8	85.1	_	181.1	228.7	245.3	247.4	247.5	247.5	247.5	247.5	247.4	243.3	228.7	207.5	184.2	160.9	138.4	103.4	39.1	0.0	0.0
27 (156°)	0.0	0.5	13.1	28.9	51.7	83.5		177.8	226.3	245.0	247.4	247.5	247.5	247.5	247.5	247.4	243.4	228.9	207.7	184.3	161.0	138.5	107.3	39.1	0.0	0.0
28 (162°)	0.0	0.4	13.0	29.0	52.0	83.8	_	178.6	226.7	245.1	247.4	247.5	247.5	247.5	247.5		243.4	228.8	207.6	184.3	161.0	138.5	107.2	39.1	0.0	0.0
29 (168°)	0.0	0.6	14.1	30.6	54.7	88.1		186.4	231.5	245.8			247.5	_	247.5		242.4	226.8	205.3	181.8	158.4	136.2	98.5	30.4	0.0	0.0
30 (174°)	0.0	0.8	14.5	31.3	55.8	89.8	_	189.4	233.1				247.5		247.5		242.3	226.7	205.1	181.7	158.3	136.1	96.5	30.4	0.0	0.0
31 (180°)	0.0	1.0	14.7	31.7	56.5	90.9	136.2	191.4	234.3	246.1	247.5	247.5	247.5	247.5	247.5	247.1	242.3	226.6	205.1	181.6	158.2	136.1	98.4	30.4	0.0	0.0
32 (186°)	0.0	1.1	14.9	32.0	57.0	91.7	137.3	192.5	234.2	246.1	247.5	247.5	247.5	247.5	247.5	247.1	242.2	226.6	205.0	181.6	158.2	136.1	98.4	32.3	0.0	0.0
33 (192°)	0.0	1.0	14.9	32.0	57.1	91.8	137.4	192.6	234.4	246.1	247.5	247.5	247.5	247.5	247.5	247.1	242.2	226.6	205.0	181.6	158.2	136.1	98.4	32.3	0.0	0.0
34 (198°)	0.0	3.7	17.7	37.3	66.2	106.2	158.3	214.7	242.2	247.1	247.5	247.5	247.5	247.5	247.4	243.0	227.1	204.9	180.2	155.9	132.6	78.1	19.2	4.1	0.0	0.0
35 (204°)	0.0	3.4	17.3	36.5	64.9	104.2	155.6	213.0	242.5	247.2	247.5	247.5	247.5	247.5	247.4	243.2	227.3	205.0	180.3	155.9	132.6	78.0	19.1	4.1	0.0	0.0
36 (210°)	0.0	3.5	17.0	35.9	63.9	102.7	153.5	211.4	242.4	247.2	247.5	247.5	247.5	247.5	247.4	243.3	227.4	205.1	180.4	156.0	132.6	78.0	19.1	4.1	0.0	0.0
37 (216°)	0.0	3.7	17.4	36.8	65.3	104.9		213.5	242.6				247.5	_	247.4	243.1	227.2	204.9	180.2	155.9	132.6	78.0	19.1	4.1	0.0	0.0
38 (222°)	0.0	3.7	17.7	37.3	66.1	106.2	_	215.2	242.9	247.2	247.5	247.5	247.5	247.5	247.4	243.1	227.1	204.9	180.2	155.8	130.6	78.0	19.1	4.1	0.0	0.0
39 (228°)	0.0	3.7	17.7	37.3	66.2	106.2		214.2	242.2	247.1	247.5	247.5	247.5		247.4	242.8	227.0	205.2	180.7	156.6	133.2	73.1	24.2	8.3	2.0	0.0
40 (234°)	0.0	3.6	17.4	36.7	65.1	104.6	_	212.9	242.2	247.1	247.5	247.5	247.5	247.5	247.4	243.0	227.1	205.3	180.8	156.7	133.3	71.2	24.2	8.3	2.0	0.0
41 (240°)	0.0	3.3	16.9	35.8	63.6	102.3		210.2	241.5	247.1	247.5	247.5	247.5	247.5	247.4	243.1	227.3	205.5	181.0	156.8	133.4	73.1	24.2	8.3	2.0	0.0
42 (246°)	0.0	3.4	16.5	35.1	62.4	100.4		206.7	240.6	247.0	247.5	247.5	247.5	247.5	247.4	243.2	227.5	205.7	181.1	156.9	133.5	69.3	24.2	8.3	2.0	0.0
43 (252°) 44 (258°)	0.0	3.4 1.3	16.4	34.9	62.1 55.5	99.8 89.5	_	205.1 189.2	240.2	247.0 246.3	247.5 247.5	247.5 247.5	247.5 247.5	247.5 247.5	247.4	243.2	227.6	205.8	181.2 199.8	157.0 175.7	133.5 152.3	71.3	74.3	8.3 16.1	0.0	0.0
44 (256) 45 (264°)	0.0	1.0	14.4	31.3	55.9	90.1		190.8	235.1	246.4	247.5	247.5	247.5	247.5	247.5	247.1	240.3	222.2	199.7	175.7	152.3	129.9	74.3	16.1	0.0	0.0
46 (270°)	0.0	1.3	14.3	30.9	55.2	89.0	_	188.7	234.0		247.5	247.5	247.5		247.5	247.1	240.2	222.3	199.8	175.7	152.3	130.0	74.3	18.0	0.0	0.0
47 (276°)	0.0	1.2	13.9	30.2	54.1	87.2		185.7	232.9		247.5	247.5	247.5	247.5	247.5	247.1	240.5	222.5	199.9	175.8	152.4	130.0	74.3	18.0	0.0	0.0
48 (282°)	0.0	1.4	14.0	30.5	54.6	88.0	_	186.8	233.2		247.5	247.5	247.5		247.5	247.1	240.4	222.4		175.8	152.4	130.0	72.4	18.0	0.0	0.0
49 (288°)	0.0	1.6	14.5	31.4	56.0	90.2		191.3	235.5	246.5			247.5				237.9	218.4		170.9	147.4	119.7	58.4	6.0	0.0	0.0
50 (294°)	0.0	1.6	14.7	31.8	56.7		137.0													_				6.0	0.0	0.0
51 (300°)	0.0	1.7	15.1	32.5	57.9	93.2	139.6	195.7	236.7	246.6	247.5	247.5	247.5	247.5	247.5	246.6	237.7	218.2	195.0	170.7	147.3	119.7	58.4	6.0	0.0	0.0
52 (306°)	0.0	1.7	15.1	32.4	57.8	93.1	139.5	195.2	236.6	246.6	247.5	247.5	247.5	247.5	247.5	246.6	237.7	218.2	195.0	170.7	147.3	119.7	58.4	6.0	0.0	0.0
53 (312°)	0.0	1.3	14.5	31.4	56.1	90.5	135.8			246.5	247.5	247.5	247.5	247.5	247.5	246.6	237.9	218.4	195.2	170.9	147.4	119.7	58.4	6.0	0.0	0.0
54 (318°)	0.0	1.8	14.5	31.4	56.1	90.4	-	191.5				_	_	_			237.1		193.5	_	_	123.5	41.6	9.9	0.0	0.0
55 (324°)	0.0	2.0	15.0	32.2	57.5	92.6		195.1					247.5						193.3			123.4	39.7	9.9	0.0	0.0
56 (330°)	0.0	2.1	15.2	32.7	58.3	93.8		195.8					247.5						193.3	_	_	123.4	43.6	9.9	0.0	0.0
57 (336°)	0.0	2.1	14.8	32.0	57.2	92.1		192.5	_				247.5				_		193.4			123.5	45.6	9.9	0.0	0.0
58 (342°)	0.0	2.1	14.9	32.2	57.4	92.4	-	193.3					247.5					216.9		169.0		123.5	43.6	9.9	0.0	0.0
59 (348°)	0.0	2.0	15.3	32.8	58.4	94.0	140.8											_	195.6			122.6	48.2	18.8	2.1	0.0
60 (354°)	0.0	1.9	15.6	33.4	59.5	95.7	143.2	199.4	23/.1	246.5	247.5	247.5	247.5	247.5	241.5	246.5	23/.1	218.3	195.5	1/1.4	148.1	122.5	48.2	18.8	2.1	0.0

Figure A.7: Plant level power curve for Chernihiv. Values in MW calculated with WAsP. Wind speed bins (first row) in m/s, direction bins (first column) in degrees.

100		2	3	4	5	6	7	8	9	10	11	12	13	14	15	16	17	18	19	20	21	22	23	24	25	26	27
	1 (0°)		_		_	_			_						-												
						_	_		_				_				_										
Heart 10			_			_	_				_		_									_					_
Fig8 10		0.0	2.3	16.9	35.8	63.7	102.2	152.5	209.2	240.8	247.0	247.5	247.5	247.5	247.5	247.5	246.6	237.0	216.9	193.6	169.3	145.2	120.2	48.4	0.0	0.0	0.0
Fig. 10	5 (24°)	0.0	2.3	16.8	35.6	63.2	101.5	151.5	208.4	240.7	247.0	247.5	247.5	247.5	247.5	247.5	246.7	237.1	216.9	193.7	169.3	145.2	120.2	48.4	0.0	0.0	0.0
9 (42) 00 0 12 199 192 345 61 391 82 345 934 301 8 152 289 249 247 247 2475 2475 2475 2475 2475 2475 2	6 (30°)	0.0	2.2	16.7	35.4	63.0	101.1	151.0	208.1	240.6	247.0	247.5	247.5	247.5	247.5	247.5	246.7	237.1	216.9	193.7	169.3	145.2	122.1	48.4	0.0	0.0	0.0
9 (48) 9 (48) 9 (48) 9 (48) 9 (48) 9 (48) 9 (48) 2	7 (36°)	0.0	2.4	16.7	35.4	62.9	101.1	150.9	208.2	240.8	247.0	247.5	247.5	247.5	247.5	247.5	246.7	237.1	216.9	193.7	169.3	145.2	122.1	48.4	0.0	0.0	0.0
19 19 19 19 19 18 18 18 19 19 20	8 (42°)	0.0	2.4	16.9	35.7	63.4	101.8	152.0	208.9	240.7	247.0	247.5	247.5	247.5	247.5	247.5	246.7	237.0	216.9	193.6	169.3	145.2	122.1	50.4	0.0	0.0	0.0
1 1 1 1 1 1 1 1 1 1		0.0			_		_																	_	_		_
					_	_	_		_								_										_
1			_			_	_				_													_	_		_
					_	_	_							_	-		_	_									_
15 16 17 18 18 18 18 18 18 18							_				_																_
1					_		_																	_			_
							_																				_
16 16 16 16 16 16 16 16						_	_										_							_			_
19 1 1 1 1 1 1 1 1 1 1 1 1 1 1 1 1 1 1					_	_	_																				_
					_	_	_										_							_	_		_
2					_	_	_		_				_				_										_
24 13 25 27 27 28 28 28 28 28 28	21 (120°)	0.0	1.1	14.4	31.2	55.7	89.6	134.3	188.5	231.9	245.8	247.5	247.5	247.5	247.5	247.5	247.3	242.9	227.9	206.6	183.3	159.8	136.4	87.8	36.4	0.0	0.0
24 143 0.0	22 (126°)	0.0	1.1	14.5	31.2	55.7	89.7	134.4	188.9	232.5	245.9	247.5	247.5	247.5	247.5	247.5	247.3	242.9	227.9	206.6	183.3	159.8	136.4	87.8	36.4	0.0	0.0
	23 (132°)	0.0	1.2	14.5	31.2	55.8	89.8	134.5	189.0	232.8	245.9	247.5	247.5	247.5	247.5	247.5	247.3	242.9	227.9	206.6	183.3	159.8	136.4	87.8	38.4	0.0	0.0
							_																				_
					_	_	_																	_			_
28 16 18 18 18 18 18 18 1					_	_	_		_		_		_														_
					_	_	_								_		_					_		_	_		_
30 (174") 0.0 17 153 329 586 93 4141 970 235 2464 275 2475 2475 2475 2475 2475 2486 285 2193 1963 1721 1480 1247 614 39 00 0.0 0.0 1161 158 383 80 2 988 1448 2011 237 2465 2475 2475 2475 2475 2475 2475 2475 2486 283 2191 1961 1719 1479 1246 834 39 00 0.0 0.0 33 (192") 0.0 15 165 350 623 1901 494 2060 236 2468 2475 2475 2475 2475 2475 2475 2475 2487 2881 2188 1959 1717 1477 1245 613 39 00 0.0 34 (198") 0.0 2.1 165 36 0.0 0.2 999 1491 2058 297 2469 2475 2475 2475 2475 2475 2475 2475 2487 2881 2188 1959 1717 1477 1245 613 39 0.0 0.0 36 (204") 0.0 2.1 165 36 0.0 0.2 999 1491 2058 297 2469 2475 2475 2475 2475 2475 2475 2475 2475					_	_	_						_														_
31 (180°) 00 15 168 338 602 968 1448 2011 2372 2465 2475 2475 2475 2475 2475 2475 2475 247			_		_	_	_															_		_			_
32 (186°) 0.0 1.8 16.4 34.8 61.9 94. 148.5 205.2 239.2 248.8 247.5					_	_	_										_	_									_
33 (192°) 0.0 1.5 16.5 35.0 62.3 10.1 149.4 26.0 239.6 24.8 247.5	· ,						_				_																_
$ \begin{array}{c c c c c c c c c c c c c c c c c c c $						_	_										_							_			_
36 (210°) 0.0 2.1 16.4 34.8 61.9 99.4 148.6 205.5 2397 248.9 247.5		0.0	2.0	16.6	35.2	62.6	100.5	150.0	206.8	240.0	246.9	247.5	247.5	247.5	247.5	247.5	246.7	238.0	219.0	196.1	172.0	147.9	123.2	54.4	8.0	0.0	0.0
37 (216°) 0.0 2 2 164 348 619 995 1486 2055 2397 2468 2475 2475 2475 2475 2475 2475 2467 2380 2191 1962 1721 1480 1232 545 80 0.0 0.0 0.0 38 (222°) 0.0 21 165 351 624 1001 1495 2063 2398 2469 2475 2475 2475 2475 2475 2475 2476 2487 2380 2190 1961 1721 1480 1232 545 80 0.0 0.0 0.0 39 (228°) 0.0 3.1 175 37.0 666 650 1042 1553 2111 2411 2470 2475 2475 2475 2475 2475 2475 2475 2475	35 (204°)	0.0	2.1	16.5	35.0	62.2	99.9	149.1	205.8	239.7	246.9	247.5	247.5	247.5	247.5	247.5	246.7	238.0	219.0	196.2	172.1	148.0	123.2	54.5	8.0	0.0	0.0
38 (222°) 0.0 2.1 16.5 35.1 62.4 100.1 149.5 266.3 239.8 246.9 247.5 247	36 (210°)	0.0	2.1	16.4	34.8	61.9	99.4	148.6	205.5	239.7	246.9	247.5	247.5	247.5	247.5	247.5	246.7	238.0	219.1	196.2	172.1	148.0	123.2	54.5	8.0	0.0	0.0
39 (228°) 0.0 3.1 174 36.6 65.0 104.2 155.3 211.1 241.1 247.0 247.5 247.	37 (216°)	0.0	2.2	16.4	34.8	61.9	99.5	148.6	205.5	239.7	246.8	247.5	247.5	247.5	247.5	247.5	246.7	238.0	219.1	196.2	172.1	148.0	123.2	54.5	8.0	0.0	0.0
$ \begin{array}{c ccccccccccccccccccccccccccccccccccc$		0.0	2.1	16.5	35.1	62.4	100.1	149.5	206.3	239.8	246.9	247.5	247.5	247.5	247.5	247.5	246.7	238.0	219.0	196.1	172.1		123.2	54.5	8.0	0.0	0.0
41 (240°) 0.0 28 17.4 36.7 66.1 10.4 165.5 211.8 241.3 247.0 247.5 247.5 247.5 247.5 247.4 245.1 234.4 214.4 191.1 166.7 142.9 101.0 49.9 2.0 0.0 0.0 42 (246°) 0.0 2.7 17.1 36.1 64.1 10.2 153.5 210.6 241.1 247.0 247.5 247.5 247.5 247.5 247.4 245.2 234.5 214.5 191.2 166.8 142.9 101.0 49.9 2.0 0.0 0.0 43 (252°) 0.0 2.7 16.8 36.6 63.3 101.6 151.7 208.2 240.6 247.0 247.5 247.5 247.5 247.5 247.5 247.4 245.2 234.6 214.7 191.3 166.9 143.0 101.0 49.9 2.0 0.0 0.0 44 (258°) 0.0 3.1 17.0 35.9 63.8 102.5 153.0 210.4 241.7 247.1 247.5					_	_	_										_	_						_			_
42 (246°) 0.0 27 17.1 36.1 64.1 102.9 153.5 210.6 241.1 247.0 247.5 247.5 247.5 247.5 247.5 247.4 245.2 234.5 214.5 191.2 166.8 142.9 101.0 49.9 2.0 0.0 0.0 43 (252°) 0.0 27 16.8 35.6 63.3 101.6 151.7 208.2 240.6 247.0 247.5 247.5 247.5 247.5 247.5 247.2 245.2 234.6 214.7 191.3 166.9 143.0 101.0 49.9 2.0 0.0 0.0 44 (258°) 0.0 3.1 17.0 35.9 63.8 102.5 153.0 210.4 241.7 247.1 247.5 2							_				_																_
43 (252°) 0.0 27 16.8 35.6 63.3 101.6 151.7 208.2 240.6 247.0 247.5 247.					_	_	_										_	_						_			_
44 (258°) 0.0 3.3 17.3 36.6 64.9 104.2 155.4 212.2 242.0 247.2 247.5 247							_																				_
45 (264°) 0.0 3.1 17.0 35.9 63.8 102.5 153.0 210.4 241.7 247.1 247.5 247					_		_																	_			_
46 (270°) 0.0 3.2 17.2 36.3 64.5 103.6 154.7 212.2 242.1 247.2 247.5 247	· · ·				_	_	_				_																_
47 (276°) 0.0 3.0 17.0 35.9 63.9 102.6 153.2 210.7 241.7 247.2 247.5 247					_	_	_																	_	_		_
48 (282°) 0.0 3.2 16.8 36.6 63.3 101.7 151.8 208.8 241.2 247.1 247.5 247					_	_	_		_				_														_
49 (288°) 0.0 3.1 165 35.0 624 1002 1497 206.6 240.6 247.0 247.5 2			_			_	_				_											_		_	_		_
51 (300°) 0.0 3.3 16.8 35.6 63.2 101.5 151.4 206.4 239.7 246.9 247.5 247	49 (288°)	0.0	3.1	16.5	35.0	62.4	100.2	149.7	206.6	240.6	247.0	247.5	247.5	247.5	247.5	247.4	245.2	233.0	211.8	187.9	163.2	138.9	98.9	28.6	0.0	0.0	0.0
$\begin{array}{cccccccccccccccccccccccccccccccccccc$	50 (294°)	0.0	3.0	16.5	35.1	62.4	100.3	149.8	205.6	239.5	246.9	247.5	247.5	247.5	247.5	247.4	245.1	233.0	211.9	187.9	163.3	139.0	99.0	28.6	0.0	0.0	0.0
53 (312°) 0.0 3.1 16.8 35.6 63.2 101.5 151.5 208.0 247.0 247.5 24	51 (300°)	0.0	3.3	16.8	35.6	63.2				239.7	246.9	247.5	247.5	247.5	247.5	247.4	245.0	232.9	211.8	187.9	163.2	138.9	99.0	28.6	0.0	0.0	0.0
54 (318°) 0.0 3.0 16.4 34.8 61.9 995 148.7 204.8 2398 247.0 247.5							_					_								-							_
55 (324°) 0.0 3.2 16.6 35.3 62.8 100.9 150.6 206.5 240.2 247.0 247.5 247							_						_														_
56 (330°) 0.0 2.9 17.1 36.1 64.1 102.9 153.6 210.5 241.4 247.1 247.5 247																				_						_	_
57 (336°) 0.0 3.0 17.2 36.4 64.6 103.7 154.7 211.7 241.5 247.1 247.5 247																				_							_
58 (342°) 0.0 3.2 16.9 35.9 63.8 102.4 152.8 209.5 240.9 247.0 247.5 247.5 247.5 247.5 247.5 247.5 247.5 247.5 247.1 240.3 222.1 199.5 175.4 151.5 127.9 66.9 2.0 0.0 0.0 59 (348°) 0.0 1.6 14.9 32.2 57.4 92.4 138.4 193.4 234.0 246.3 247.5 247.5 247.5 247.5 247.5 247.5 247.5 247.1 240.3 222.1 199.5 175.4 151.5 127.9 66.8 2.0 0.0 0.0 60 (354°) 0.0 1.6 14.9 32.2 57.4 92.4 138.4 193.4 234.0 246.3 247.5 247.5 247.5 247.5 247.5 247.5 247.1 240.3 222.1 199.6 175.5 151.5 127.9 68.8 2.0 0.0 0.0 0.0 0.0 0.0 0.0 0.0 0.0 0.0						_																_					
59 (348°) 0.0 1.8 15.0 32.3 57.6 92.7 138.8 193.7 234.4 246.3 247.5 247.5 247.5 247.5 247.5 247.1 240.3 222.1 199.5 175.4 151.5 127.9 66.9 2.0 0.0 0.0 60 (354°) 0.0 1.6 14.9 32.2 57.4 92.4 138.4 193.4 234.0 246.3 247.5 247.5 247.5 247.5 247.5 247.5 247.1 240.3 222.1 199.6 175.5 151.5 127.9 68.8 2.0 0.0 0.0					_												_										_
60 (354°) 0.0 1.6 14.9 32.2 57.4 92.4 138.4 193.4 234.0 246.3 247.5 247.5 247.5 247.5 247.1 240.3 222.1 199.6 175.5 151.5 127.9 68.8 2.0 0.0 0.0																											_
					_												_									_	_
	. ,						-						-				-										

Figure A.8: Plant level power curve for Kirovohrad. Values in MW calculated with WAsP. Wind speed bins (first row) in m/s, direction bins (first column) in degrees.

	2	3	4	5	6	7	8	9	10	11	12	12	14	15	16	17	10	19	20	21	22	23	24	25	26	27
1 (0°)	0.0	4.3	18.4	38.5	68.3	109.5	163.1	219.7	243.9	11 247.3	12 247.5	13 247.5	14 247.5	15 247.5	247.4	243.5	18 227.2	204.6	179.8	154.5	128.7	65.1	6.3	0.0	0.0	0.0
2 (6°)	0.0	4.1	18.3	38.4	68.1	109.1	162.6	219.2	243.7	247.3		247.5	247.5	247.5	247.4	243.5	227.2	204.6	179.8	154.5	128.7	65.1	6.3	0.0	0.0	0.0
3 (12°)	0.0	3.9	18.1	37.9	67.3	107.9	160.8		243.4		247.5	247.5	247.5		247.4	243.5		204.7	179.9	154.6	128.8	65.2	6.3	0.0	0.0	0.0
4 (18°)	0.0	4.3	18.1	38.0	67.4	108.1	161.1	217.6	243.5		247.5	247.5	247.5		247.4	_	225.2	202.1	177.0	151.4	126.2	52.4	8.0	0.0	0.0	0.0
5 (24°)	0.0	3.9	17.1	36.2	64.3	103.3	154.5		241.7	247.2		247.5			247.4		225.6	202.5	177.3	151.7	126.4	52.5	8.0	0.0	0.0	0.0
6 (30°)	0.0	3.6	16.3	34.8	61.9	99.5	149.0	206.1	240.1	247.1		247.5			247.4	_	225.9	202.8		151.9	126.5	52.5	8.0	0.0	0.0	0.0
7 (36°)	0.0	3.4	16.3	34.7	61.8	99.4	149.1	207.5	241.7	247.2	247.5	247.5	247.5	247.5	247.4	242.9	225.8	202.7	177.5	151.9	126.5	52.5	8.0	0.0	0.0	0.0
8 (42°)	0.0	3.4	16.7	35.5	63.2	101.6	152.2	210.8	242.4	247.3	247.5	247.5	247.5	247.5	247.4	242.8	225.7	202.6	177.4	151.8	126.4	52.5	8.0	0.0	0.0	0.0
9 (48°)	0.0	2.9	16.2	34.5	61.4	98.8	148.1	205.2	239.9	247.0	247.5	247.5	247.5	247.5	247.4	243.5	228.6	206.6	182.0	156.6	129.5	75.3	14.8	4.0	0.0	0.0
10 (54°)	0.0	3.0	16.5	35.1	62.5	100.5	150.5	208.3	241.2	247.1	247.5	247.5	247.5	247.5	247.4	243.5	228.5	206.4	181.9	156.4	129.3	75.3	14.8	4.0	0.0	0.0
11 (60°)	0.0	2.7	16.5	35.1	62.4	100.4	150.4	208.2	241.1	247.1	247.5	247.5	247.5	247.5	247.4	243.4	228.4	206.4	181.9	156.5	129.4	75.3	14.8	4.0	0.0	0.0
12 (66°)	0.0	2.8	16.6	35.2	62.6	100.6	150.7	207.9	240.9	247.1	247.5	247.5	247.5	247.5	247.4	243.4	228.4	206.4	181.9	156.4	129.4	75.3	14.8	4.0	0.0	0.0
13 (72°)	0.0	2.8	16.6	35.2	62.7	100.7	150.8	207.2	240.4	247.0	247.5	247.5	247.5	247.5	247.4	243.4	228.4	206.4	181.9	156.4	129.4	75.3	14.8	4.0	0.0	0.0
14 (78°)	0.0	0.7	13.7	29.9	53.4	86.1	129.3	182.9	229.8	245.6	247.4	247.5	247.5	247.5	247.5	247.4	243.8	229.0	207.8	184.5	160.7	135.9	94.7	22.3	0.0	0.0
15 (84°)	0.0	0.7	13.5	29.7	53.0	85.5	128.4	181.9	229.3	245.4	247.4	247.5	247.5	247.5	247.5	247.4	243.8	229.0	207.9	184.5	160.8	136.0	94.7	22.3	0.0	0.0
16 (90°)	0.0	8.0	13.2	29.1	52.2	84.2	126.5	179.4	227.6	245.1	247.4	247.5	247.5	247.5	247.5	247.4	243.8	229.1	208.0	184.6	160.8	136.1	94.7	22.3	0.0	0.0
17 (96°)	0.0	8.0	13.0	28.8	51.7	83.4	125.3	177.9	226.3	244.8	247.4	247.5	247.5		247.5		243.8	229.2	208.0	184.7	160.9	136.1	94.7	24.2	0.0	0.0
18 (102°)	0.0	8.0	13.3	29.4	52.7	85.0	127.6	180.8	228.3	245.1	247.4	247.5	247.5		247.5	247.4	243.7	229.0	207.9	184.6	160.8	136.0	94.7	24.2	0.0	0.0
19 (108°)	0.0	0.3	13.0	28.5	51.0	82.3	123.6	175.4	225.2	244.5	247.3	247.5	247.5	247.5	247.5	247.5	245.8	235.4	216.2	194.0	170.7	147.0	120.4	58.0	6.0	0.0
20 (114°)	0.0	0.3	13.0	28.6	51.2	82.7	124.2	176.0	225.4	244.5	247.4	247.5	247.5		247.5	247.5	245.8	235.4	216.1	193.9	170.7	147.0	120.4	59.9	6.0	0.0
21 (120°)	0.0	0.3	13.3	29.2	52.3	84.3	126.5	178.8	226.3	244.6		247.5	247.5		247.5	_		235.3		193.8	170.6	146.9	120.3	59.9	6.0	0.0
22 (126°)	0.0	0.3	13.0	28.6	51.2	82.6	124.1	175.8	224.2	244.2		247.5	247.5		247.5			235.4	216.1	194.0	170.7	147.0	120.4	58.0	6.0	0.0
23 (132°)	0.0	0.3	12.9	28.4	50.8	82.0	123.3	174.8	223.8		247.3	247.5			247.5	_		235.4		194.0	170.7	147.0	120.4	58.0	6.0	0.0
24 (138°)	0.0	0.7	14.0	30.4	54.3	87.5	131.1	184.9	230.6		247.4	247.5				247.2		229.9	209.0	185.7	162.3	135.7	101.6	26.4	0.0	0.0
25 (144°)	0.0	0.7	14.5	31.2	55.7	89.7	134.4	188.7	232.9		247.5		247.5			247.2		229.7	208.8	185.6	162.2	135.7	101.6	26.3	0.0	0.0
26 (150°)	0.0	0.7	14.4	31.1	55.5	89.4	133.9	188.2	232.7	_	247.5	_	247.5			247.2	_	229.7	208.8	185.6	162.2	135.7	101.6	26.3	0.0	0.0
27 (156°)	0.0	0.7	14.3	30.8	55.1	88.7	133.0	187.2	232.0	245.8		247.5	247.5		247.5	_		229.7	208.9	185.7	162.2	135.7	101.6	26.4	0.0	0.0
28 (162°) 29 (168°)	0.0	0.7 2.7	14.2 16.0	30.8	55.0 60.5	97.3	132.8 145.6	187.0 203.2	231.6	245.7 246.9	247.4	247.5 247.5	247.5 247.5		247.5 247.5	247.2	244.0	229.8	208.9 195.8	185.7 171.4	162.2 146.8	135.7 118.8	101.6 42.8	0.0	0.0	0.0
30 (174°)	0.0	2.6	16.5	35.1	62.3	100.1	149.6	206.7	240.3	246.9	247.5	247.5	247.5		247.5	246.7	238.2	218.5	195.6	171.2	146.6	118.8	42.8	0.0	0.0	0.0
31 (180°)	0.0	2.6	16.4	34.8	62.0	99.5	148.6	205.4	239.7	246.9	247.5	247.5	247.5	247.5	247.5	246.7	238.1	218.6	195.6	171.3	146.7	118.8	42.9	0.0	0.0	0.0
32 (186°)	0.0	2.8	16.3	34.7	61.7	99.1	148.1	205.0	239.5	_	247.5	247.5			247.5	246.7	238.2	218.6	195.7	171.3	146.7	118.8	42.9	0.0	0.0	0.0
33 (192°)	0.0	2.3	16.1	34.2	60.9	97.8	146.3	203.3	239.0	246.8		247.5	247.5	247.5	247.5	246.7	238.3	218.7	195.8	171.4	146.8	118.9	42.9	0.0	0.0	0.0
34 (198°)	0.0	4.8	18.5	38.8	68.8	110.3	164.2	219.7	243.9	247.3		247.5	247.5		246.9	240.6	222.6	199.1	173.8	148.2	110.9	50.0	3.9	0.0	0.0	0.0
35 (204°)	0.0	4.1	17.5	37.0	65.7	105.5	157.5	213.2	242.5	247.3	247.5	247.5	247.5		246.9	240.8	223.0	199.5	174.1	148.5	111.1	50.0	3.9	0.0	0.0	0.0
36 (210°)	0.0	3.7	16.7	35.6	63.3	101.8	152.1	207.5	241.1	247.2	247.5	247.5	247.5	247.5	246.9	241.0	223.3	199.8	174.3	148.7	111.2	50.1	3.9	0.0	0.0	0.0
37 (216°)	0.0	3.5	16.8	35.6	63.3	101.8	152.3	209.2	241.7	247.2	247.5	247.5	247.5	247.5	247.0	240.9	223.3	199.7	174.3	148.7	111.2	50.1	3.9	0.0	0.0	0.0
38 (222°)	0.0	3.7	17.2	36.3	64.6	103.8	155.4	212.9	242.2	247.2	247.5	247.5	247.5	247.5	247.0	240.8	223.1	199.5	174.2	148.5	111.1	50.1	3.9	0.0	0.0	0.0
39 (228°)	0.0	2.8	15.7	33.6	59.9	96.3	144.4	201.4	238.8	246.9	247.5	247.5	247.5	247.5	247.5	245.4	232.2	210.6	186.3	161.5	135.5	89.6	16.1	0.0	0.0	0.0
40 (234°)	0.0	2.9	16.1	34.3	61.1	98.3	147.1	204.2	239.2	246.9	247.5	247.5	247.5	247.5	247.5	245.3	232.0	210.4	186.1	161.4	135.4	89.6	16.1	0.0	0.0	0.0
41 (240°)	0.0	3.0	16.0	34.2	60.9	98.0	146.9	204.4	239.6	246.9	247.5	247.5	247.5	247.5	247.5	245.3	232.0	210.4	186.1	161.4	135.3	89.6	16.1	0.0	0.0	0.0
42 (246°)	0.0	2.8	16.1	34.3	61.0	98.2	147.0	204.0	239.4		247.5	247.5			247.5			210.4	186.1	161.4	135.3	89.6	16.1	0.0	0.0	0.0
43 (252°)	0.0	2.9	16.1	34.2	61.0	98.1	146.9	203.8	239.3		247.5		247.5			245.3		210.4	186.1	161.4	135.4	89.6	14.2	0.0	0.0	0.0
44 (258°)	0.0	0.9	14.4	31.2	55.7	89.8	134.8	190.5	234.8	246.4		247.5			247.5		_	223.7	201.4	177.2	153.6	127.4	82.5	0.0	0.0	0.0
45 (264°)	0.0	0.7	14.3	31.0	55.3	89.2	133.9	189.4	234.4	246.3		247.5			247.5	_		223.8	201.5	177.2	153.7	127.4	82.5	0.0	0.0	0.0
46 (270°)	0.0	0.9	14.0	30.5	54.5	87.8	131.9	186.8	232.9	246.2		247.5	247.5		247.5	247.4	_	223.9	201.6	177.4	153.7	127.4	82.6	0.0	0.0	0.0
47 (276°)	0.0	0.9	13.8	30.2	54.0	87.1	130.7	185.1	231.7	246.1	247.5	247.5	247.5	247.5	247.5	247.4	242.1	224.0	201.7	177.4	153.8	127.5	86.5	0.0	0.0	0.0
48 (282°)	0.0	1.2	14.2	30.7	54.9	88.5	132.9	188.0	233.6	246.3		247.5	247.5		247.5	_		223.8	201.6	177.3	153.7	127.4	86.5	0.0	0.0	0.0
49 (288°)	0.0	1.8	15.2	32.6	58.1	93.5	140.1	196.7	237.6	246.7		247.5	247.5		247.5		239.3	220.2	197.3	173.1	148.5	124.0	55.0	2.0	0.0	
50 (294°) 51 (300°)	0.0	2.0	15.3 15.7	32.9	58.6 59.7	94.3	141.1						247.5 247.5						197.3 197.2		148.4		53.1	2.0	0.0	0.0
51 (300°) 52 (306°)	0.0	1.8	15.7	32.8	58.5	94.0		199.5				_	247.5						197.4			124.0	53.1	2.0	0.0	0.0
52 (300°) 53 (312°)	0.0	1.8	15.1	32.5	58.0	93.4	_	195.8					247.5						197.4	_	148.5		55.0	2.0	0.0	0.0
54 (318°)	0.0	2.8	15.8	33.8	60.1	96.7		200.9					247.5						193.5			115.7	30.6	12.3	0.0	0.0
55 (324°)	0.0	2.8	16.3	34.7	61.8	99.3		204.8	-				247.5	-					-	_		115.6	28.6	12.3	0.0	0.0
56 (330°)	0.0	2.8	16.3	34.6	61.6	99.0		204.2					247.5									115.6	30.6	12.3	0.0	0.0
57 (336°)	0.0	2.6	16.1	34.3	61.1	98.2		203.4					247.5	_		_			-		143.6		30.6	12.3	0.0	0.0
58 (342°)	0.0	2.8	16.1	34.2	60.8	97.8	_	203.1					247.5	-								115.6		12.3	0.0	0.0
59 (348°)	0.0	3.6	17.9	37.7	66.9			_	243.5	_										_	128.8		6.3	0.0	0.0	0.0
60 (354°)	0.0	4.5	18.6	38.9	_				243.9							_							6.3	0.0	0.0	0.0
Eiguro																									. .	

Figure A.9: Plant level power curve for Ternopil. Values in MW calculated with WAsP. Wind speed bins (first row) in m/s, direction bins (first column) in degrees.